# Global View of the Upper Level Outflow Patterns Associated with Tropical Cyclone Intensity Change during FGGE

By
Lianshou Chen and William M. Gray

Department of Atmospheric Science
Colorado State University
Fort Collins, Colorado

NASA NAG 5-299

Colorado State University

Department of Atmospheric Science

Paper No. 392

# GLOBAL VIEW OF THE UPPER LEVEL OUTFLOW PATTERNS ASSOCIATED WITH TROPICAL CYCLONE INTENSITY CHANGES DURING FGGE

By

Lianshou Chen(*)

and

William M. Gray

Department of Atmospheric Science

Colorado State University

Fort Collins, Colorado 80523

October, 1985

Atmospheric Science Paper No. 392

---

(*) On leave from the Chinese National Meteorological Bureau.

## ABSTRACT

This paper discusses the characteristics of the upper tropospheric outflow patterns which occur with tropical cyclone intensification and weakening over all of the global tropical cyclone basins during the year long period of the First GARP Global Experiment (FGGE). By intensification we mean the change in the tropical cyclone's maximum wind or central pressure, not the change of the cyclone's outer 1-3° radius mean wind which we classify as cyclone strength. All the 80 tropical cyclones which existed during the FGGE year are studied. 200 mb wind fields were derived from the analysis of the European Centre for Medium Range Weather Forecasting (ECMWF) which made extensive use of upper tropospheric satellite and aircraft winds. Corresponding satellite cloud pictures from the polar orbiting U.S. Defense Meteorological Satellite Program (DMSP) and other supplementary polar and geostationary satellite data are also used.

Intensifying tropical cyclones within the different global ocean basins typically show upper level outflow patterns of three basic types: Single channel (S) outflow which includes either poleward ($S_P$) or equatorward ($S_E$) outflow; Double channel outflow in both poleward and equatorial directions (D); or No-channel (N) outflow (only 17% of cases). Depending on the location of the tropical cyclone and its associated anticyclone and the surrounding 200 mb environmental wind fields, these outflow patterns can each be further divided into three to four sub-patterns. Mid-latitude troughs and low latitude anticyclones of the other hemisphere often play an important role in specifying the location and strength of these outflow channels. Outflow patterns have distinct seasonal and geographic differences. In general poleward outflow channels are dominant for tropical cyclones in the Southern Hemisphere and for spring and autumn Northern Hemisphere cyclones. Equatorward outflow channels are dominant for tropical cyclones in the Northern Hemisphere in summer.

The sudden weakening of tropical cyclones over tropical oceans also appears to be often associated with the characteristics of the upper level surrounding cyclone wind fields. When the existing outflow channels of a tropical cyclone become cut off, it typically undergoes a weakening of its intensity.

A short discussion of some of the likely physical processes which may be involved with this observed association of 200 mb outflow patterns and cyclone intensity change is also given.

TABLE OF CONTENTS


| | | Page |
|---|---|---|
| 1. | Introduction | 1 |
| 2. | Data Analysis | 8 |
| 3. | Characteristics of the Outflow Patterns and Satellite Images of Intensifying Cyclones | 12 |
| 4. | Types of Synoptic Flow Patterns which Enhance Outflow Channel Change | 51 |
| 5. | Regional and Seasonal Outflow Differences as a Response To Background 200 mb Climatology | 72 |
| 6. | Outflow Channel Changes Associated with Tropical Cyclone Weakening | 91 |
| 7. | How Upper Level Outflow Channels May Be Related to Cyclone Intensification | 103 |
| 8. | Concluding Discussion | 115 |
| Acknowledgements. | | 118 |
| References | | 119 |
| APPENDIX A: W. M. GRAY'S FEDERALLY SUPPORTED RESEARCH PROJECT REPORTS SINCE 1967 | | 121 |

## LIST OF SYMBOLS AND ACRONYMS

| | |
|---|---|
| DMSP | U.S. Defense Meteorological Satellite Program |
| ECMWF | European Center for Medium Range Weather Forecasting |
| FGGE | First GARP Global Experiment |
| GARP | Global Atmospheric Research Program |
| GMS | Geostationary Meteorological Satellite |
| JTWC | Joint Typhoon Warning Center, Guam |
| NE | Northeast |
| NW | Northwest |
| TUTT | Tropical Upper Tropospheric Trough |

## 1. Introduction

For many years forecasters have often noted an association between the characteristics of a tropical cyclone's upper tropospheric outflow at radius of 5 to 10° or beyond and the cyclones' current and subsequent rate of intensity change. Intensification is frequently observed to occur when a cyclone develops one or two concentrated upper tropospheric outflow channels on its poleward or equatorial flanks. Although a number of individual case studies have been made on this topic, there has yet to be a systematic observational study of this subject in all the global storm basins where upper level analysis procedures are the same for all regions. It would appear that some systematic study of these upper level outflow channels and their possible role in intensity change is warranted. This study was undertaken to try to help document this likely upper outflow channel and cyclone intensity change link.

Observations so far have shown that the establishment of concentrated tropical cyclone outflow channels is almost always a consequence of the favorable positioning about the cyclone of synoptic scale 200 mb anticyclones or troughs such as a Tropical Upper Tropospheric Trough (TUTT), a low latitude 200 mb anticyclone of the opposite hemisphere, or other distinctive surrounding cyclone upper level flow features. Furthermore, it appears that if a tropical cyclone's 5 to 10° radius outflow circulation is indeed concentrated into narrow channels there can result a more important influence on the cyclone's inner-core deep cumulus convection and rate of intensification than would have occurred if the same amount of upper level mass outflow were more uniformaly spread out over a broader circle around the cyclone.

Studies by Sadler (1976, 1978) and others have shown an association of these synoptic scale influences on tropical cyclone intensification such as favorable positions of the TUTT for intensification of west Pacific typhoons and Atlantic hurricanes. Sadler observes that intensification often occurs when a cyclone's outflow becomes concentrated into one or two channels which extend outward to large radius. The first author (Chen 1974) has also pointed out that the interactions between Southern and Northern Hemisphere upper tropospheric circulations can have an important influence on northwestern Pacific cyclone intensification. Likewise, R. Simpson (1970) has stated that upper tropospheric wind patterns can have strong triggering and suppressive influences on tropical cyclone mass circulation and intensity.

This paper discusses tropical cyclone intensity change as it is related to a storm's 200 mb environmental wind fields and satellite observed cloud patterns. All 80 tropical cyclones which occurred during the 1978-79 First GARP Global Experiment (FGGE) are studied. Use is made of the large-scale 200 mb wind analysis of the European Center for Medium Range Weather Forecasting (ECMWF) where upper level satellite and aircraft winds have been used in addition to the normal and special rawinsondes employed during the FGGE year. This paper attempts to identify the characteristic upper troposphere outflow patterns which are associated with tropical cyclones undergoing intensity change and how these outflow patterns may vary geographically and seasonally. By intensification we mean the change in the cyclone's inner-core maximum wind or central pressure.

Global analysis of upper air observations is now available from the

ECMWF for the FGGE (December 1978 through November 1979) year. Global upper-air coverage as provided during the FGGE year offers a chance to examine this question of the link between intensity change and upper level outflow from a global observational perspective. Using the complete ECMWF upper tropospheric analysis of the 1978-79 FGGE year, this paper attempts to more systematically investigate this likely association of favorable 200 mb outflow with intensification for the 80 FGGE year tropical cyclones. We also analyze cases of cyclone weakening over tropical waters. Cloud image data consists primarily of the polar orbiting high resolution U.S. Defense Meteorological Satellite Program (DMSP) visual (1/2 n mi resolution) pictures. Where DMSP images were occasionally missing supplementary satellite data has been obtained from geostationary and polar orbiting image sources.

Although cyclone intensification does not always require strong outflow channels, they were observed in 80-85% of the cases during the FGGE year. We believe this figure is also representative of other years. These outflow channels can, however, be quite variable as to their location and strength relative to the cyclone center. Outflow also varies by storm basin and by season.

There is at present no well accepted theory as to the causes of this apparent physical linkage between concentrated outflow and cyclone intensification. Holland and Merrill (1984) have recently hypothesized that this physical linkage is related to the presence of low inertial instability which is often established in the anticyclonic flow of the upper troposphere on the flanks of tropical cyclones. This low inertial instability occurs from the favorable superposition of troughs or other special surrounding cyclone wind features. Merrill (1985) has recently

carried these ideas much further and has developed a more integrated rationale for this apparent important physical linkage. This is not an easy task however.

Before we discuss this upper level outflow and cyclone intensity change link it is important that we first define what we mean by cyclone intensification. An important new idea coming out of our CSU research in the last few years is the concept of the necessity of distinguishing between tropical cyclone "intensity" which is a measure of a tropical cyclone's maximum sustained low level winds and/or central pressure, and that of tropical cyclone "strength", which we define as the mean tangential wind around the storm between $1-3^{o}$ n mi radius. Figure A shows these differences. We have measured both of these quantities from the Guam aircraft reconnaissance flights. (See papers by Weatherford and Gray, 1984, and Weatherford, 1985 for more details.) Weatherford (op cit) does not observe a good correlation between tropical cyclone strength and intensity (see Fig. B). This is particularly true of the more intense cyclones. It is possible to have a cyclone increase its strength and simultaneously weaken its intensity and vice-versa. She also does not find a good relationship between a cyclone's central pressure (or its maximum winds) and its radius of 30 and 50 knot winds. A cyclone's radius of 30 and 50 knot winds and rainfall is more related to cyclone strength than it is to cyclone intensity. Merrill (1984) finds that a tropical cyclone's size as defined by its mean radius of outer closed isobar correlated with tropical cyclone intensity at a value of only 0.3 and that there is hardly any correlation of the changes of these features.

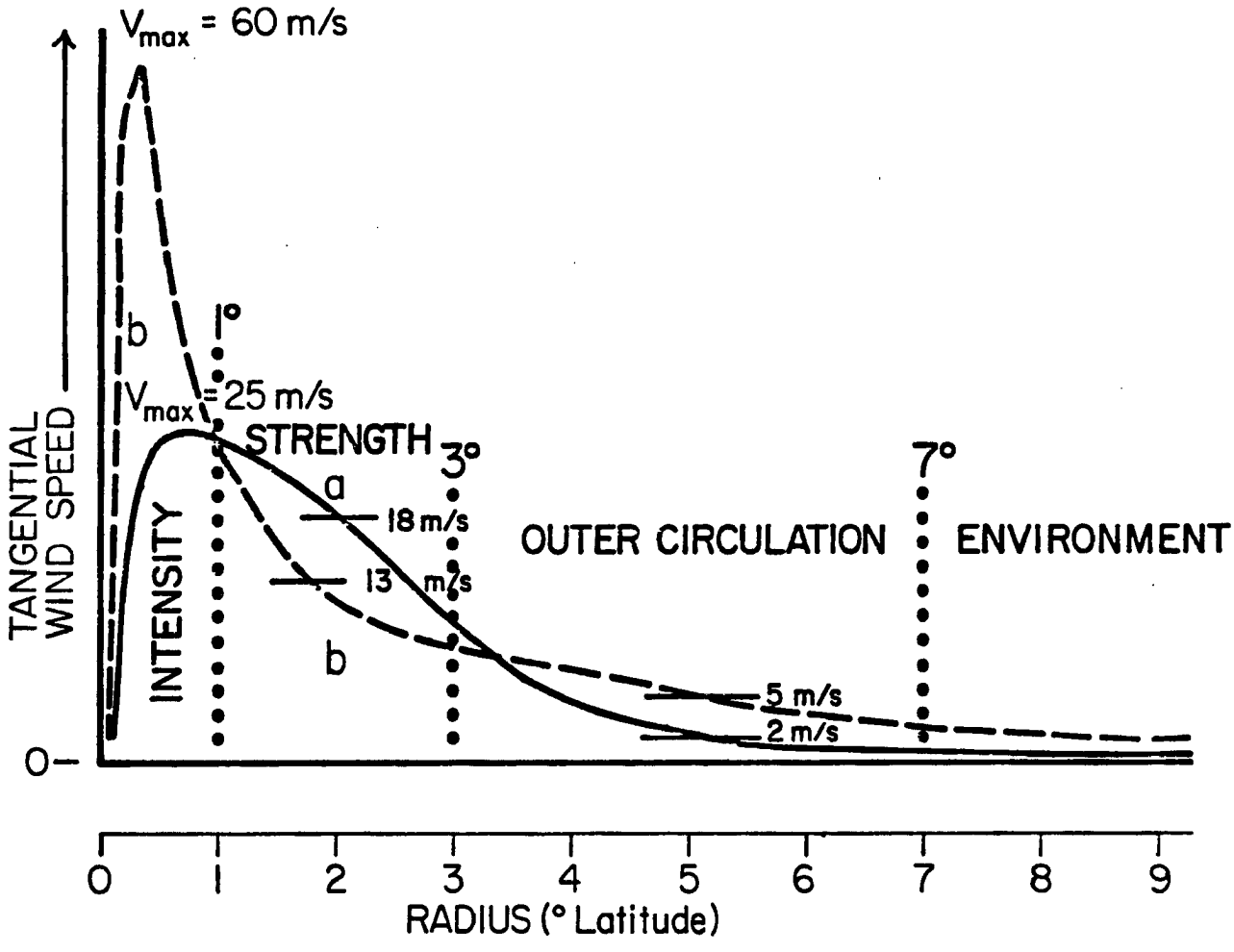


Fig. A. Definition of tropical cyclone intensity, strength, and outer circulation on a radial profile of tangential (azimuthal) winds. Note that the wind profile representative of the dashed line gives large intensity but less strength than the solid line.

Thus, the physical requirement that has more commonly been associated with the development of a tropical cyclone such as large-scale low level vorticity and broad upward vertical motion may be more related to the broader scale "strength" increase of a cyclone and may be quite different than the more specialized requirements for only inner-core (< 1° radius) cyclone "intensity" increase. We are finding that cyclone intensity and intensity change appears to be much more

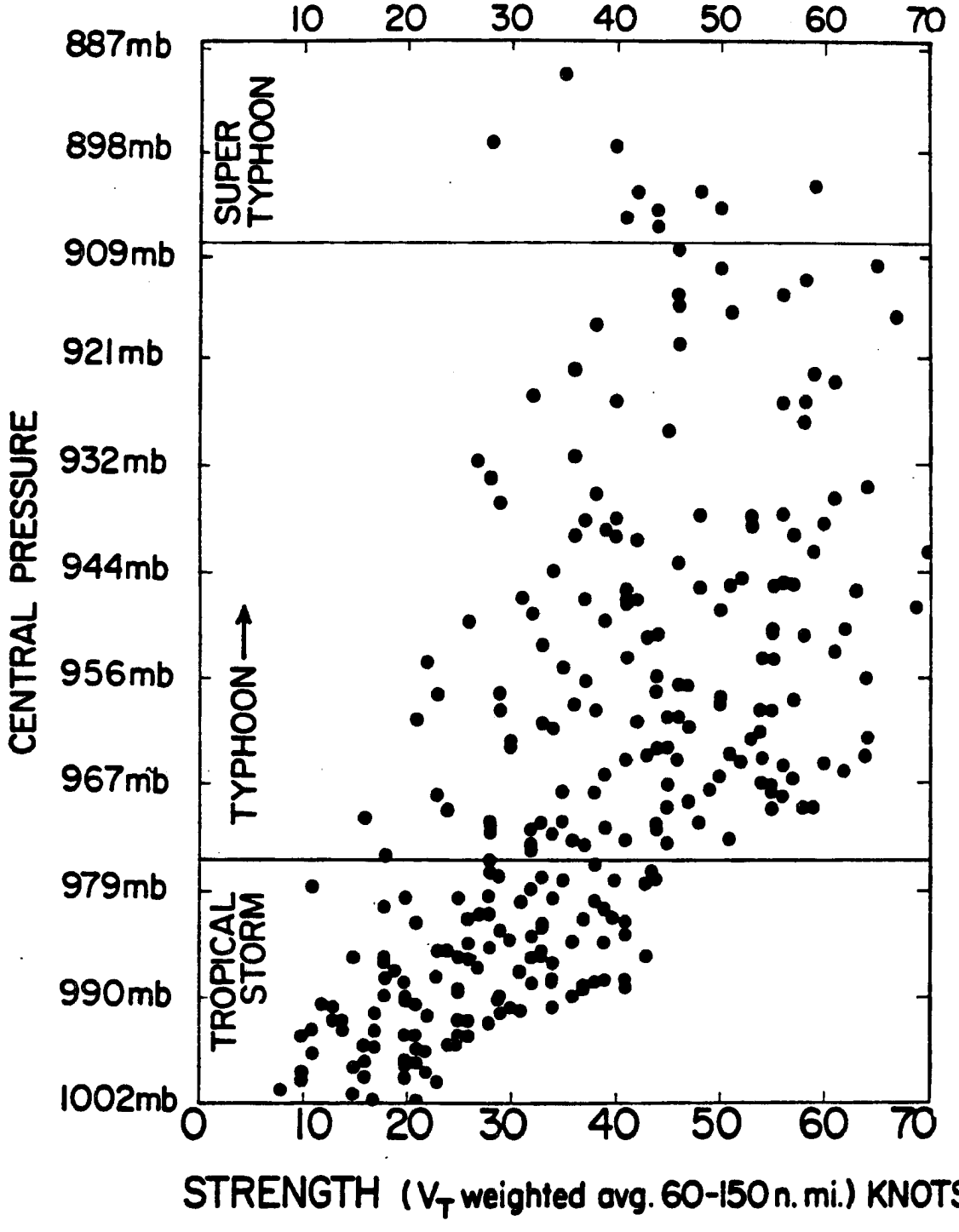


Fig. B. INTENSITY (minimum sea-level pressure) VERSUS STRENGTH SCATTER DIAGRAM (from Weatherford, 1985) of tropical cyclones of the western Pacific for 1980-1982.

related to the upper tropospheric outflow mechanisms of the cyclone and the amount of deep convection near the cyclone center. By contrast we have found that cyclone strength and its change appears to be much more related to the large-scale lower tropospheric surrounding cyclone wind fields and the net overall deep convection occurring within the entire inner 3-4° radius of the cyclone. Cyclone intensification depends not so much on the amount of deep convection occurring within the cyclone system as a whole (which was also shown by Arnold, 1976) but rather more on the amount of deep organized convection and the resulting magnitude of the 'in-up-and-out' mass circulation which takes place within the system's central 0-1° radius core.

Our project is now involved in research to try to better ascertain the different environmental conditions which lead some cyclones to develop concentrated inner-core deep convection and to increase their intensity vs. those environmental conditions which cause more net convection within the cyclone cloud area as a whole but lesser amounts of deep convection within the cyclone core.

This paper makes an extensive analysis only of the tropical cyclone's surrounding environmental 200 mb wind fields and cloud patterns as they may be related to the cyclone's intensity change. The important question of tropical cyclone "strength" change is not discussed. Other factors which may influence cyclone intensity change are also not covered.

## 2. Data Analysis

This paper will concentrate on the strong jet-like upper tropospheric outflow channels of 10-50 m/s which often emanate 10-20° or more from the cyclone. These outflow channels often extend long distances outward from the cyclone. In most cases they appear to be well resolved by the ECMWF analysis at least in the qualitative sense.

Intensification criteria for all FGGE year tropical cyclones have been determined on the basis of whether the cyclone had an intensification or weakening rate of 20 knots (kts) per 24 hours or greater for at least one 24-hour period. The locations where the tropical cyclones met this criteria are studied in this paper and are shown by the dots and X's in Fig. 1. It is believed that the FGGE year period was a representative year for tropical cyclones about the globe. Its 80 tropical cyclones compared with a previous 20 year average of 79 cyclones. There were also no significant anomalous storm frequency or track alterations in any of the cyclone basins during the FGGE year. Anomalous years occur mainly when El Nino-Southern Oscillation (ENSO) events take place such as the 1982-83 ENSO. Statistical results derived for the whole FGGE year are thus considered to be quite representative of what would have been obtained if this analysis had been performed for a multi-year period or in other individual non-ENSO years.

Intensity data for the FGGE year storms were obtained from aircraft measurements and "best track" information. For those ocean basins which lacked reconnaissance aircraft determined wind speed data, maximum winds have been determined from satellite derived T-numbers as specified by the well-known Dvorak, (1975) scheme. US Military DMSP satellite

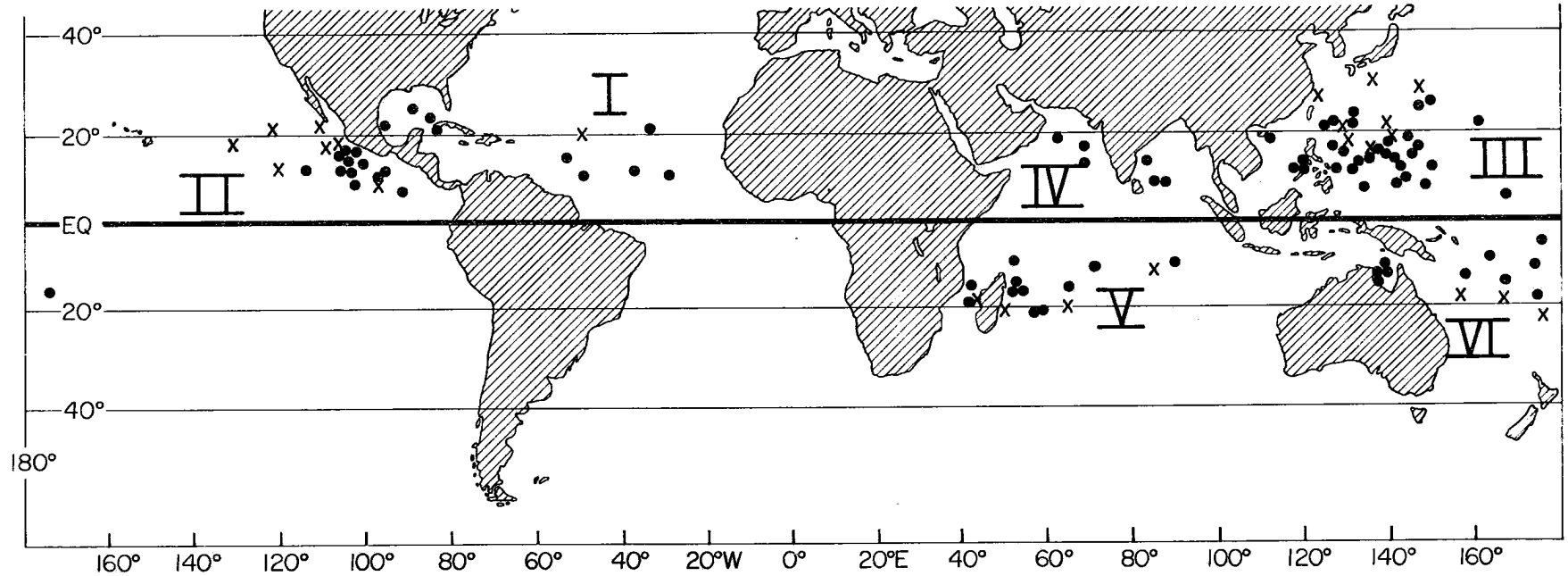


Fig. 1. Distribution of intensity change cases over the six ocean storm basins (● represent the location of tropical cyclones undergoing intensification and X the location of tropical cyclones undergoing a weakening).

imagery has been obtained for most of our cases with some augmentation from NOAA polar orbiting satellite data plus the FGGE year GMS picture images.

The outflow channels that are discussed in this paper refer to the narrow high speed near jet like features of the upper tropospheric outflowing air that can move out a considerable distance from a tropical cyclone's center as seen by satellite imagery or the upper-level wind charts. These outflow channels usually have an anticyclonic turning component and are usually observable in satellite images of cirrus bands or lines stretching long distances outward around the storm center. In general, the direction of upper cloud outflow is approximately the same as that of the upper level wind outflow. When doubt occurred as to the direction of the wind outflow, priority was given to the satellite cloud patterns rather than the analyzed streamline outflow of the ECMWF analysis.

The ECMWF III-b 1.875$^{o}$ Mercator-grid analysis at 200 mb which has been used in this study was objectively analyzed in all of the ocean basins. It is considered to be the best objective analysis that can be obtained. This analysis made extensive use of satellite and jet aircraft winds. Many extra upper-air rawinsonde were made during the FGGE year. The ECMWF center uses a longer cut-off time for data receipt than most other operational centers. This assists with a better data coverage. All the 200 mb analysis shown in this paper are for 00 GMT (Z) of the day shown. All multi-day changes refer to change from 00 GMT on one day to 00 GMT in the other day.

It is known that the initializing procedures of the ECMWF analyses act to suppress the divergent component of the tropical wind field on

the smaller scales. This divergent component suppression is not believed, however, to unduely alter the character and the general magnitude of the quite broadscale outflow channels which are studied here.

The 200 mb winds used in this study were obtained from the maps of the atlases distributed by the ECMWF center in Reading, U.K. (Bjorheim, 1981, 1982).

## 3. Characteristics of the Outflow Wind Patterns and Satellite Images of Intensifying Cyclones

At upper troposphere levels, almost every tropical cyclone has a corresponding anticyclone and an outward directed wind field.

In most cases a mesoscale anticyclone is generally found directly over or near the center of the tropical cyclone and represents the location in the upper troposphere where there is a build-up of temperature from the rising convective motion within the center of the cyclone. On the other hand, it is often found that there is another larger, synoptic scale anticyclone that pre-existed within the vicinity of the intensifying tropical cyclone. This synoptic scale anticyclone usually is a major component of the upper equatorial ridge in which the tropical cyclone develops. The exact location of this larger upper level anticyclone with respect to its center of the tropical cyclone can vary depending upon many environmental factors -- including the lower level forcing mechanisms that are helping to create the cyclone. The relative location of this large-scale anticyclone with respect to the tropical cyclone center whether it is to its east, west, north, south or superimposed over the smaller cyclone mesoscale anticyclone will help to dictate the direction of the outflow patterns away from the cyclone. These can vary greatly in size and strength. These outflow patterns when linked to the environment generally result in one or more outflow channels. It is the relative positions of these larger scale anticyclones to the center of the tropical cyclone that will be discussed in the rest of this chapter.

The majority of tropical cyclones have some type of outflow channel to their poleward or equatorward side. A few cyclones do not.

Satellite imagery typically shows outgoing cirrus bands or lines corresponding to these outflow channels. For an anticyclone without an outflow channel, a synoptic-scale dense overcast cloud shield without major outflow bands is typically seen in the satellite imagery. Short lateral cirrus plumes often exist around this type of anticyclone -- indicating a more uniform circular spread of the cyclone's upper level outflow.

Upper level outflows can almost always be classified into one of three basic categories depending on the number of channels:

1) Single-channel outflow (S)

2) Double-channel outflow (D), and

3) Systems without distinct outflow channels or non-channel outflow (N)

Each of these outflow patterns may be divided into three to four subpatterns based on the position of the upper level anticyclone relative to the tropical cyclone center and the resulting outflow channel direction. The following sections present and discuss these various 200 mb outflow models with examples of each pattern in the Northern and Southern Hemisphere. Each pattern is identified by a combination of one or more of the following terms:

S = Single channel

D = Double channel

N = Non-channel

P = Poleward outflow

E = Equatorward outflow

w = cyclone center is west of the 200 mb anticyclone center

e = cyclone center is east of the 200 mb anticyclone center

s = cyclone center is south of the 200 mb anticyclone center

c = cyclone center is near the center of the 200 mb anticyclone center

For example $S_E$ means a cyclone with a single channel outflow towards the equator. $S_{Pe}$ means a cyclone with a single channel outward towards the pole where the cyclone center is to the east of the 200 mb anticyclone center.

Examples of these various classes of outflow patterns and the relative positions of the 200 mb large scale anticyclonic centers which are associated with these intensifying cyclones will now be given.

a) Basic Northern Hemisphere Patterns

(1) Single Channel (S) Outflow.

This single channel outflow may be divided into four subpatterns based on the direction of the outflow and the position of the upper anticyclone center relative to the cyclone center.

$S_{Pw}$. The tropical cyclone center is located to the west of an upper anticyclone that has a poleward outflow channel (Fig. 2a). For example, Typhoon Bess on 22 March 1979 and was located to the west of a NW Pacific anticyclone that had an outflow channel directed towards the northeast (Fig. 2b). In the satellite imagery for the same day, a poleward cloud outflow pattern is observed (Fig. 2c). After this upper level flow pattern was formed, the maximum sustained wind speed of Bess increased from 55 kts to 90 kts during the time period 22-24 March.

$S_{Pc}$. A poleward outflow extends from a tropical cyclone whose center is located underneath the center of the 200 mb anticyclone (Fig. 3a). On 18 September 1979, a tropical depression moved into the

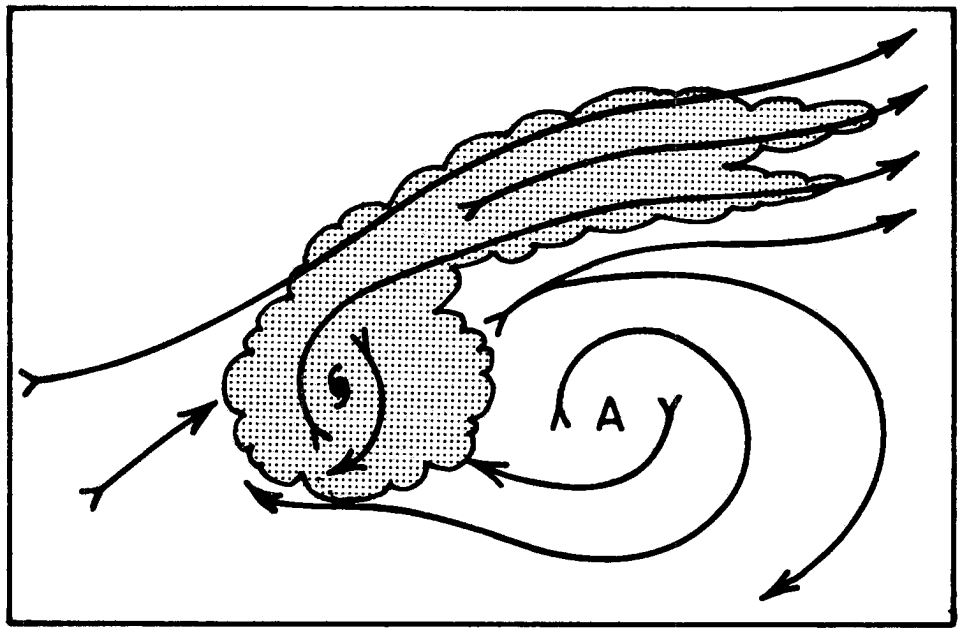


(a)

200 mb

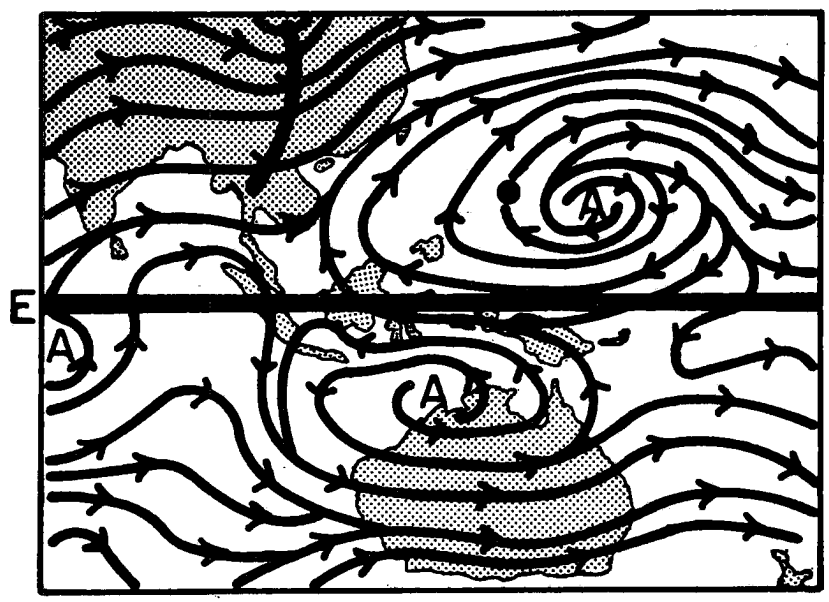


(b)

22 MARCH 00Z

Fig. 2a-c. Pattern $S_{PW}$: Diagram (a) is an idealized picture of a single poleward 200 mb outflow channel with the cyclone center to the west of the 200 mb anticyclone center. Diagram (b) 200 mb winds on 22 March 1979 for future Typhoon Bess. Diagram (c) 1600Z 22 March 1979 DMSP display (Typhoon Bess). From 22 to 24 March the maximum sustained wind increased from 55 to 90 kts.

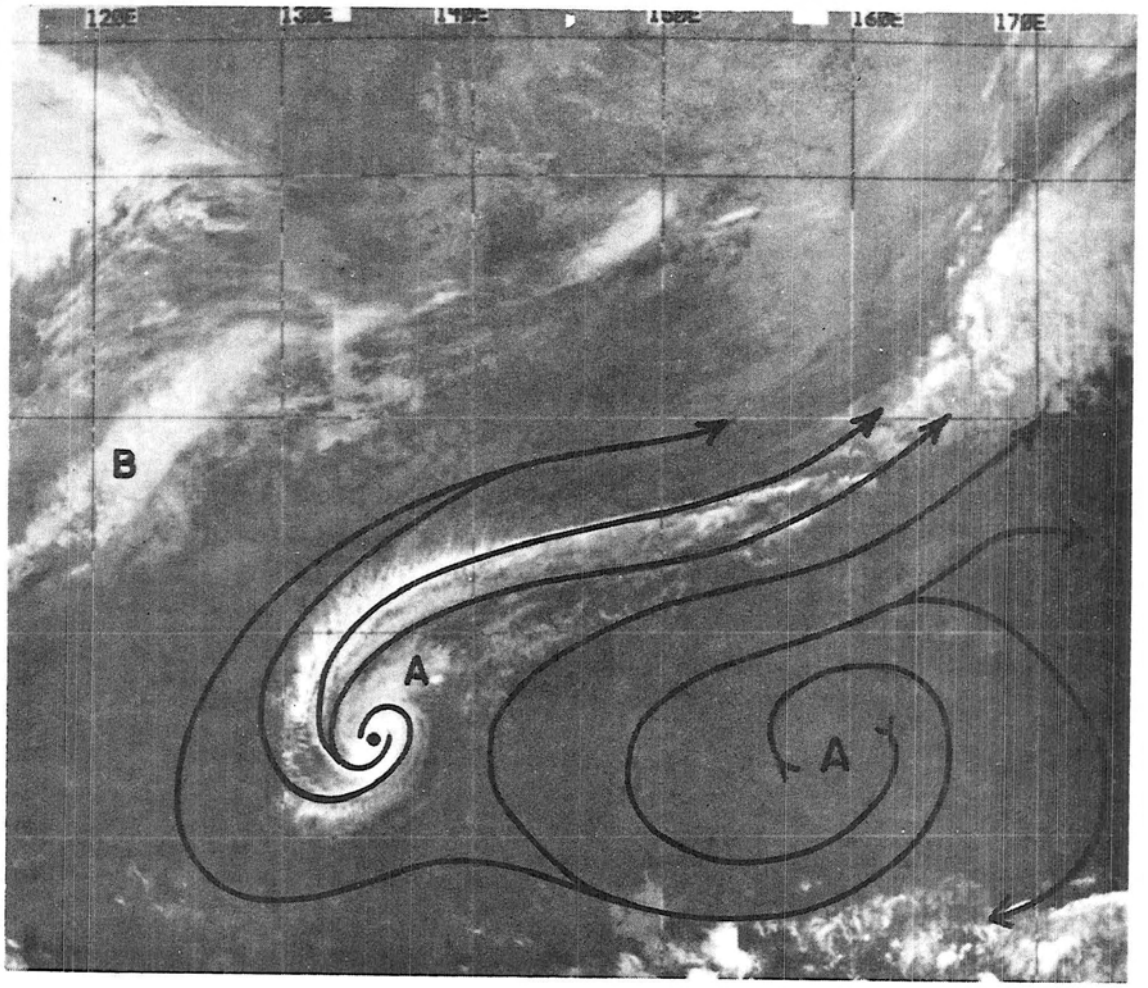


(c)

Fig. 2c. Continued.

northern part of the South China Sea and under an anticyclone. Figure 3b shows the upper level stream field at the time this tropical storm (Nancy) intensified. Figure 3c shows the cloud picture which goes with this. Outflow is to the northeast. For 18 to 19 September the maximum winds increased from 25 to 45 kts.

$S_{Ec}$. Example of a single equatorial directed outflow (Fig. 4a) where the cyclone is underneath the 200 mb anticyclone (Fig. 4b). The corresponding satellite cloud picture shows a large area of equatorward

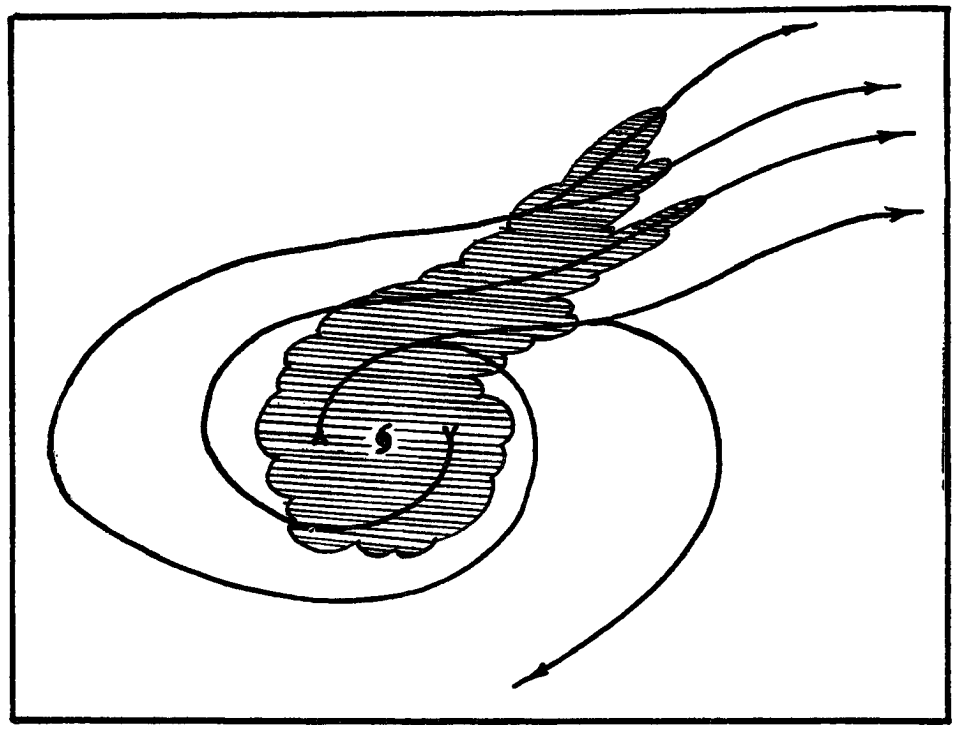

(a)

200 mb

(b)

18 SEPTEMBER 00Z

Fig. 3a-c. Pattern $S_{Pc}$: Diagram (a) shows a typical case of a single 200 mb poleward outflow channel with the 200 mb anticyclone center located directly over the cyclone center. Diagram (b) 200 mb flow on 18 September 1979 for Tropical Storm Nancy. Diagram (c) 0629 GMT 18 September 1979 DMSP display of Tropical Storm Nancy.

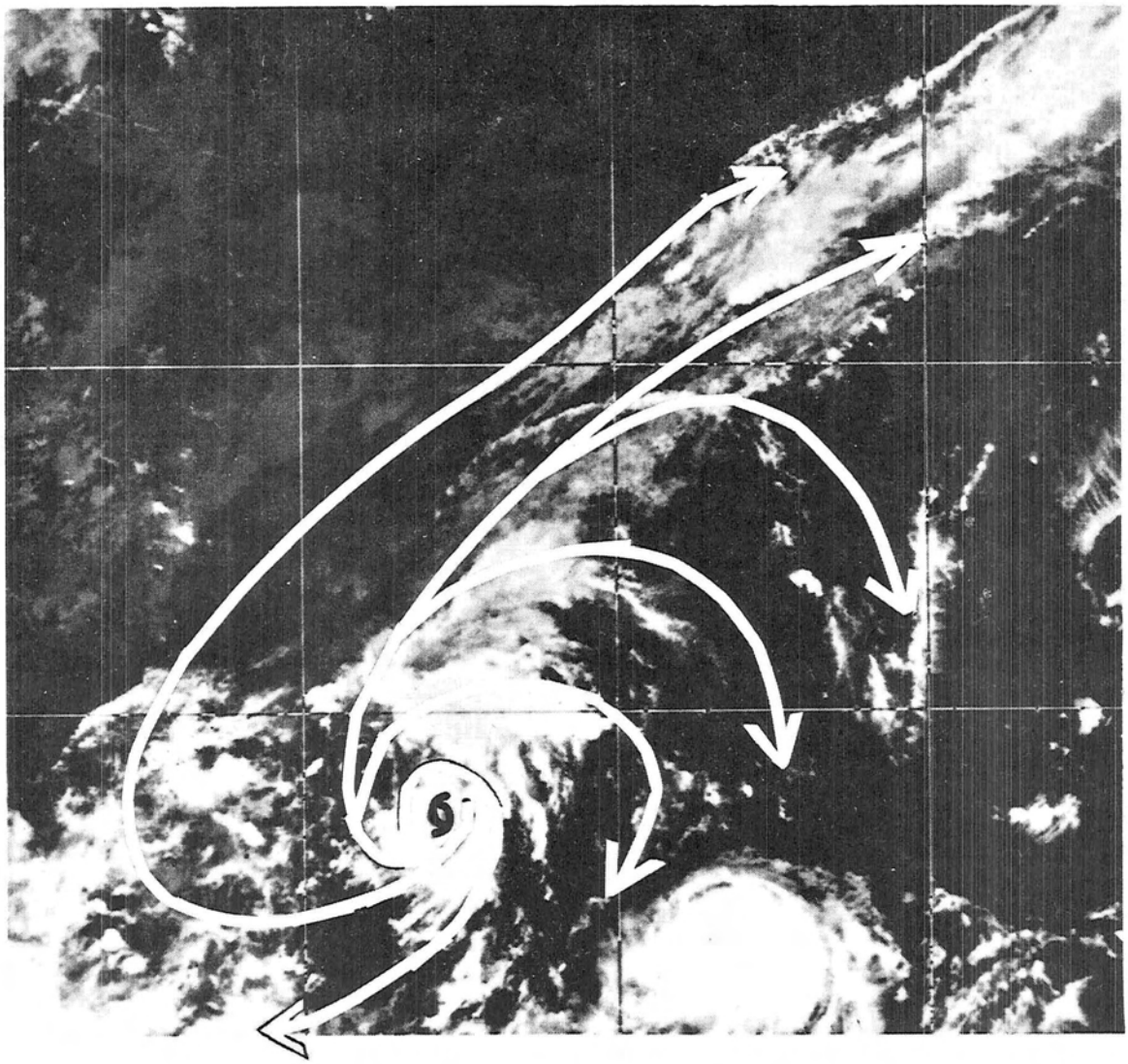

(c)

Fig. 3c. Continued.

cloud outflow (Fig. 4c). Between 9 and 11 September, the maximum sustained wind speed of this system (Guillermo) increased from 30 to 65 kts.

$S_{Ee}$. The tropical cyclone center is located to the east of the center of an upper level anticyclone that has an equatorward outflow channel (Fig. 5a).

Two examples are given. In its tropical storm stage, future Typhoon Irving was located northeast of the Philippines and below the northeast 200 mb flow in the eastern sector of the South Asian summer

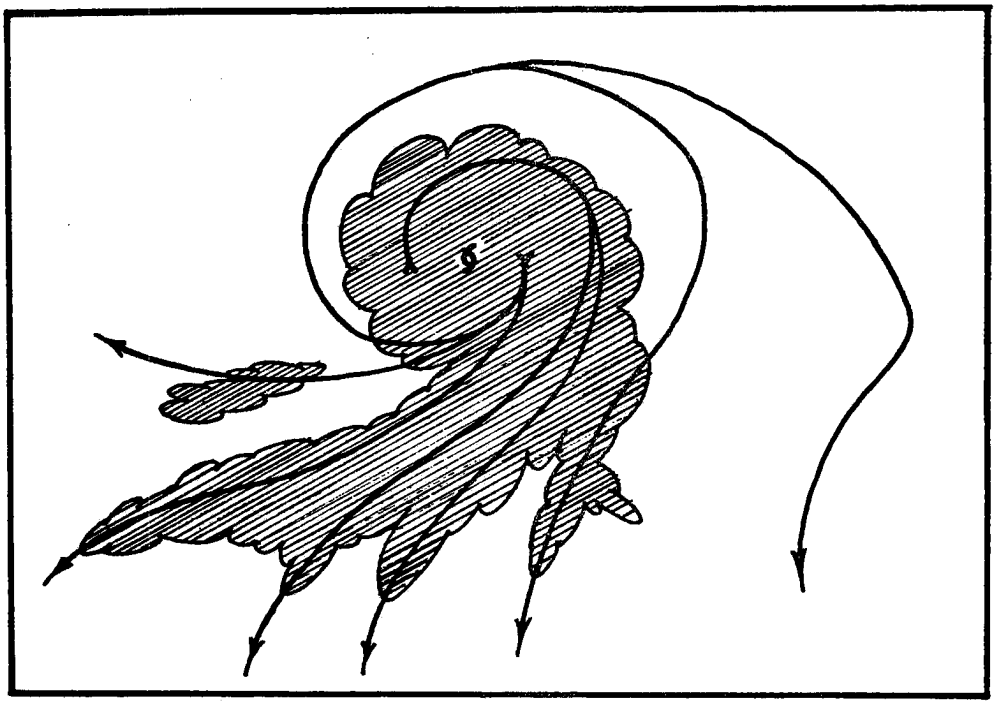

(a)

200 mb

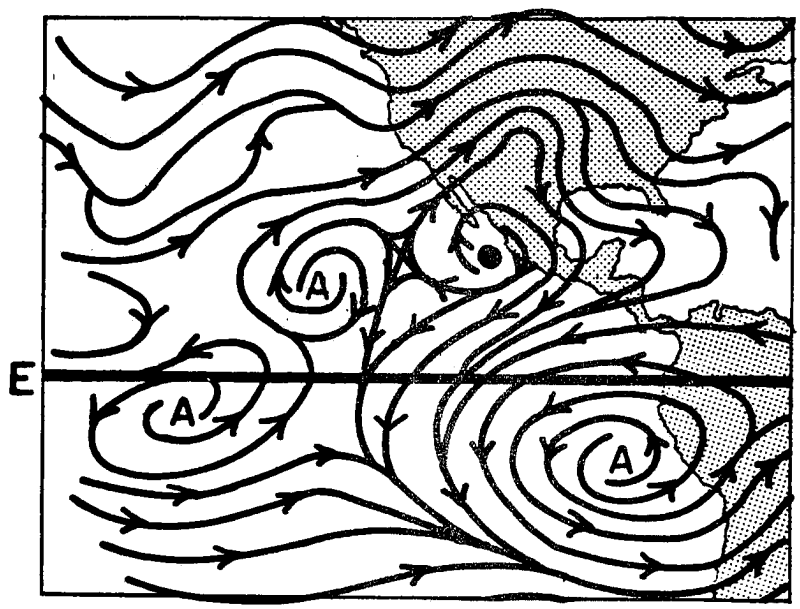


(b)

10 SEPTEMBER 00Z

Fig. 4a-c. Pattern $S_{EC}$: Diagram (a) is a typical case of a single equatorward outflow channel when the anticyclone center is located directly over the cyclone center. Diagram (b) 200 mb winds on 10 September 1979 for future Hurricane Guillermo. Diagram (c) 1626 GMT 9 September 1979 DMSP display of future Hurricane Guillermo.

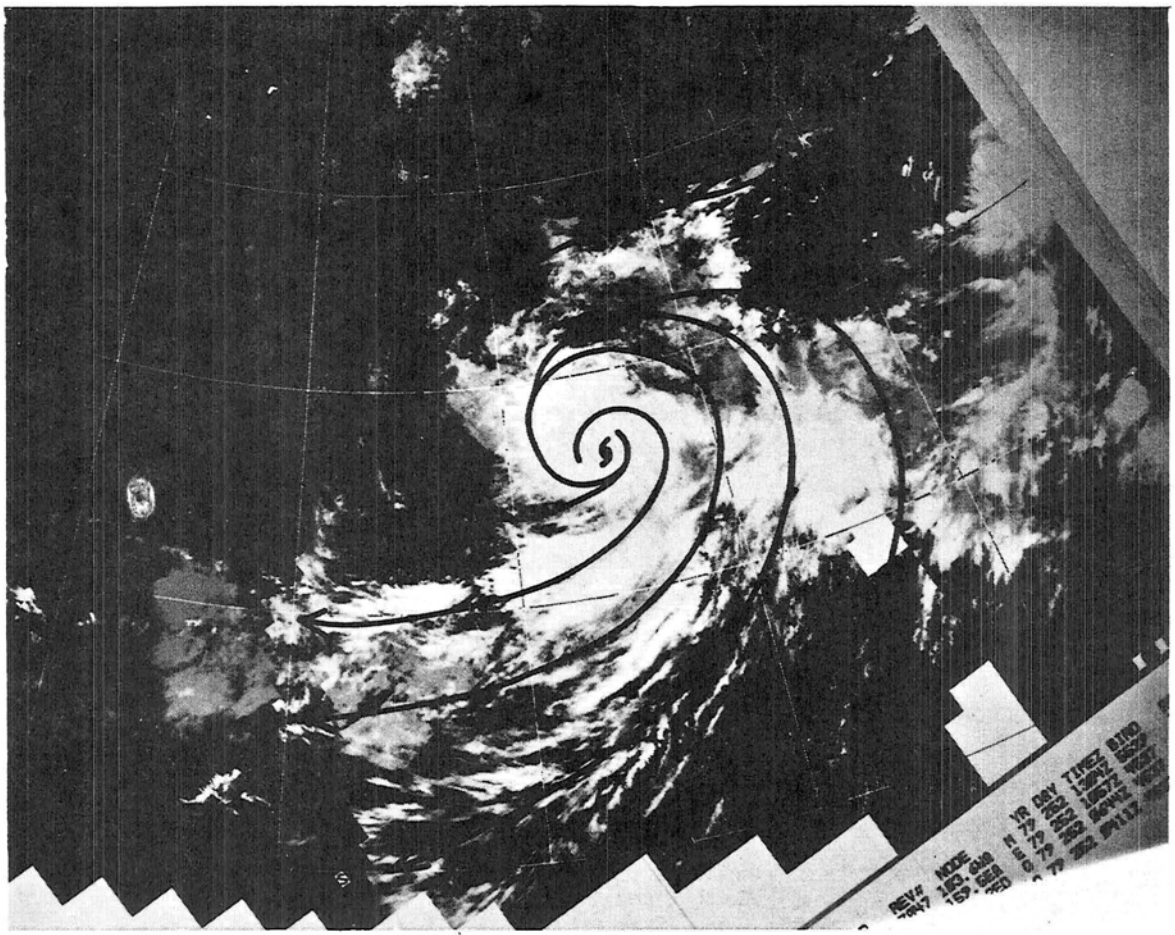

(c)

Fig. 4c. Continued.

anticyclone. An equatorward outflow channel was present (Fig. 5b). The corresponding satellite cloud picture also showed an area of equatorward cloud outflow. Lateral cirrus lines at the cloud tail part indicated quite strong upper level outflow (Fig. 5c). Within three days (i.e., 12-15 August), the maximum sustained wind speed for Irving increased from 50 to 90 kts. Typhoon Irving's equatorward outflow channel is typical of the upper level flow pattern found in intensifying tropical cyclones over the northwestern Pacific Ocean during mid-summer.

Equatorward outflow channels also frequently occur with northeast Pacific tropical cyclones. For example, Hurricane Andres, a tropical

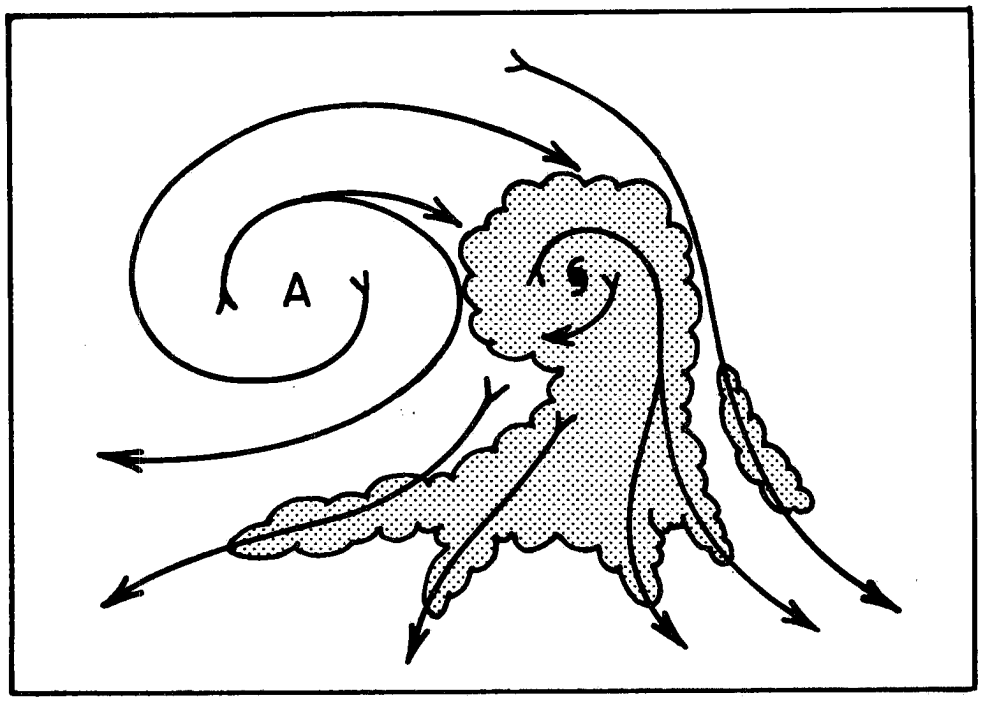


(a)

200 mb

(b)

13 AUGUST 00Z

Fig. 5a-c. Pattern $S_{Ee}$: Diagram (a) a single equatorward channel for a cyclone center to the east of the anticyclone center. Diagram (b) 200 mb flow for Typhoon Irving on 13 August 1979. Diagram (c) 0611 GMT 12 August 1979 DMSP display (Typhoon Irving). From 12 to 15 August the maximum sustained winds increased from 50 to 90 knots.

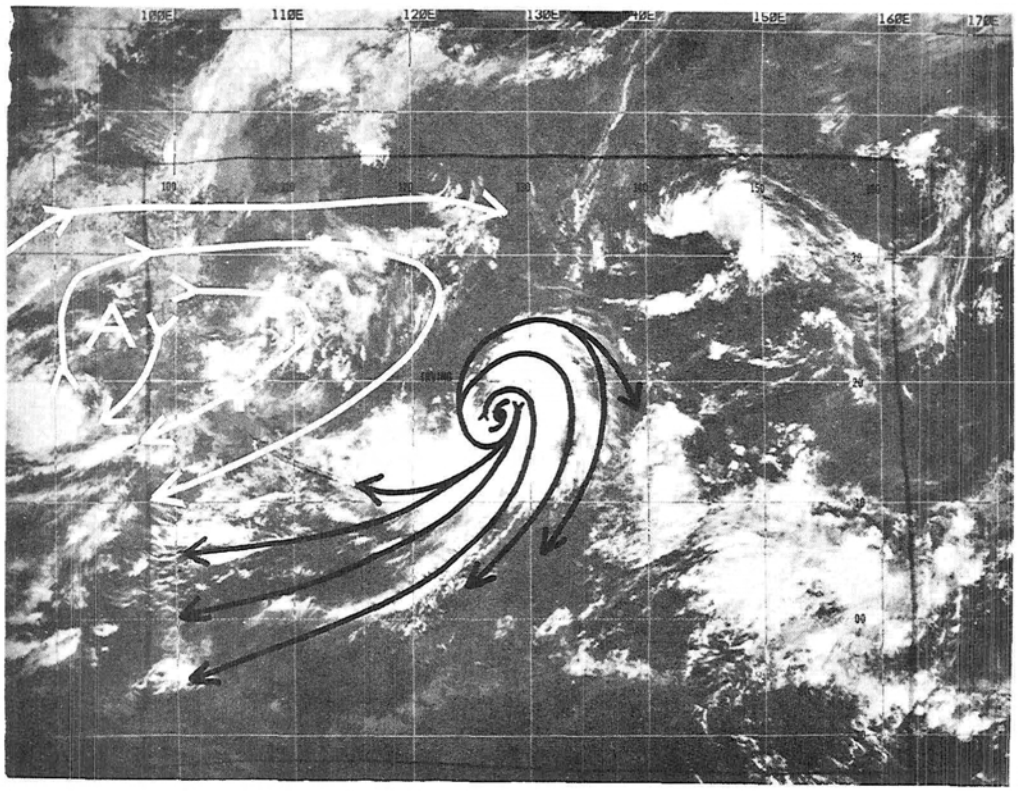


C)

Fig. 5c. Continued.

depression on 1 June, was located to the east of an upper level anticyclone that resulted in northeast air flow over the system (Fig. 6a). A corresponding area of equatorward outflow cirrus lines, which shows the existence of strong upper level outflow is seen in the satellite cloud picture (Fig. 6b). The maximum sustained wind speed of Andres increased from 30 kts to 65 kts in three days beginning on 1 June.

When a quasi-stationary 200 mb TUTT or shear line oriented northeast to southwest exists east of a tropical cyclone as is often the case in summer over the central North Pacific, the poleward cloud outflow from the cyclone often flows out to the northeast and then

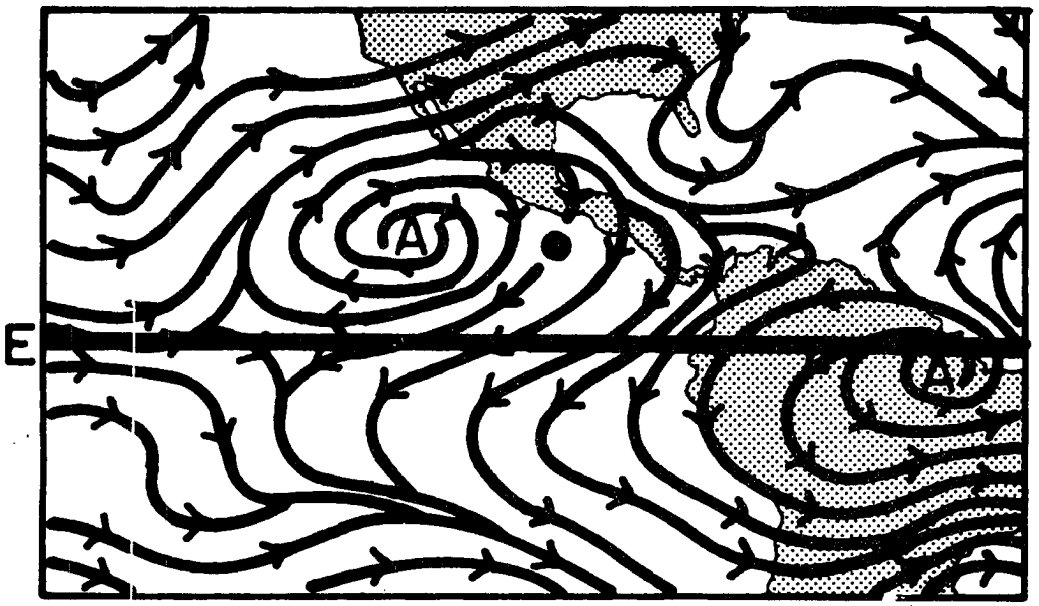


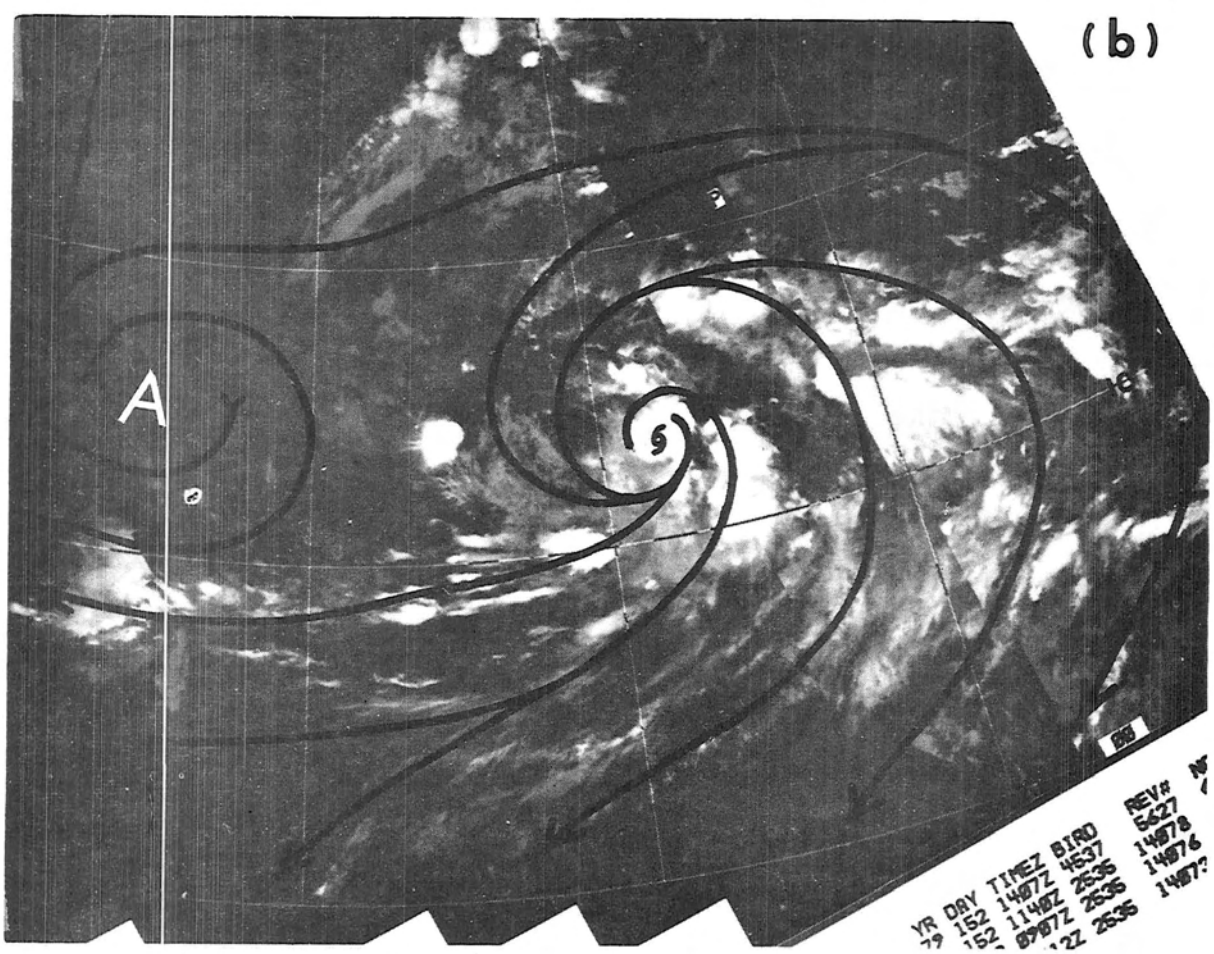


Fig. 6a-b. The typical case of pattern $S_{EC}$ in the north eastern Pacific. Diagram (a) 200 mb flow on 1 June 1979 for Hurricane Andres. Diagram (b) 1627 GMT 1 June 1979 DMSP display. From 1 to 3 June the maximum sustained winds increased from 30 to 65 kts.

curves around and reverses itself into a southeastward directed cloud band. Though such a pattern may appear to have a double-channel cloud outflow both cloud outflows are ultimately oriented only in an equatorward direction. This pattern is thus included in the $S_E$ category.

(2) Double-channel (D) Outflow.

Some tropical cyclone patterns have both poleward and equatorward outflow channels. These double channel outflow cyclones typically exhibit more rapid intensification. Based on the relative position of the cyclone center to the 200 mb anticyclone center, three sub-patterns of double channel outflow can be identified.

$D_W$. The tropical cyclone center is located to the west of an upper anticylone center (Fig. 7a). Take, for example, Hurricane Henri over the Atlantic. Its predecessor depression developed over the Caribbean Sea and to the west of an anticyclone and moved into the Gulf of Mexico on 15 September. It can be seen from Fig. 7b that the tropical depression at this time is located between north and south outflow patterns. These two outflow channels are also reflected in the satellite cloud picture (Fig. 7c). In two days from 15 to 17 September, the maximum sustained wind speed of this tropical cyclone (to be Hurricane Henri) increased from 25 to 75 kts.

$D_C$. The tropical cyclone center is located underneath the center of the anticyclone (Fig. 8a). For example the center of Typhoon Owen over the northwest Pacific coincided with that of an upper level anticyclone (Fig. 8b). Two channels of outflow on each side of the

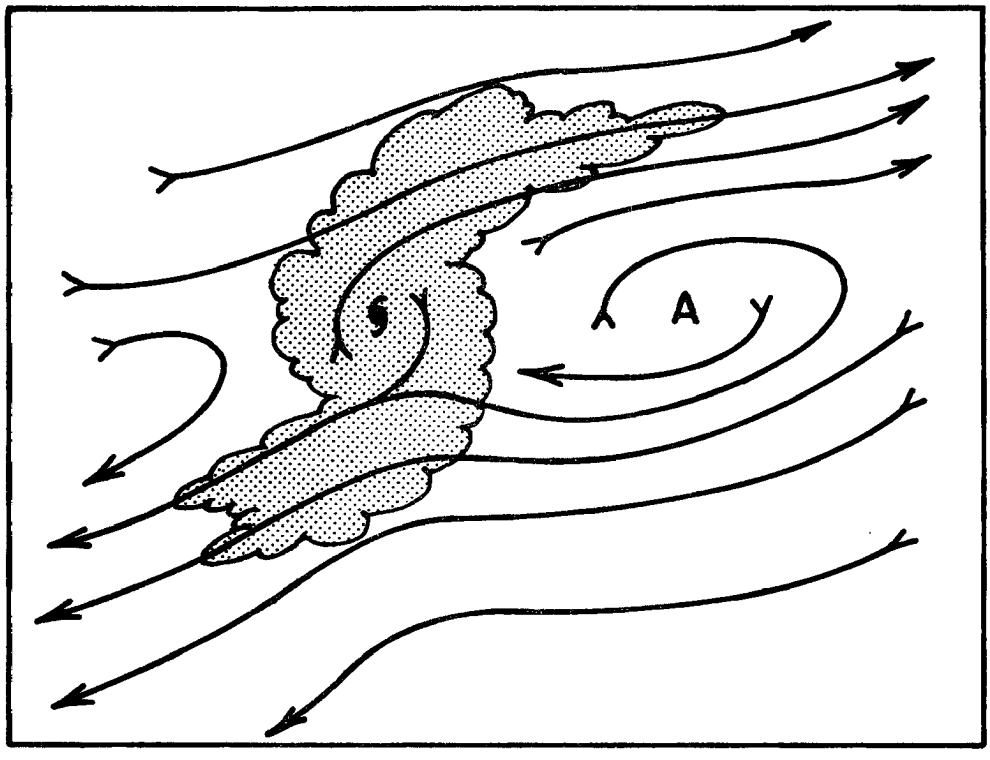


200 mb

16 SEPTEMBER 00Z

Fig. 7a-c. Pattern $D_W$: Typical example of a double outflow channel with the cyclone center to the west of the anticyclone center Diagram (a). Diagram (b) 200 mb 16 September 1979 of future Hurricane Henri. Diagram (c) 1621 GMT 16 September 1979 DMSP display of future Hurricane Henri. From 15 to 17 September the maximum winds increased from 25 to 75 kts.

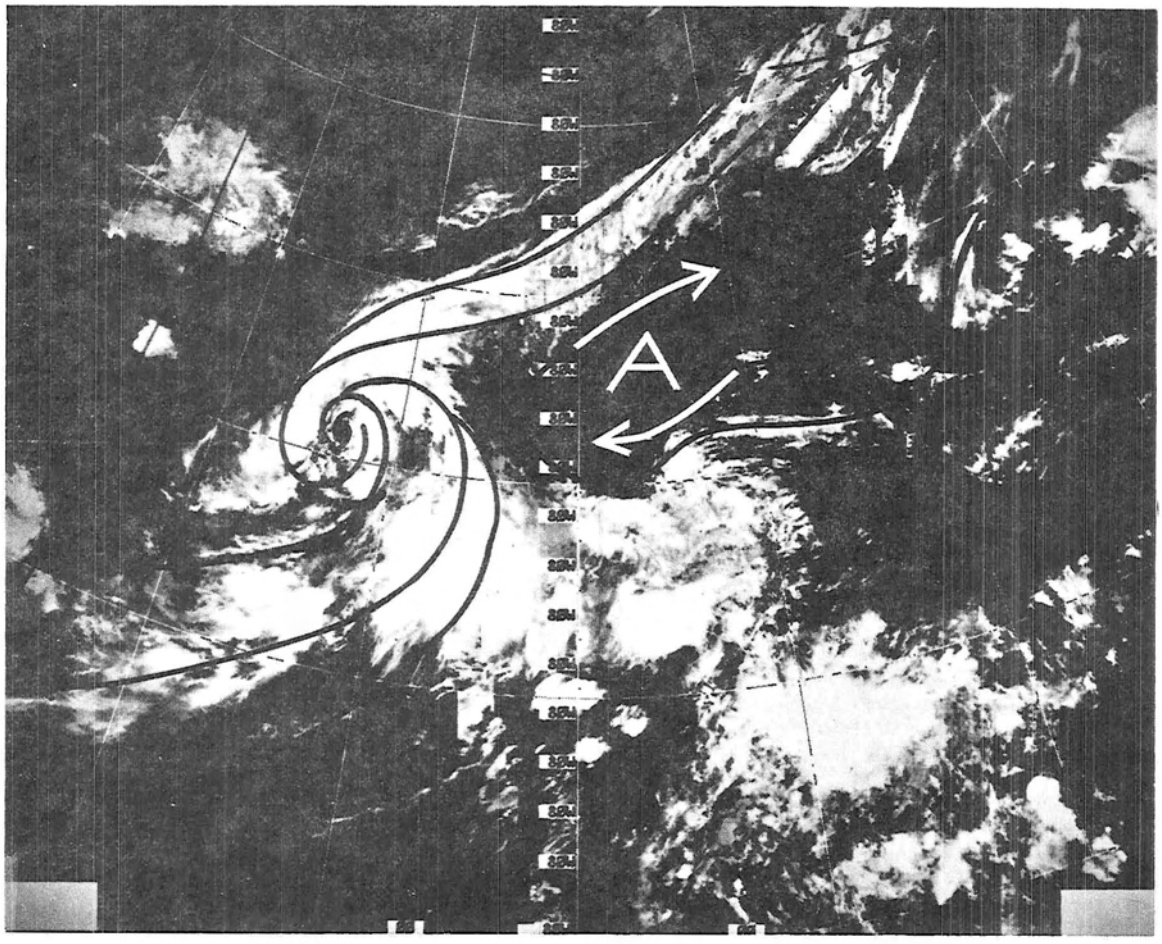


Fig. 7c. Continued.

anticyclone are directed poleward and equatorward. The satellite cloud picture shows corresponding poleward and equatorward cloud outflows (Fig. 8c). These double outflow patterns contributed to Owen's rapid intensification into a strong typhoon. The maximum sustained wind speed of Owen increased from 45 kts on 24 September to 110 kts on 26 September.

$\underline{D_e}$. The tropical cyclone center is located to the east of an upper level anticyclone (Fig. 9a). Super Typhoon Tip possessed these features during the stage of its very rapid development. Tip reached typhoon intensity on 9 October and moved to the east of an anticyclone over the

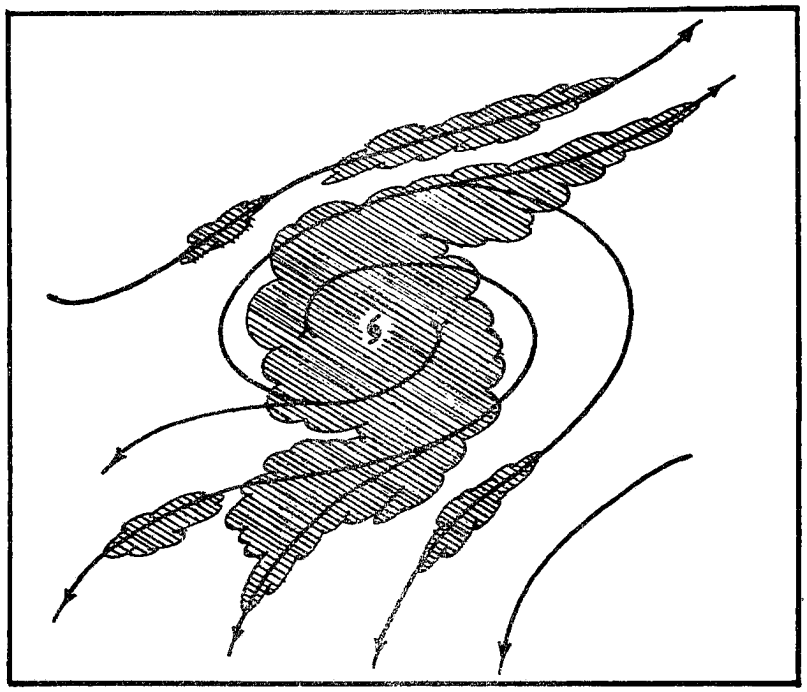

(a)

200 mb

(b)

25 SEPTEMBER 00Z

Fig. 8a-c. Pattern $D_c$: Idealized case of a double channel outflow pattern where the anticyclone center is located directly over the cyclone center, Diagram (a). Diagram (b) 200 mb flow pattern on 25 September 1979 for future Typhoon Owen. Diagram (c) 1652 GMT 25 September DMSP display of future Typhoon Owen. From 24 to 26 September the maximum winds increased from 45 to 110 kts.

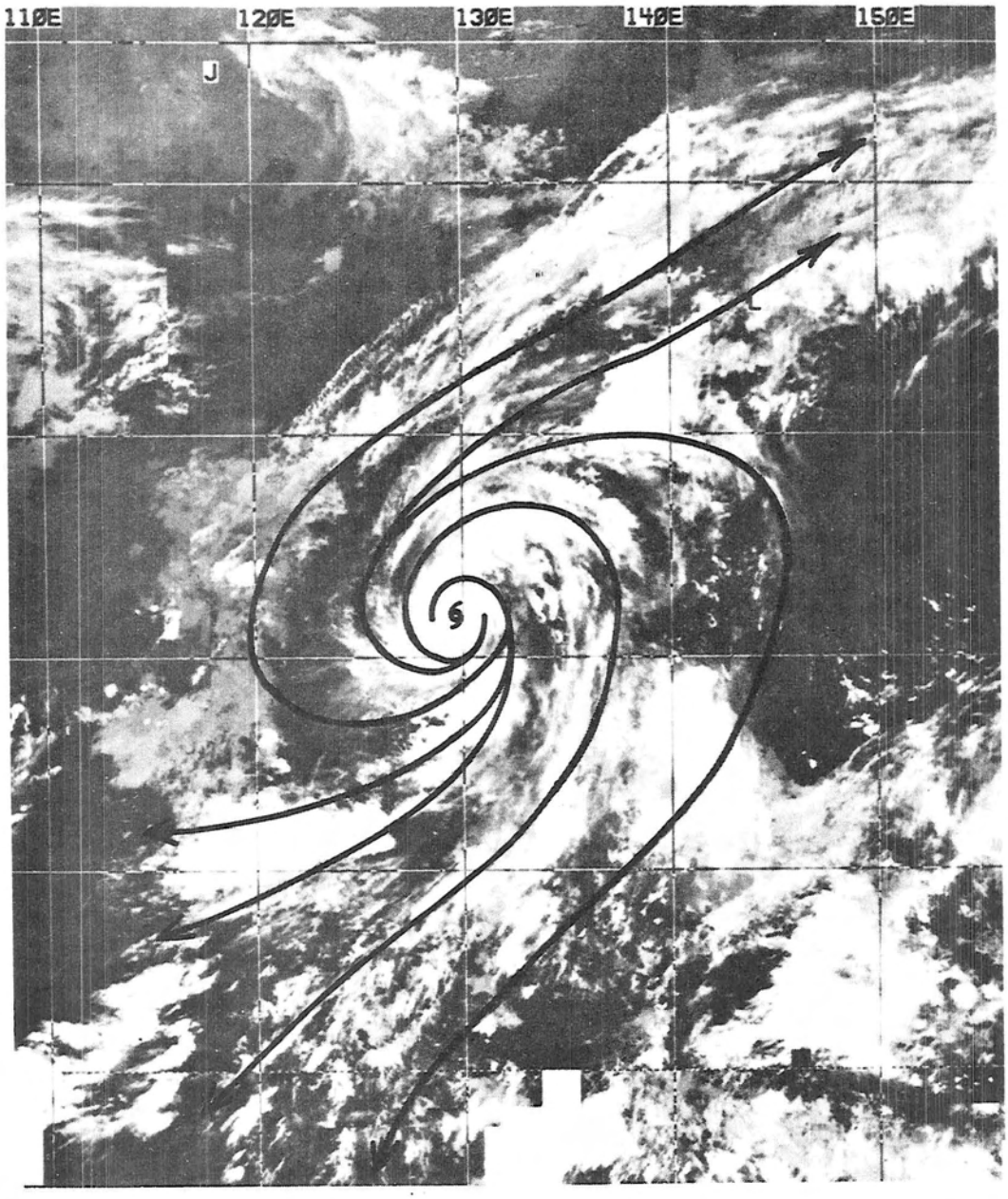


(C)

Fig. 8c. Continued.

South China Sea from 10 to 12 October. The southern and the northern flows of the anticyclone were thus linked up to form strong poleward and equatorward outflow channels (Fig. 9b). Tip eventually reached a central pressure of 870 mb which is the lowest pressure on record. Corresponding poleward and equatorward cloud outflow patterns appeared in the satellite cloud pictures (Fig. 9c). Upper level outflow from the cyclone appears very strong. In two days the maximum sustained wind speed of Tip increased from 80 to 165 kts. Such double channel outflow patterns often lead to very rapid and very deep cyclone intensification.

(3) No Outflow Channel (N).

When upper tropospheric environmental winds around the typical cyclone are weak or, though strong, do not form an outflow link with the tropical cyclone, then distinct outflow channels are not observed. The tropical cyclone (anticyclone over a cyclone) without a channel is reflected in satellite cloud pictures as a dense overcast above the cluster without distinct cloud outflow channels. The periphery of the dense overcast is often feathery with short lateral cirrus lines, indicating that the cyclone's upper level outflow is more azimuthally spread out over a broad area around the cyclone and is not concentrated into one or two outflow channels.

Depending on the relative position of the tropical cyclone center and the upper anticyclone center, the upper level stream field for a non-channel intensifying cyclone has one of the following four patterns.

Pattern $N_W$. The tropical cyclone center is located to the west of the center of an upper level anticyclone (Fig. 10a). For example in the Pacific, Tropical Storm Ken was located to the west of an upper

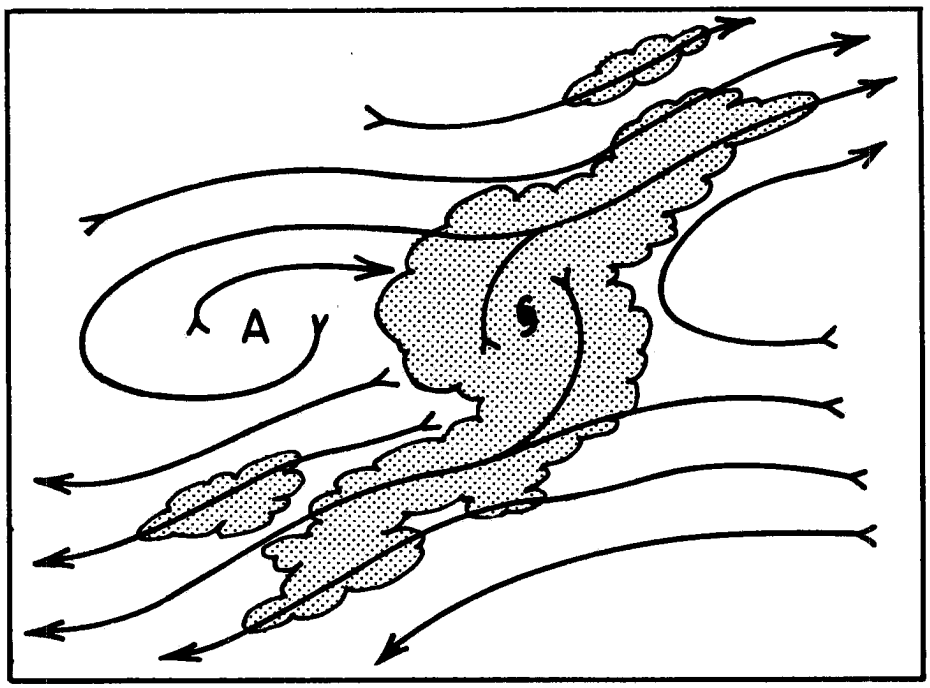


200 mb

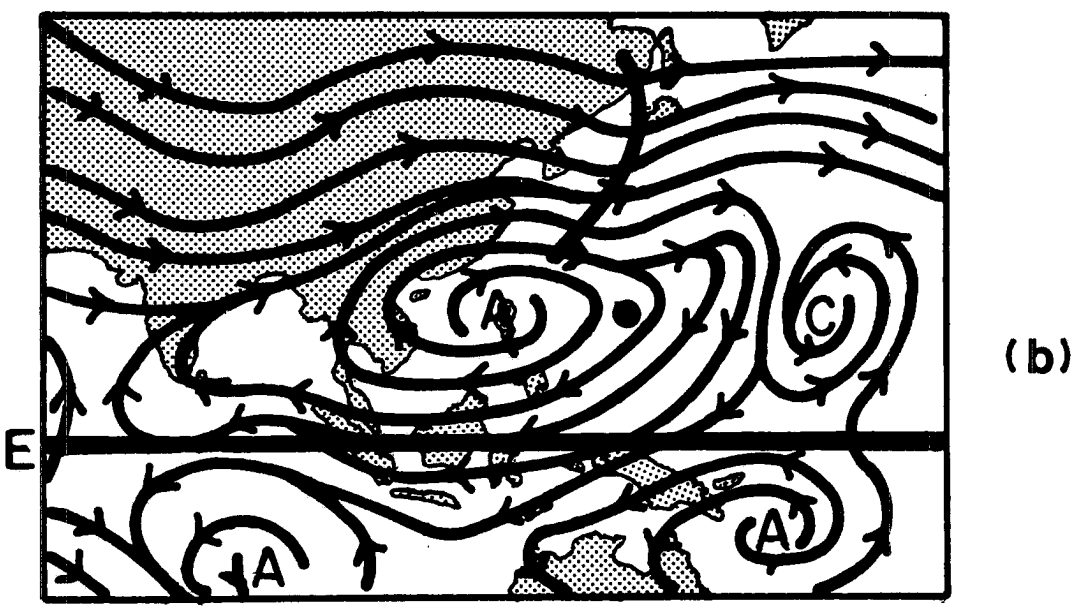


12 OCTOBER 00Z

Fig. 9a-c. Pattern $D_e$: Typical case of a double channel outflow with the cyclone center east of the anticyclone center, Diagram (a). Diagram (b), 200 mb 12 October 1979 for Typhoon Tip. Diagram (c) 1601 GMT 12 October 1979 DMSP display Typhoon Tip. From 10 to 12 October the maximum winds increased from 80 to 165 knots.

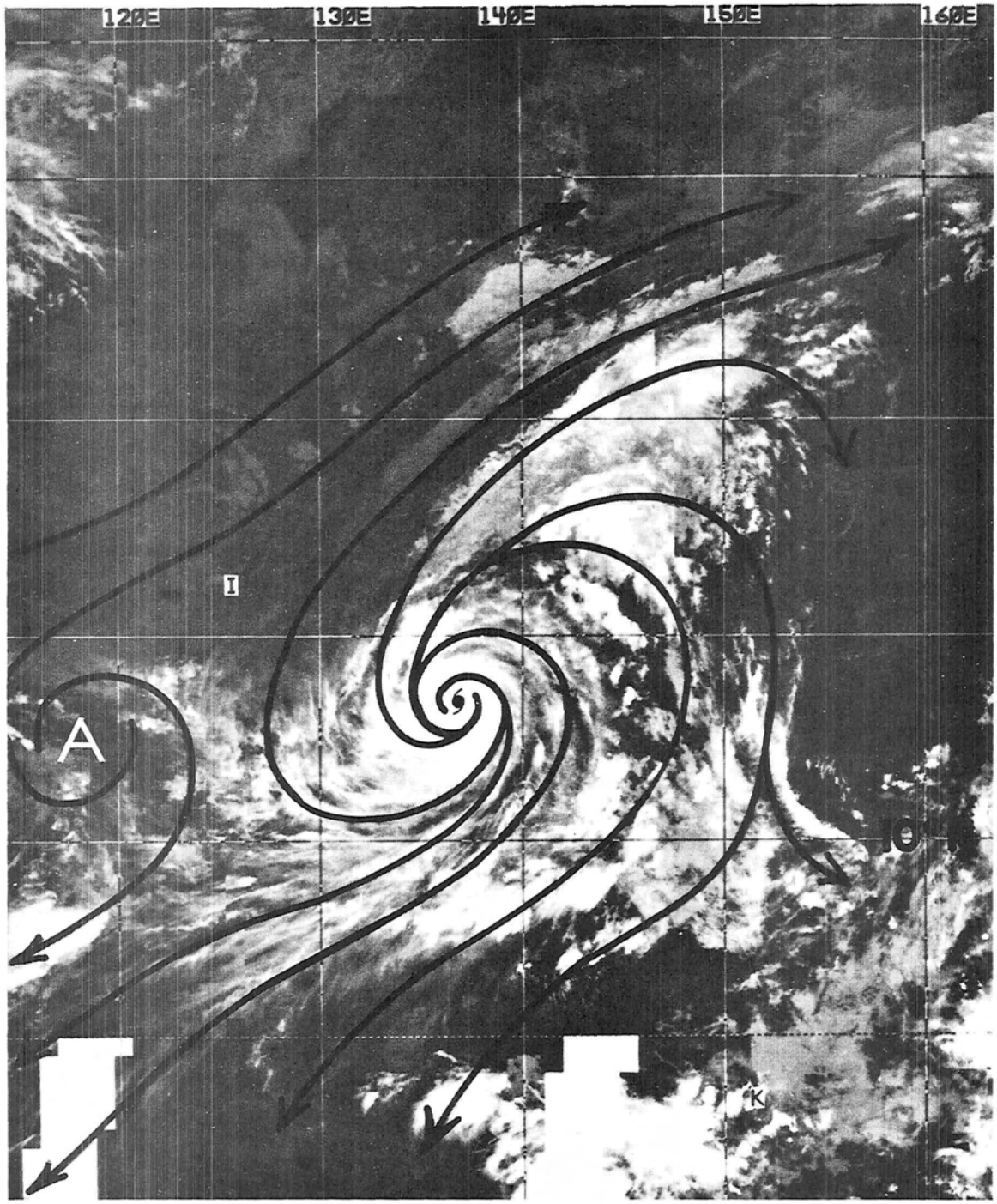


(c)

Fig. 9c. Continued.

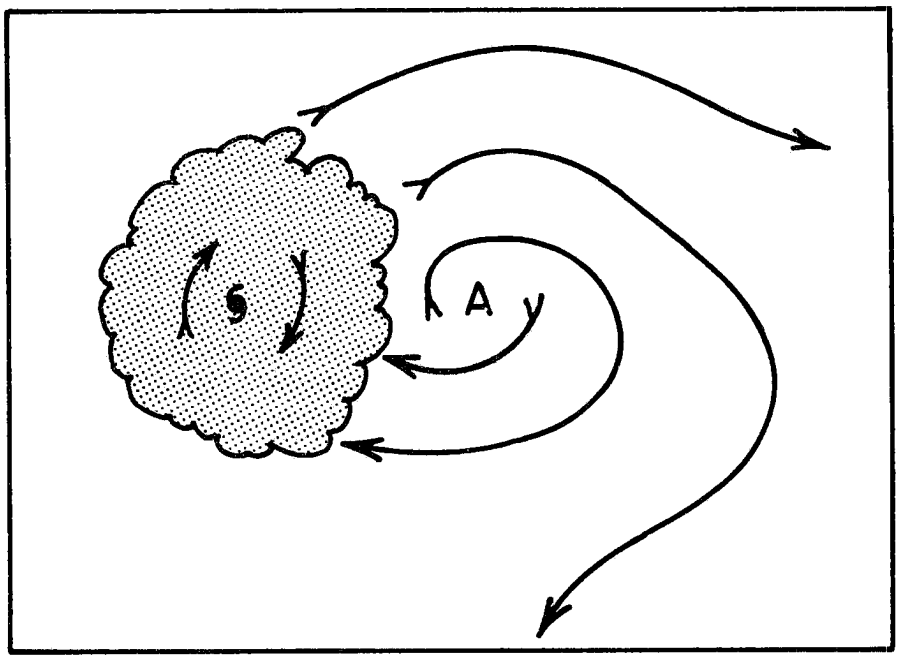


200 mb

2 SEPTEMBER 00Z

Fig. 10a-c. Pattern $N_W$: Idealized case with no outflow channel and with the cyclone center west of the anticyclone center, Diagram (a). Diagram (b), 200 mb 2 September 1979 wind for Tropical Storm Ken. Diagram (c) 0611 GMT 1 September 1979 DMSP display of Tropical Storm Ken. From 2 to 3 September the maximum winds increased from 35 to 60 kts.

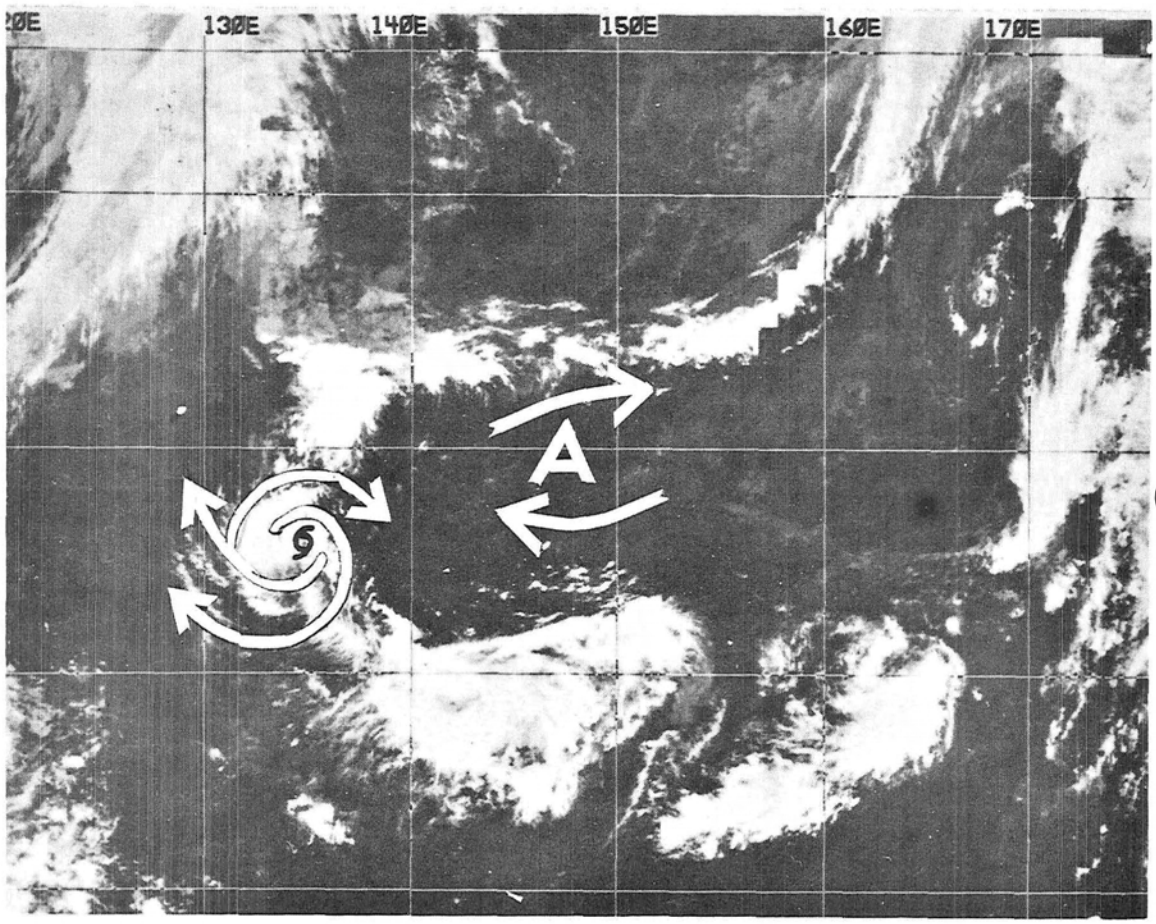


Fig. 10c. Continued.

anticyclone on 2 September. The winds in the central area of the anticyclone were weak, and the outflow channel was indistinct (Fig. 10b). In satellite imagery, Ken was reflected as a round cloud cluster without concentrated cloud outflow in one direction; to Ken's east was the cloud free region of the large scale anticyclone (Fig. 10c). However, spiral cirrus lines showed that divergence was strong at the upper level. Ken's maximum sustained wind speed increased from 35 kts on 2 September to 60 kts on 3 September.

Pattern $N_S$. The tropical cyclone center is located south of the upper anticyclone center. The cyclone center is under an east wind flow

south of the upper anticyclone (Fig. 11a). Figure 11b shows the upper level stream field of forming Typhoon Vera. After forming Verna moved continuously westward. On 3 November, its center moved south of the strong upper anticyclone. The cirrus lines around the cloud cluster (Fig. 11c) indicate strong but unconcentrated upper level outflow. A very large anticyclonic cloud free area is seen to the north of the storm's cloud shield. From 2 to 4 November, this system showed a dramatic increase in its maximum sustained wind speeds from 25 to 140 kts.

Pattern $N_c$. The tropical cyclone center is located directly over the center of the upper level anticyclone (Fig. 12a). For example, future Typhoon Lola was located directly under an upper anticyclone center on 4 September (Fig. 12b). The anticyclone was surrounded by a large cloud free moat region. Cloud outflow did not extend very far from the cluster system (Fig. 12c). However, marked clockwise outward spiral cirrus lines existed around the dense cloud cluster of this cyclone system (Fig. 12c). This indicates strong but unconcentrated upper level outflow. Within one day, from 4 to 5 September, the maximum sustained wind speed of Lola increased from 45 kts to 75 kts.

Pattern $N_e$. The tropical cyclone center is located to the east of an upper level anticyclone (Fig. 13a). For example, on 13 April northwest Pacific Tropical Storm Cecil was located to the east of an anticyclone over the South China Sea. This anticyclone had a weak upper level outflow (Fig. 13b), and satellite imagery showed an isolated dense cloud shield. No cloud outflow stretched equatorward (Fig. 13c).

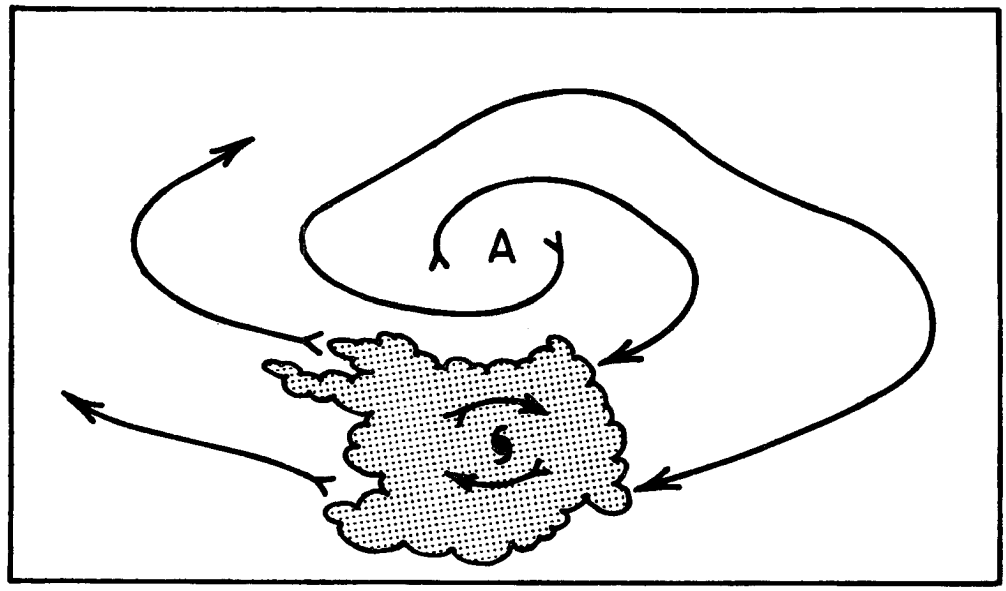


200 mb

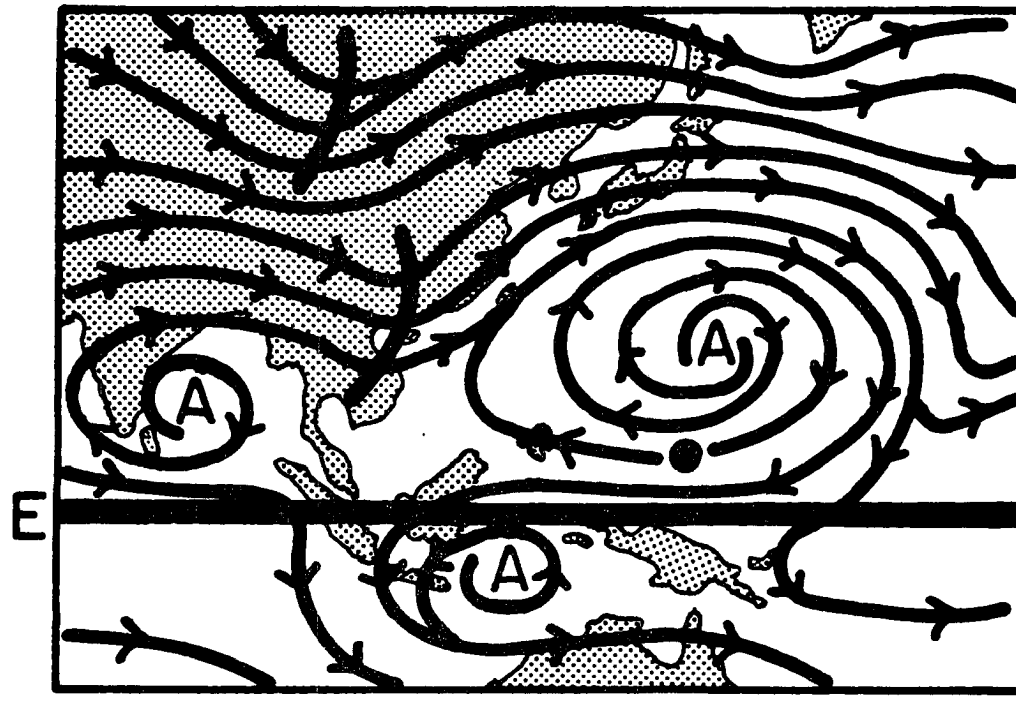


3 NOVEMBER 00Z

Fig. 11a-c. Pattern $N_S$: Idealized case with no outflow channel and with the cyclone center south of the anticyclone Diagram (a). Diagram (b), 200 mb 3 November 1979 for Typhoon Vera. Diagram (c) 1614 GMT 2 November 1979 DMSP display of Typhoon Vera. From 2 to 4 November the maximum winds increased from 25 to 140 kts.

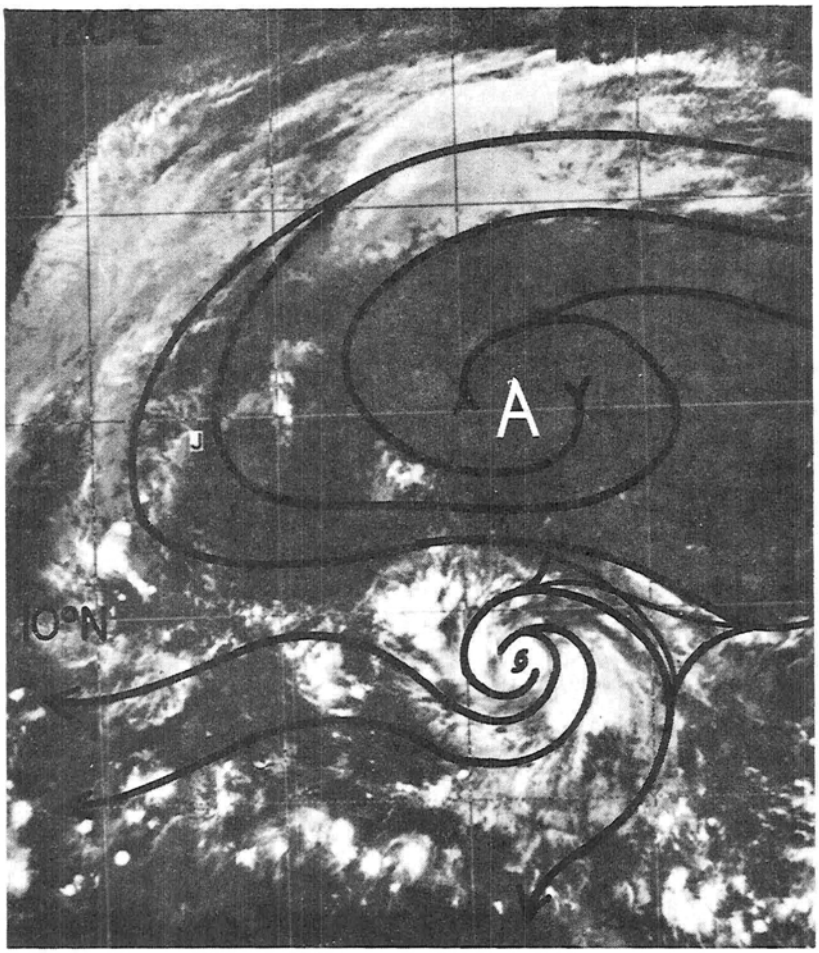


(c)

Fig. 11c. Continued.

However, divergence at the upper levels was obvious. The maximum sustained wind of tropical storm Cecil increased from 45 to 65 kts from the 13th to the 14th of April.

b. Basic Southern Hemisphere Patterns

In the Southern Hemisphere, upper level outflow patterns above tropical cyclones can be divided into only Single channel (S) and No Outflow Channel (N) categories. Very few double-channel outflow patterns occur in the Southern Hemisphere.

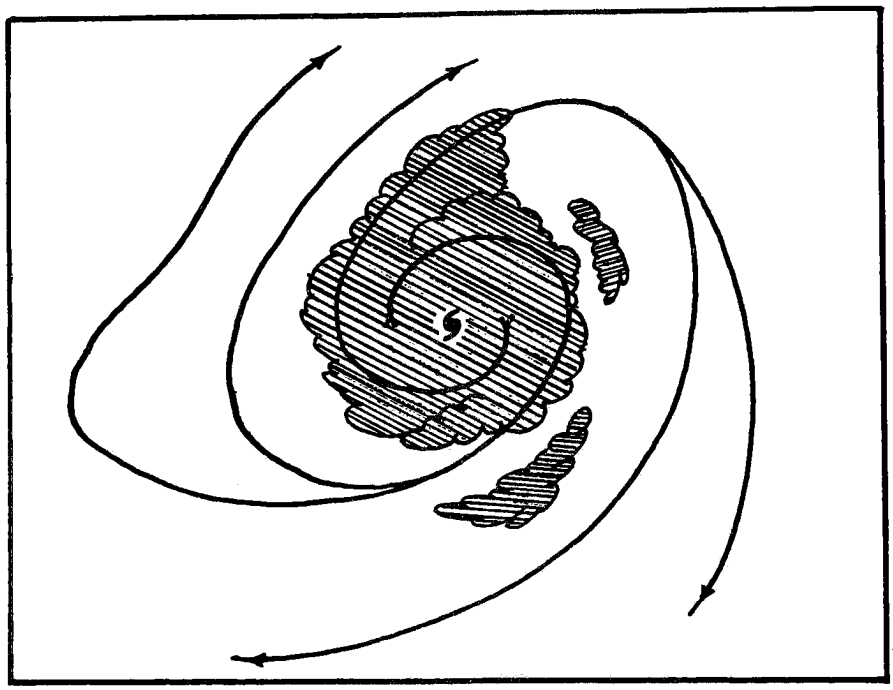

(a)

200 mb

(b)

4 SEPTEMBER 00Z

Fig. 12a-c. Pattern $N_c$: Idealized case with no outflow channel and with the anticyclone center directly over the cyclone center, Diagram (a). Diagram (b), 200 mb 4 September 1979 for Typhoon Lola. Diagram (c) 1601 GMT 4 September 1979 DMSP display of Typhoon Lola. From 4 to 5 September the maximum winds increased from 45 to 80 kts.

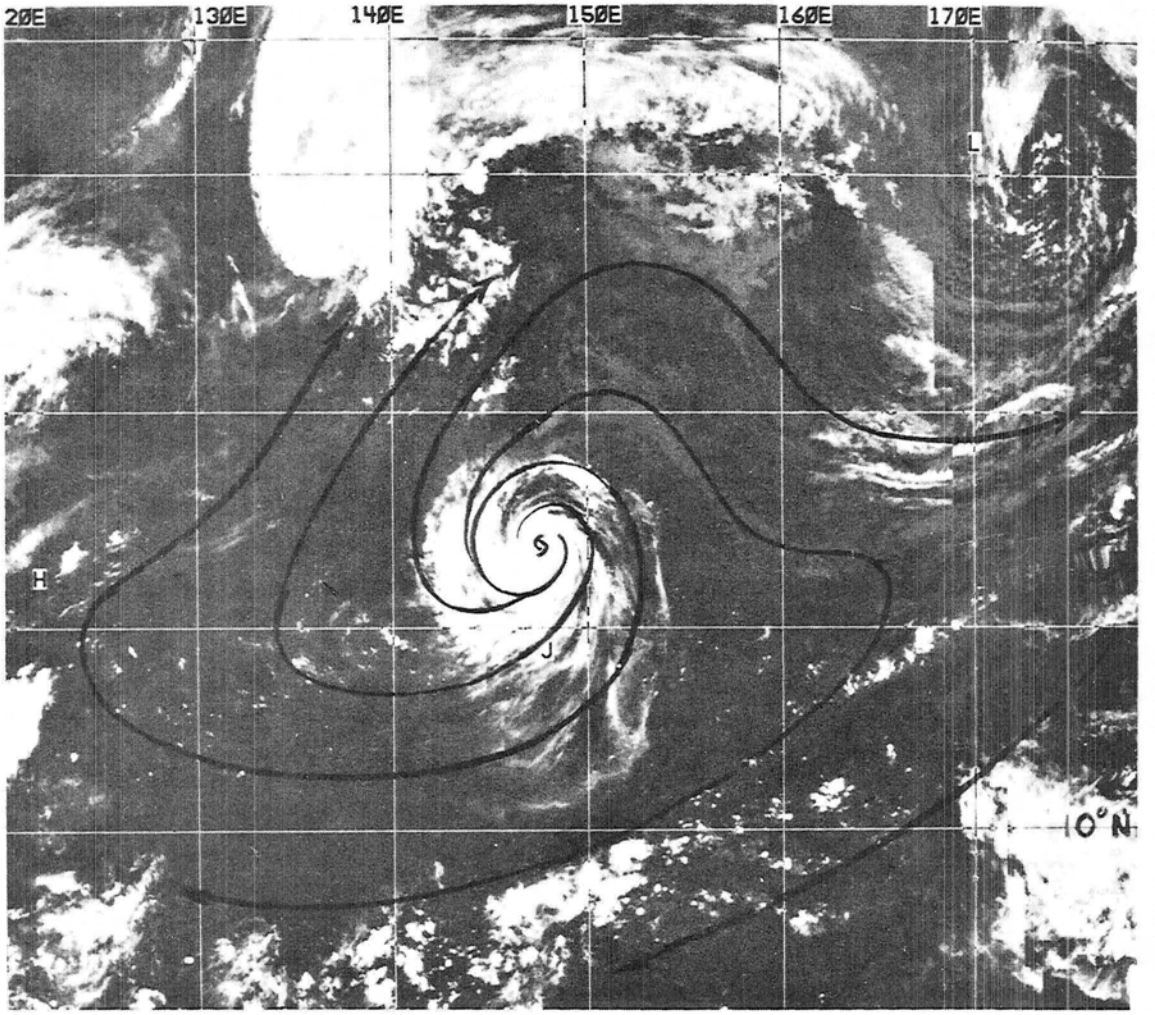


(c)

Fig. 12c. Continued.

(1) Single Channel (S).

The following two sub-patterns can be identified:

Pattern $S_{Pw}$. The usual outflow pattern with this type of intensification is seen in Fig. 14a. Tropical Storm Celine is an example. It was located in the South Indian Ocean on the poleward side of an upper anticyclone and had a poleward outflow channel (Fig. 14b).

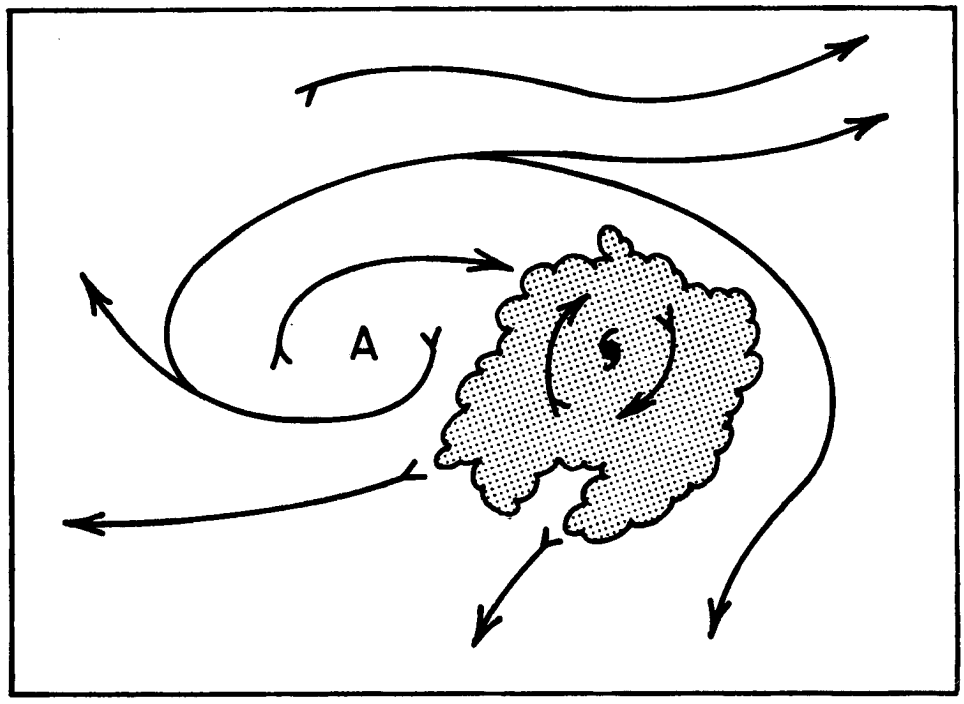


200 mb

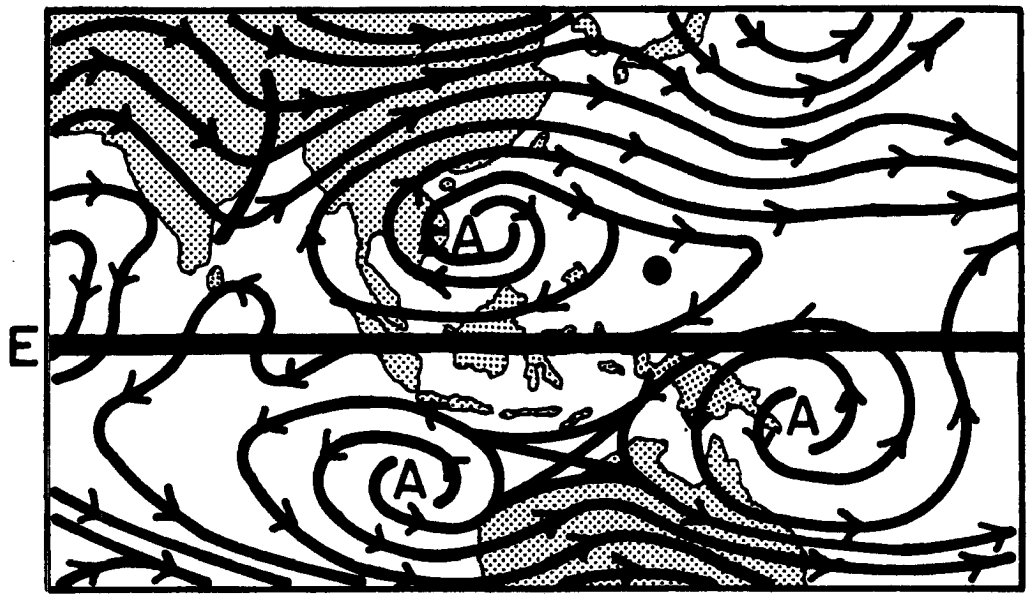


13 APRIL 00Z

Fig. 13a-c. Pattern $N_e$: Idealized case with no outflow channel and with the cyclone center east of the anticyclone center, Diagram (a). Diagram (b), 200 mb 13 April 1979 of Typhoon Cecil. Diagram (c) 1627 GMT 13 April 1979 DMSP display of Typhoon Cecil. From 13 to 14 April the maximum winds increased from 45 to 65 kts.

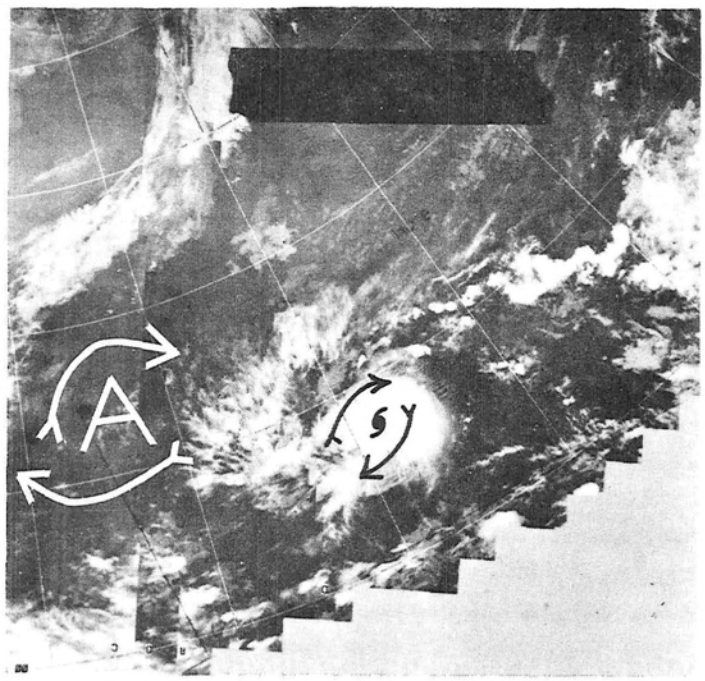


(C)

Fig. 13c. Continued.

Though an equatorward outflow was on the east side of the anticyclone, it did not link up with the tropical cyclone. There was no equatorward cloud outflow in the satellite imagery, but a marked poleward cloud outflow was evident (Fig. 14c). The T-number for Celine was T2 (~30 kts) on 3 February and T5 (~90 kts) on 7 February. The majority of tropical cyclone intensifications in the Southern Hemisphere are under such an a $S_{Pw}$ pattern.

Pattern $S_{Ec}$. This tropical storm has an equatorward outflow channel as portrayed in Fig. 15a. Figure 15b shows the 200 mb wind field for Tropical Storm Greta over the Gulf of Carpentaria adjacent to Australia. On 8 January Greta was located underneath a strong anticyclone. There was a strong equator-crossing flow between the anticyclone and the Northern Hemispheric equatorial ridge. The positioning of these anticyclones about Greta caused a substantial equatorward outflow channel (Fig. 15c). The satellite imagery also

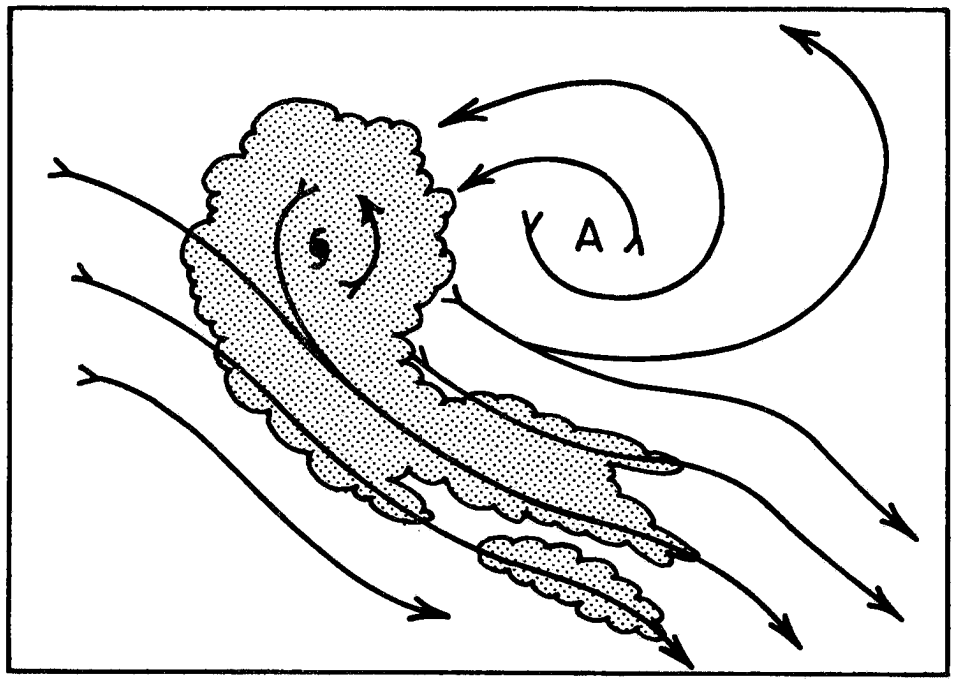


200 mb

5 FEBRUARY 00Z

Fig. 14a-c. Pattern $S_{PW}$: Typical case, Diagram (a). Diagram (b) 200 mb 5 February 1979 of Hurricane Celine. Diagram (c) 1600 GMT 5 February 1979 DMSP display of Hurricane Celine. From 3 to 7 February the intensity went from T2 (30 kts) to T5 (90 kts).

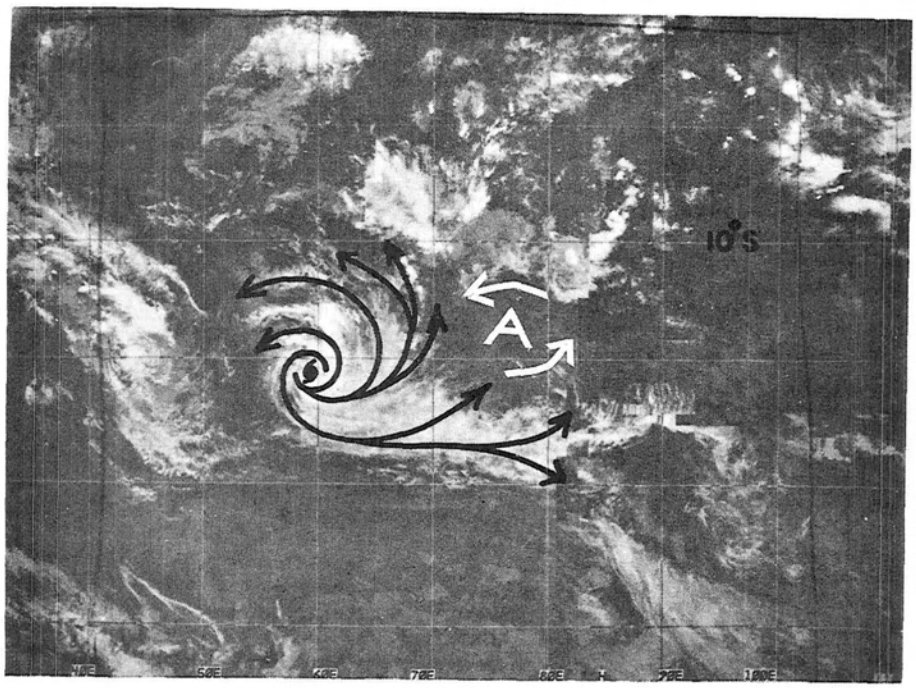


(c)

Fig. 14c. Continued.

shows a large area of equatorward cloud outflow on the equatorward side of Greta; the cirrus lines ran in the same direction as the streamlines (Fig. 15c). From 8 to 9 January, Greta developed from a tropical depression into a tropical storm.

A number of Southern Hemisphere tropical cyclones with equatorward outflow channels have their centers located east of an upper level anticyclones as Fig. 16a shows in idealized form. For example, the center of Tropical Storm Henry was located to the east of an upper anticyclone in the South Pacific on 31 January 1979. The storm was under an equatorward flowing south wind. It is believed to have formed the equatorward outflow cloud channel as seen in Fig. 16c. The upper level outflow appears rather strong. From 31 January to 3 February, Henry developed from a tropical depression into a tropical storm.

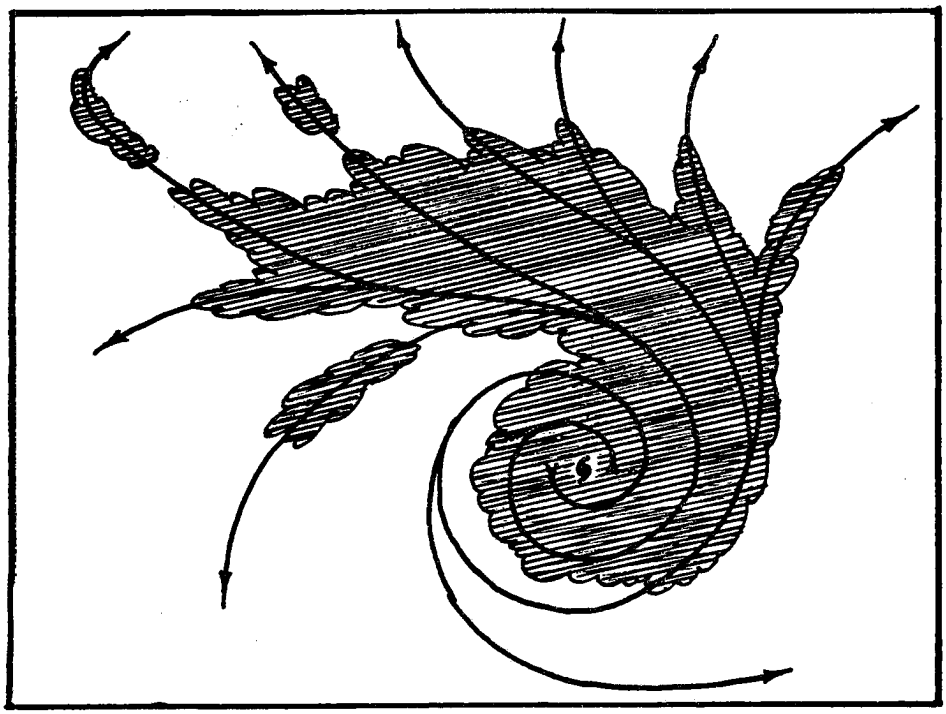

(a)

200 mb

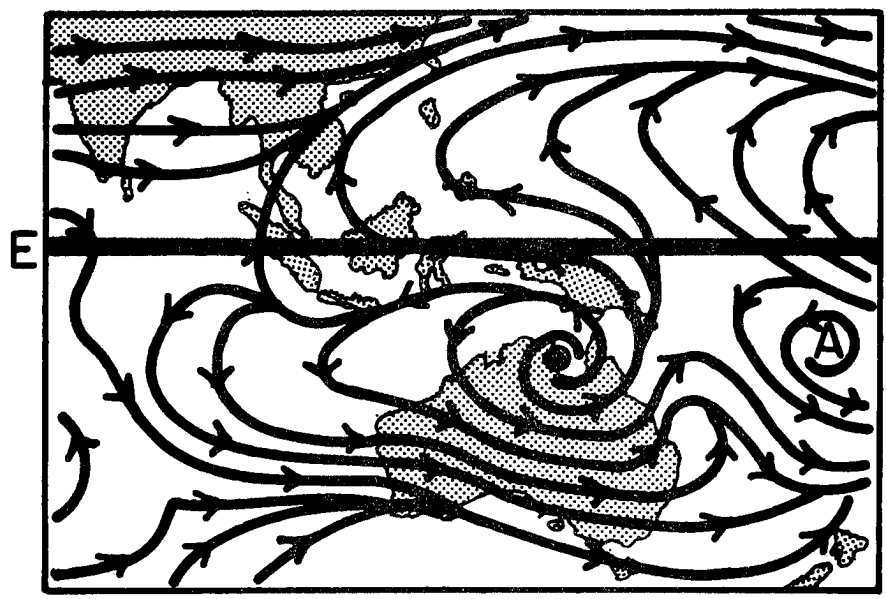


(b)

8 JANUARY 00Z

Fig. 15a-c. Pattern $S_{Ec}$: Typical case, Diagram (a). Diagram (b) 200 mb 8 January 1979 of Storm Greta. Diagram (c) 1601 GMT 8 January 1979 DMSP display of Tropical Storm Greta. Between 8 and 9 January this system went from a tropical depression to a tropical storm.

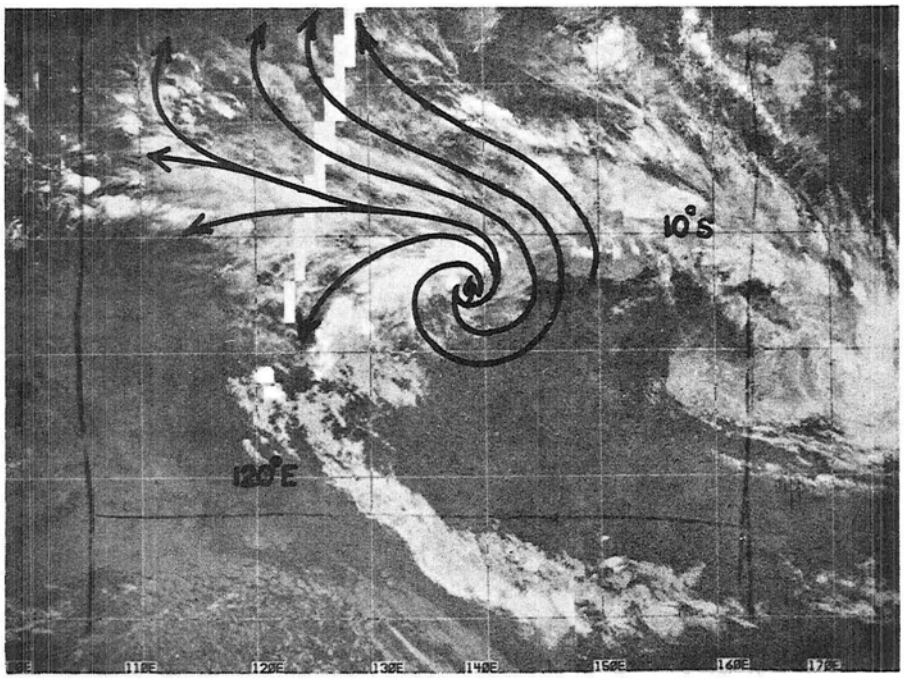


(c)

Fig. 15c. Continued.

(2) No Outflow Channel (N).

This category of tropical cyclones frequently occurs when the cyclone is on the equatorward-side of an anticyclone and when there is a weaker-wind region to the north of the upper anticyclone. Figure 17a shows the idealized picture. It is more difficult for outflow channels to form in this particular arrangement.

Figure 17b shows the upper level stream field when Tropical Cyclone Idylle was still a tropical depression over the South Indian Ocean. On 5 April the depression was in the weak east-wind region north of an anticyclone. It had no apparent wind nor cloud outflow. However, at the outer edge of the central dense overcast (Fig. 17c), there were marked counterclockwise outward spiraling cirrus lines. This indicates that strong divergence existed above the cyclone, but was just not

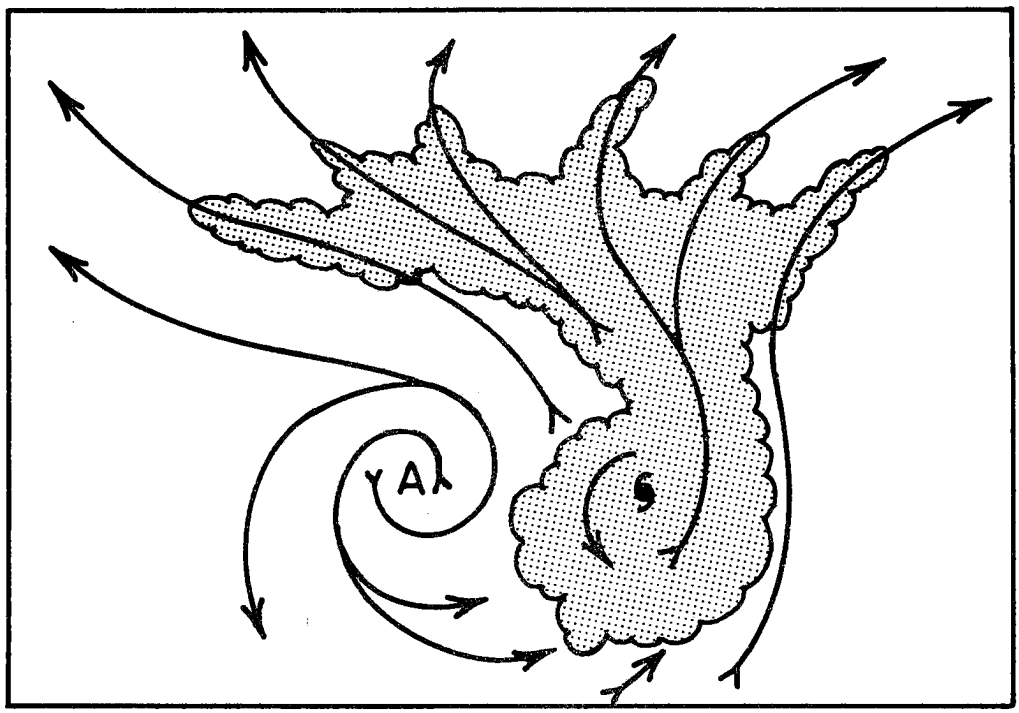


200 mb

31 JANUARY 00Z

Fig. 16a-c. Pattern $S_{Ee}$: Typical case, Diagram (a). Diagram (b) 200 mb 31 January 1979 of Storm Henry. Diagram (c) 1602 GMT 31 January 1979 DMSP display of Tropical Storm Henry. From 30 January to 3 February the system was upgraded from a tropical depression to a tropical storm.

Fig. 16c. Continued.

concentrated in any one quadrant. From 5 to 7 April, Idylle intensified from a tropical depression into a strong hurricane (T6 -- maximum winds 115 kts).

c. Synthesis of all Major Outflow Patterns

Figure 18 gives a summary of the variety of upper tropospheric outflow patterns which can occur with intensifying tropical cyclones of the Northern Hemisphere. Similar but inverted patterns occur in the Southern Hemisphere for a number of these cases.

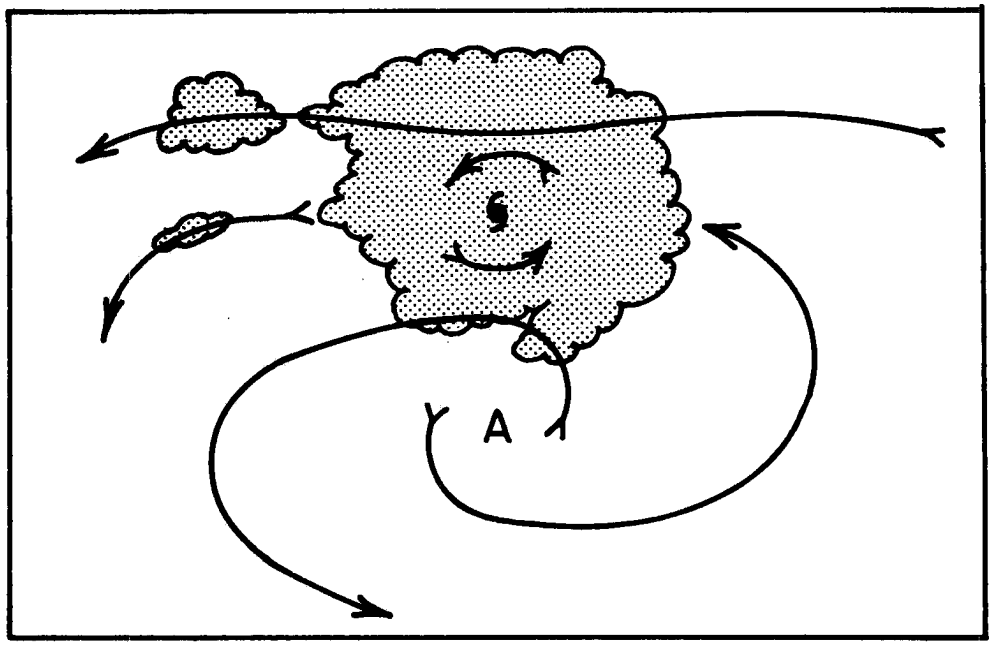


(a)

200 mb

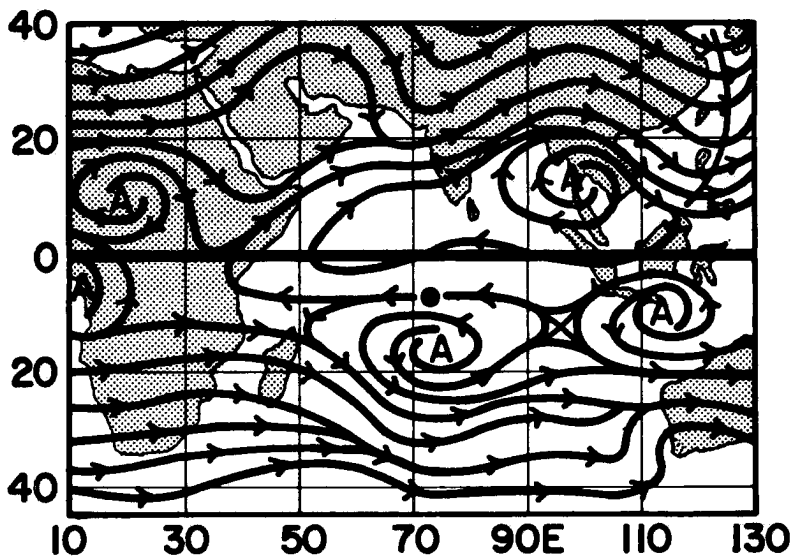


(b)

5 APRIL 00Z

Fig. 17a-c. Pattern N: Typical case, Diagram (a). Diagram (b) 200 mb 5 April 1979 of Tropical Cyclone Idylle. Diagram (c) 0613 GMT 6 April 1979 DMSP display of Hurricane Idylle. From 5 to 7 April the system intensified from a tropical depression to well above hurricane strength (T6 - 115 kts).

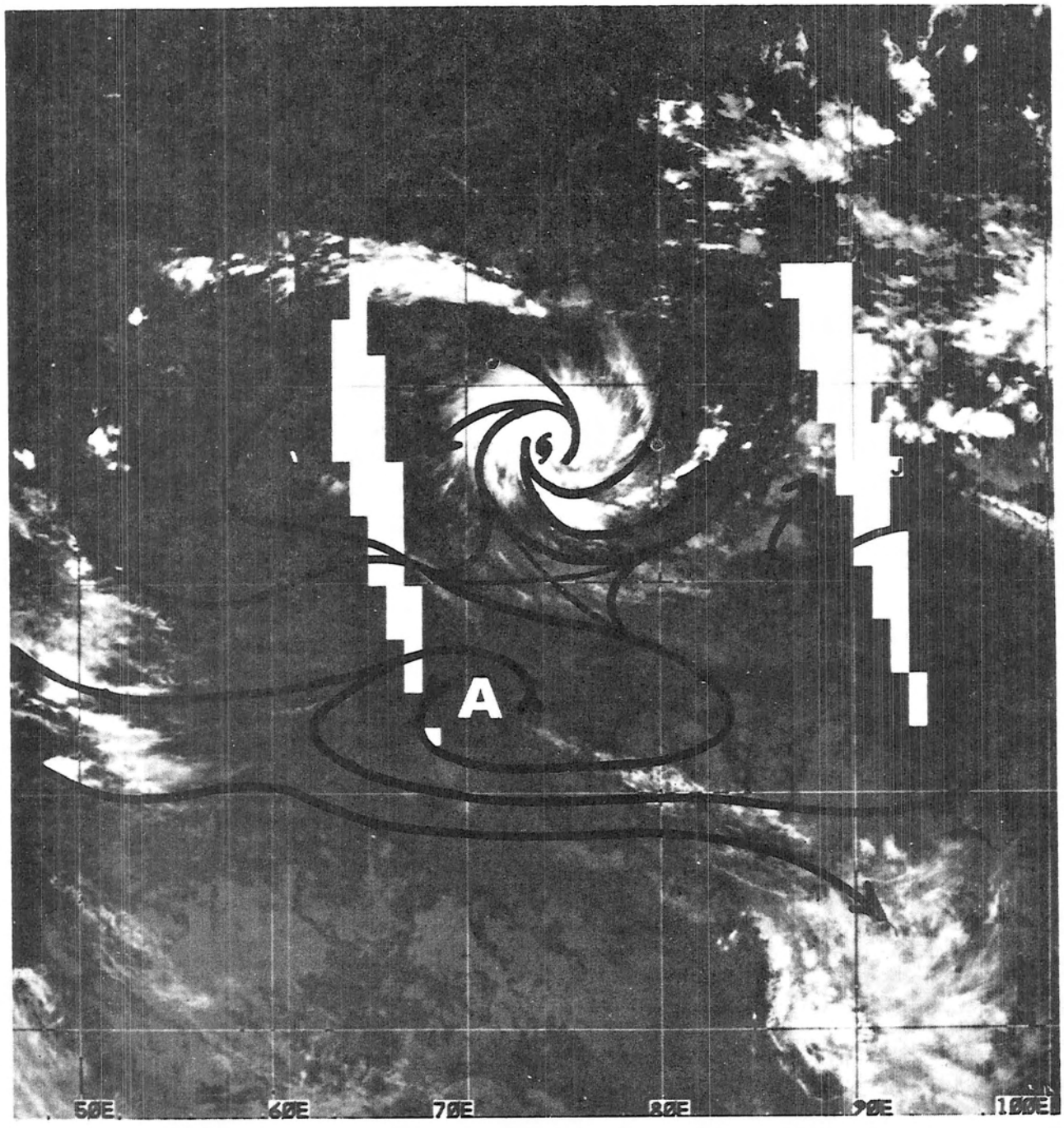


(c)

Fig. 17c. Continued.

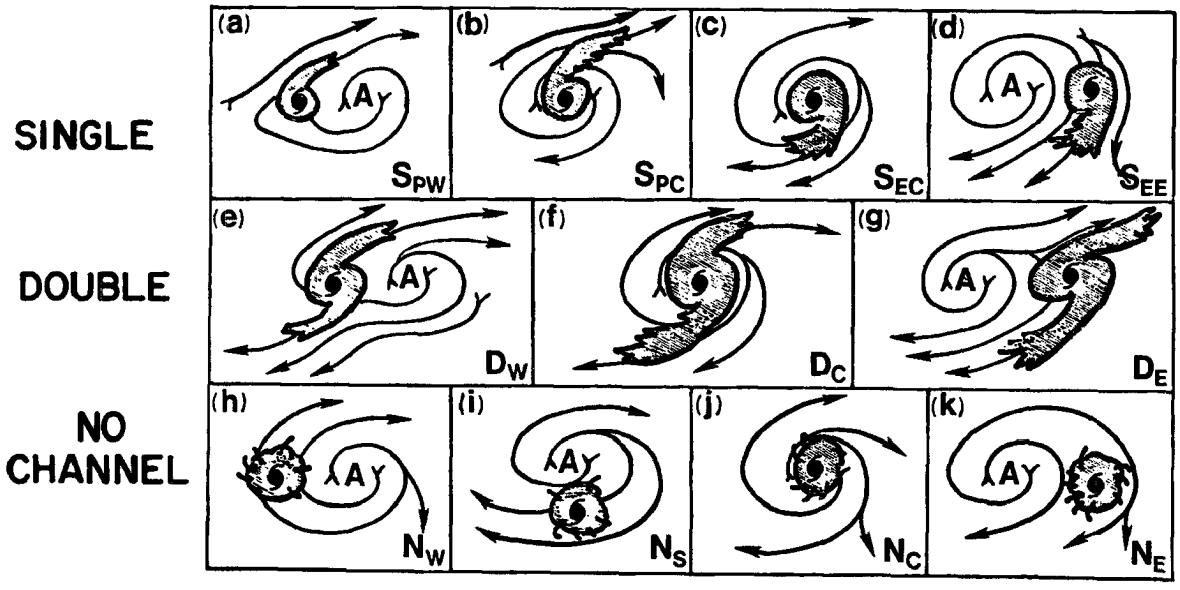


Fig. 18. Variety of outflow patterns associated with tropical cyclone intensification for Northern Hemisphere cases.

d. Intensity Changes Associated with Different Outflow Patterns

These different outflow patterns can have different effects on the magnitude of tropical cyclone intensity change. Statistical analysis of the average intensifying rates of many of these cases was also made. Intensifying rates are expressed in average wind speed increase per 24 hours as reported by reconnaissance aircraft or as inferred from satellite estimates of the Dvorak scheme (1975). A number of these averages are taken over multi-days of intensification. Figure 19 shows results.

Double-channel outflows are associated with the fastest intensification rates. For single-channel patterns, equatorial outflow channels on average lead to faster intensification rates than do poleward channel outflows.

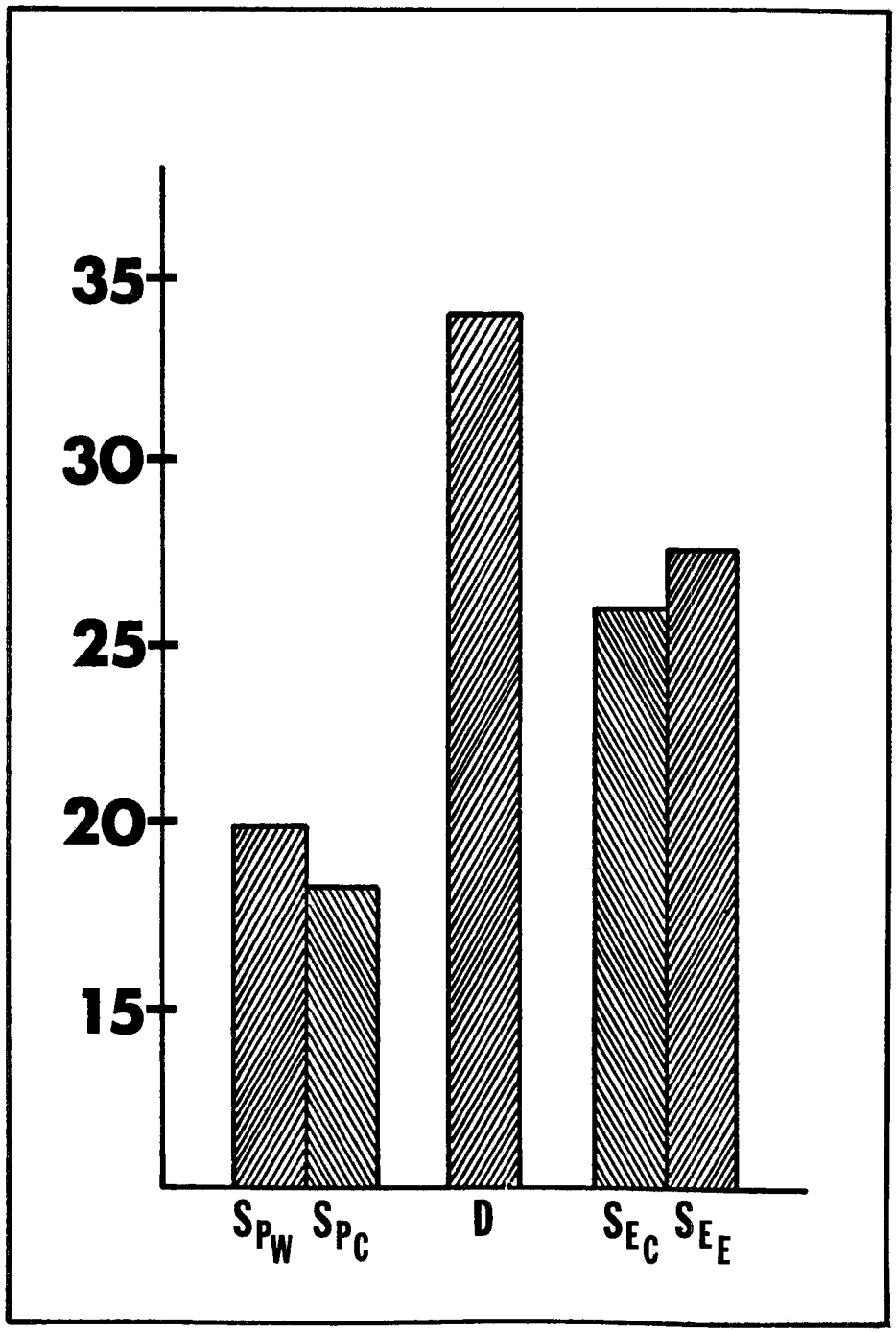


Fig. 19. Average maximum wind increase KTS/6 hr. associated with different outflow patterns.

## 4. Types of Synoptic Flow Patterns which Enhance Outflow Channel Change

The different types of outflow channels associated with tropical cyclone intensification as discussed in the previous Chapter lead one to pay close attention to changes in a cyclone's surrounding environmental upper tropospheric flow conditions which can bring about enhancements or reductions in such outflow channels. This, perhaps, can lead to some improved techniques for the forecasting of cyclone intensity change.

There are three basic types of environmental influences to be watched for:

a) Opposite hemisphere influences

b) Middle latitude upper trough and/or westerly wind influence on the poleward side of the cyclone such as a Tropical Upper Tropospheric Trough (TUTT)

c) A combination of process (a) and (b)

### a) Opposite-hemispheric Influences

An upper level anticyclone at low latitude on the opposite side of the equator can have an important influence on the equatorial outflow of a tropical cyclone existing across the equator from it.

#### (1) Impact of the Southern Hemisphere (S.H.) on the Northern Hemisphere (N.H.)

A strong equatorial upper level anticyclone in the Southern Hemisphere (S.H.) is extremely favorable for enhancing the equatorward outflow of a Northern Hemisphere (N.H.) tropical cyclone and vice versa. In particular, when a low latitude anticyclone of the opposite hemisphere increases its strength or builds from west to east into a position just equatorward of the tropical cyclone, a general

strengthening of the equatorward outflow channel of the tropical cyclone is frequently observed. This often leads to an intensification of the cyclone.

On 16 August, future Super Typhoon Judy (in the northwest Pacific) was still a tropical depression with light easterly 200 mb wind over it and weak appearing outflow (Fig. 20a). During 17-19 August, a low latitude anticyclone in the S.H. extended westward and began to build over Northern Australia (Fig. 20b, 20c). This process dramatically changed the equatorial outflow circulation above Judy. Equatorward of the cyclone the wind changed from being weakly from the east to being strongly from the northeast. A strong equatorward outflow channel was established during the 16th to 17th of August. Following the enhancement of the equatorward outflow, the tropical cyclone dramatically intensified from the 17th to the 20th (Fig. 21). A tropical storm was formed by the 17 August, and by 20 August the maximum sustained wind speed of Typhoon Judy reached their then peak value of 135 kts.

Figure 22 gives another example of this type of cross-equator enhancement for the northeast Pacific. Hurricane Andres was in a tropical depression phase during 31 May - 1 June (Fig. 22a). An equatorial anticyclone over South America moved westward and strengthened from the 31 May to the 3rd of June. Its approach to the south of the tropical depression led to the generation of an equatorward outflow channel for the tropical depression (Fig. 22b, 22c). During the course of the anticyclone's intensification and westward movement tropical depression Andres experienced a continued intensification. Its

200 mb

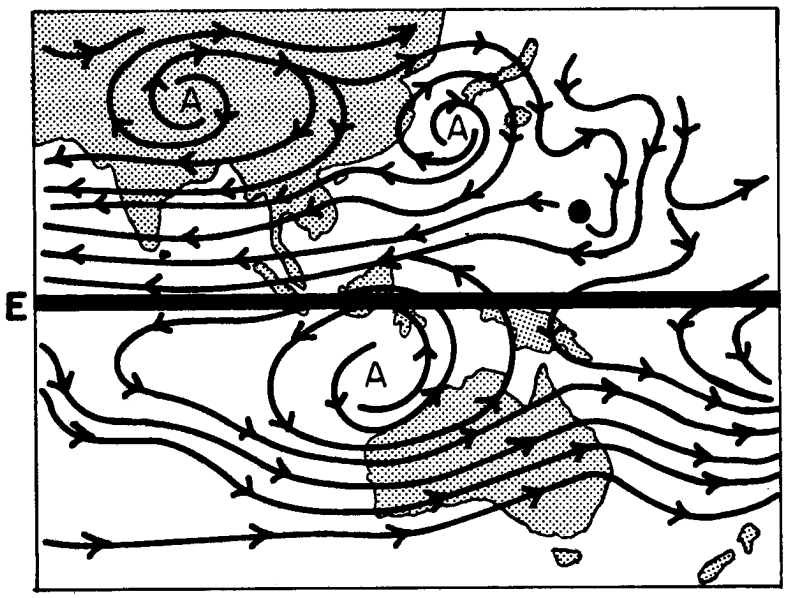


(a)

16 AUGUST 00Z

200 mb

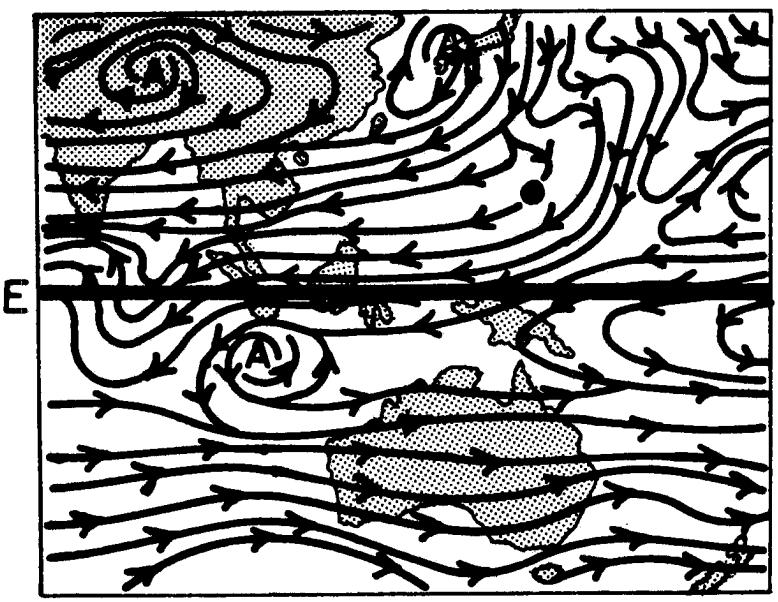


(b)

17 AUGUST 00Z

Fig. 20a-c. Illustration of how a Northern Hemisphere tropical cyclone (Judy) with an equatorward outflow channel intensified when an anticyclone over the opposite hemisphere moved close to it. From 17 to 19 August Judy's maximum sustained wind increased from 50 to 120 kts.

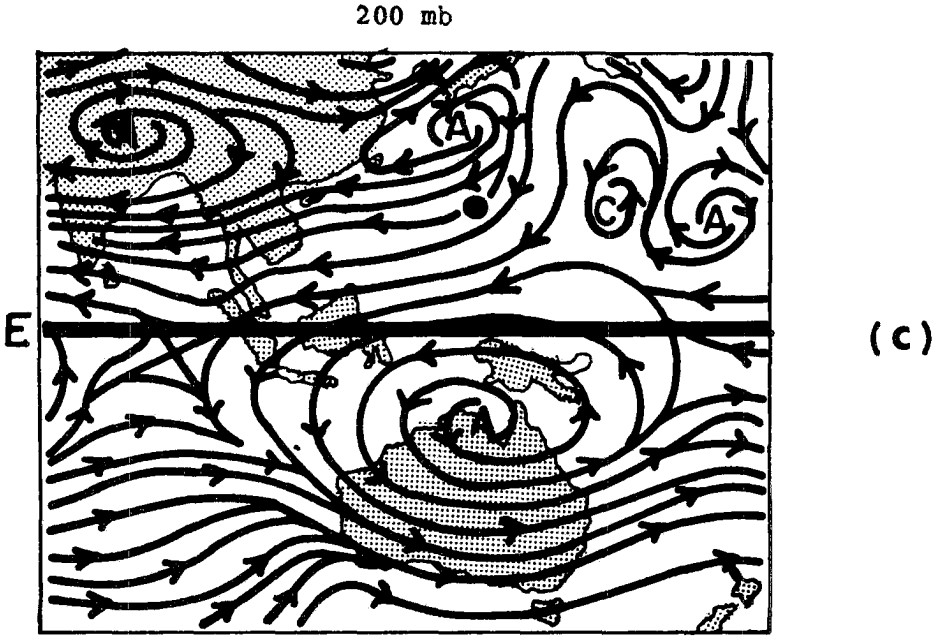


Fig. 20c. Continued.

maximum sustained wind speed increasing from 30 kts on 2 June to 85 kts on 4 June.

An opposite hemisphere anticyclone with the above-mentioned characteristics can also contribute to enhancing some non-equatorial 200 mb outflow. An example is shown in Fig. 23. Hurricane Ignacio was at tropical depression stage on 24 October. A weak low latitude S.H. anticyclone was located to its south (Fig. 23a). From 24 to 26 October, the anticyclone began to build rapidly. This acted to enhance the outflow of the cyclone to its west and contributed, we believe, to the development of this system into a strong hurricane (Fig. 23b). From 26-28 October, the maximum sustained wind speed of Ignacio (as measured by the Dvorak scheme increased from 45 kts to 120 kts.

In the opposite sense when a S.H. upper level equatorial anticyclone weakens and/or moves away from a tropical system, conditions

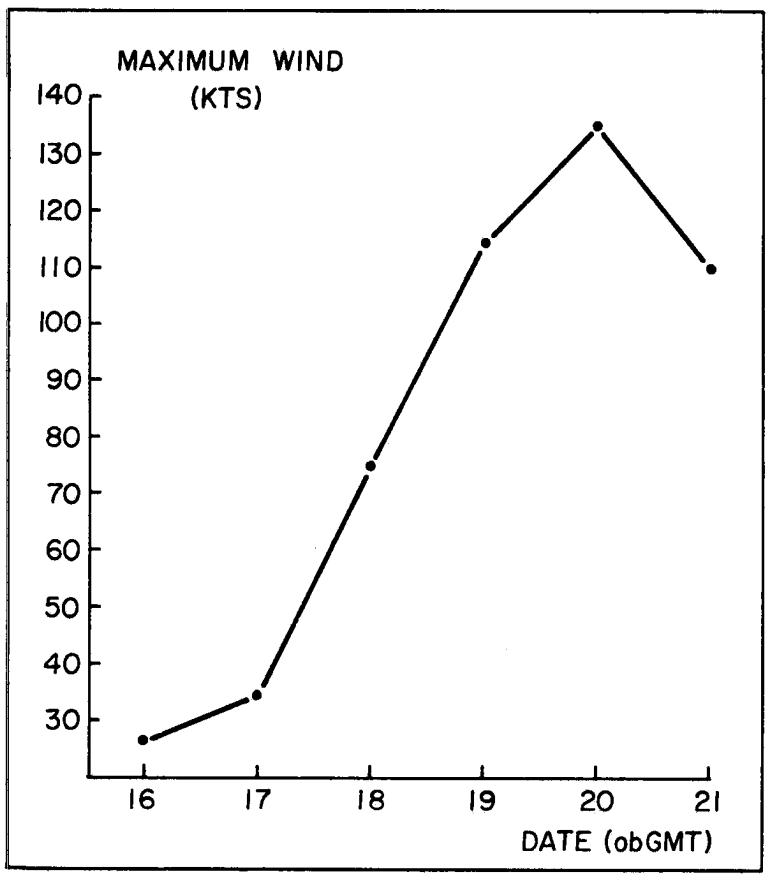


Fig. 21. Intensity (maximum wind in kts) of Typhoon Judy in the period 16-21 August.

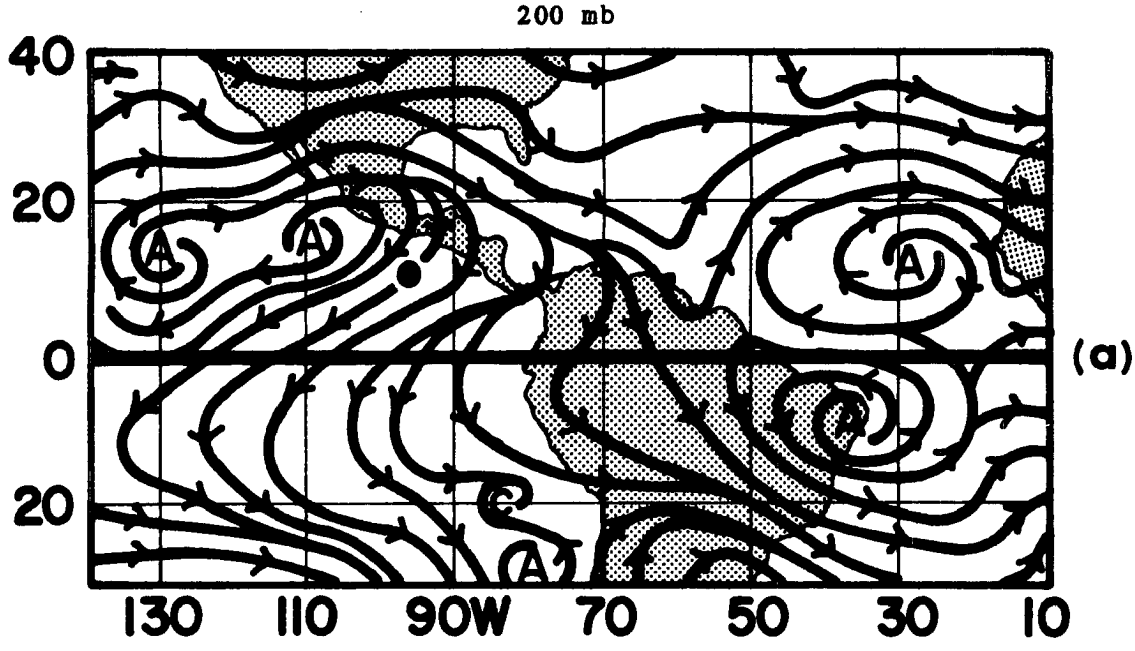


31 MAY 00Z

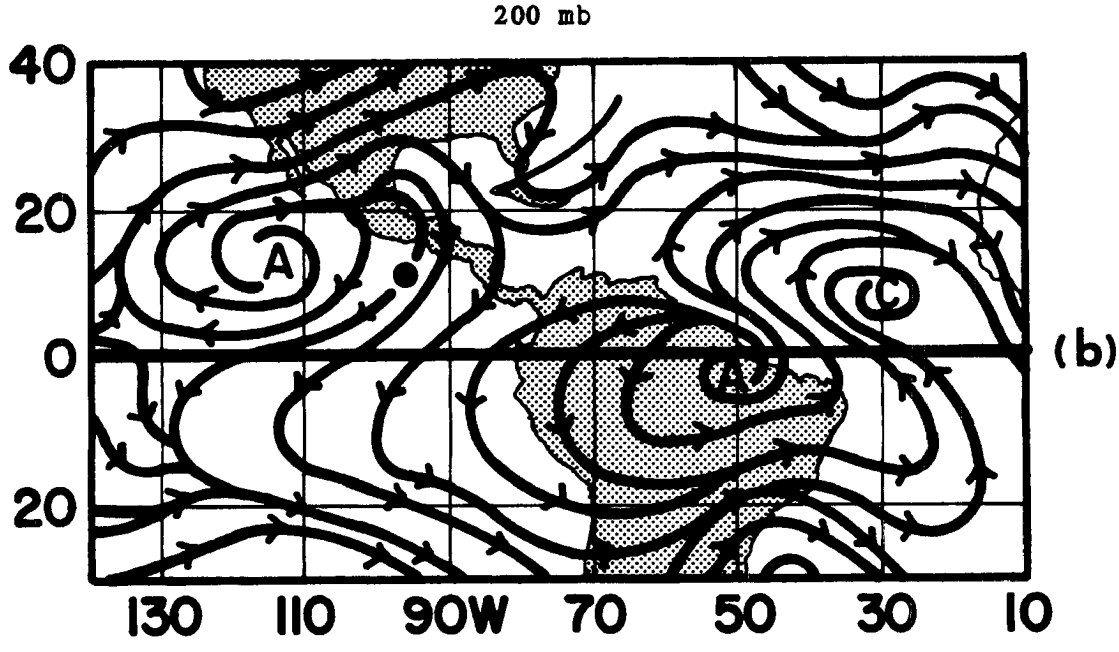


1 JUNE 00Z

Fig. 22a-c. An east Pacific tropical cyclone (Andres) with an equatorward outflow channel intensified when an anticyclone of the southern hemisphere moved close to it. From 2 to 4 June Andres maximum sustained wind increased from 30 to 85 kts.

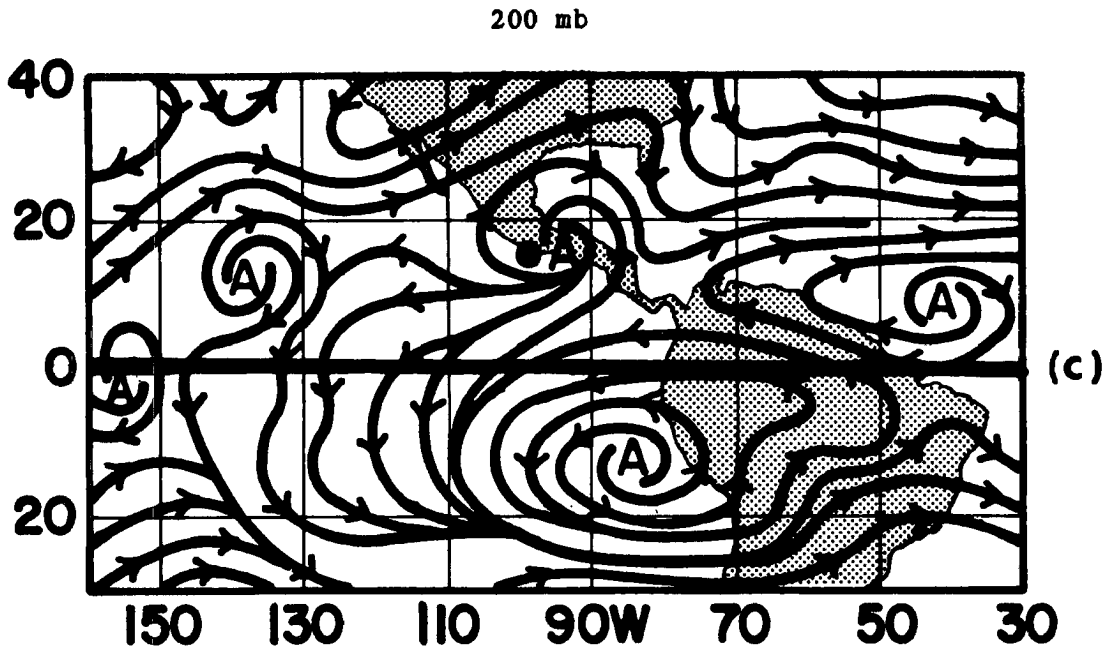


Fig. 22c. Continued.

become less favorable for either development or intensification. For example, on 23 July a tropical cyclone over the northwest Pacific joined together with a neighboring powerful S.H. equatorial anticyclone to help establish a strong equatorward outflow channel from the storm system (Fig. 24a). After 23 July, however, the anticyclone split into two weaker anticyclones. The equatorward outflow channel which was well established on the 23rd was consequently weakened (Fig. 24b). Two days later on 25 July, this system filled over the sea.

(2) Effect of the N.H. Flow Patterns on S.H. Tropical Cyclones

The movement or intensification of a low latitude N.H. upper level anticyclone to a S.H. tropical cyclone can have a similar enhancing influence on the equatorward outflow above a N.H. tropical cyclone.

Figure 25 shows the intensifying process of Tropical Cyclone Angele over the South Indian Ocean. On 15 December, a 200 mb low latitude

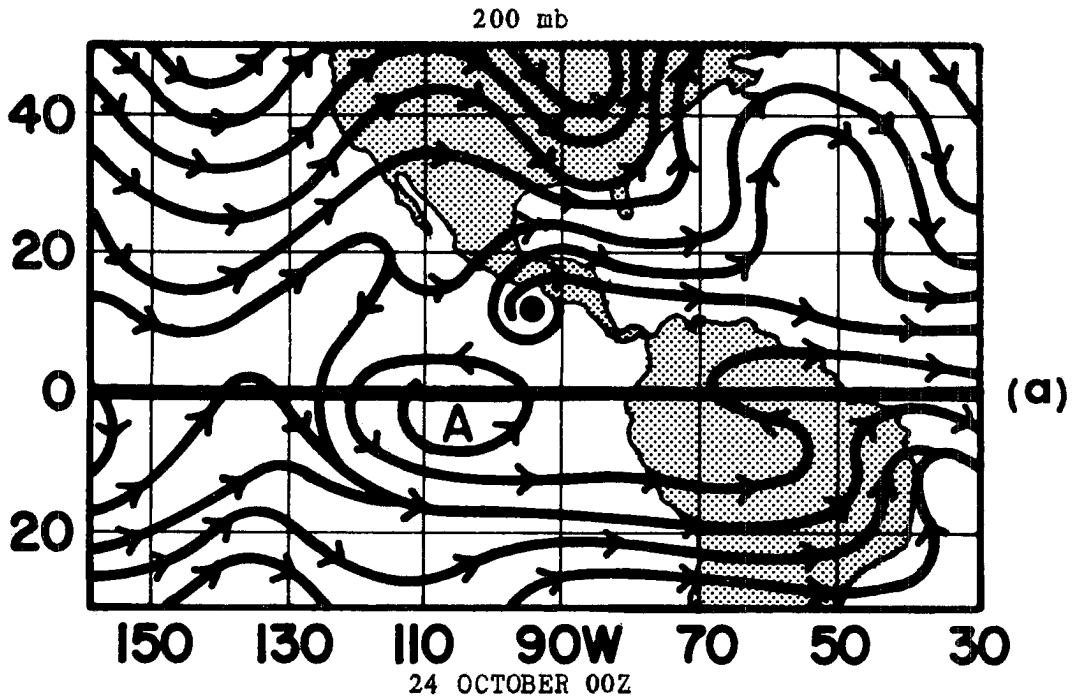


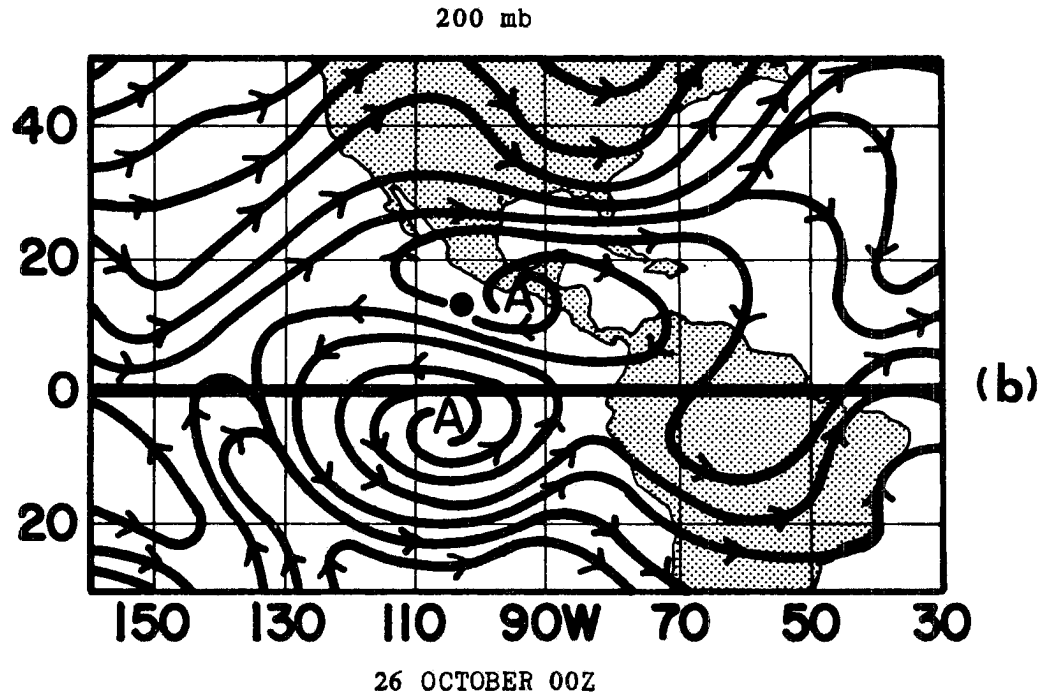


Fig. 23a-b. Illustration of a no-channel tropical cyclone (Ignacio) intensified when a stationary anticyclone near the cyclone, but in the other hemisphere intensified.

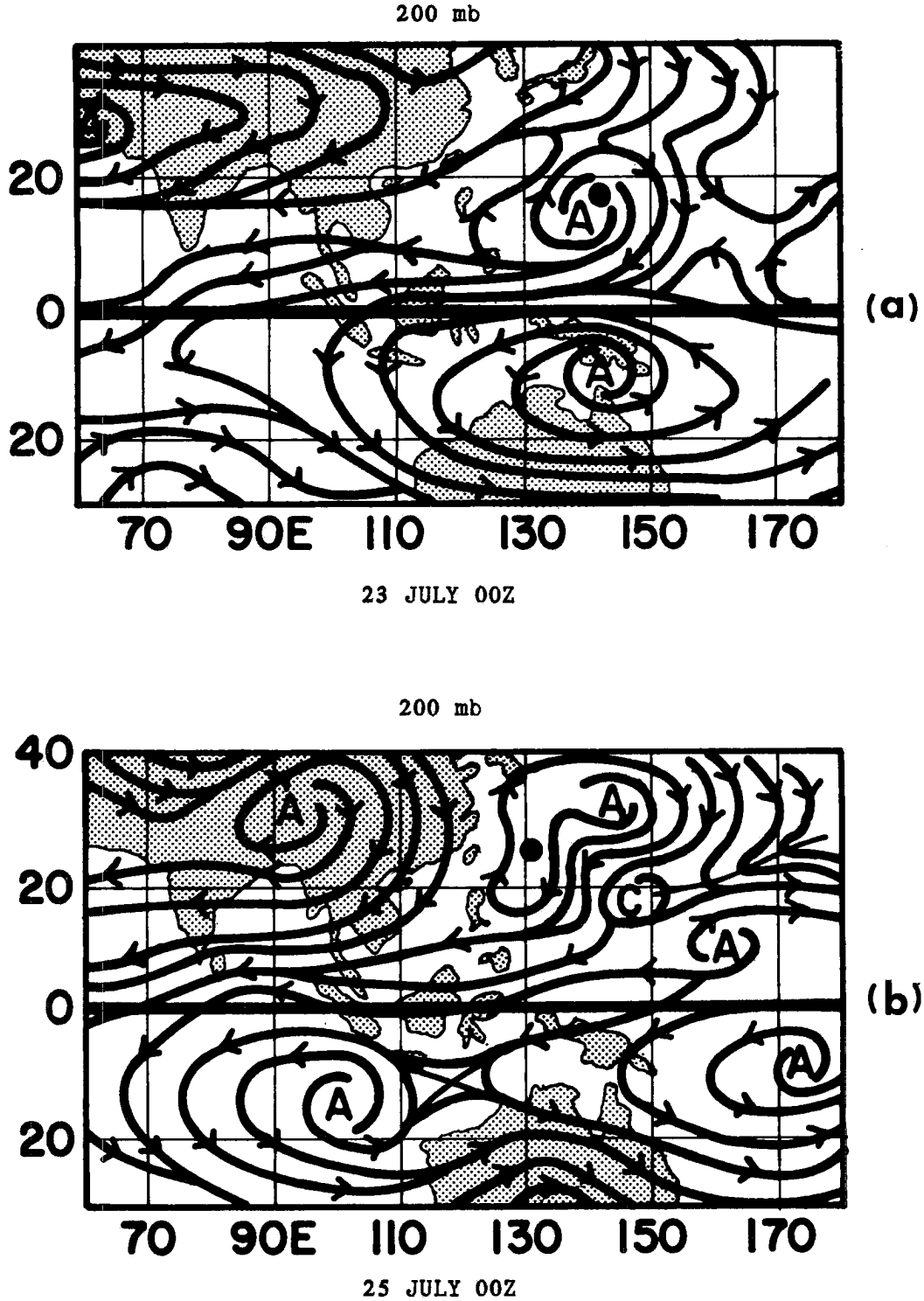


Fig. 24a-b. Example of a Northern Hemisphere tropical cyclone which weakened when a Southern Hemisphere 200 mb anticyclone moved away from the storm. a) 23 July 1979; and b) 25 July 1979.

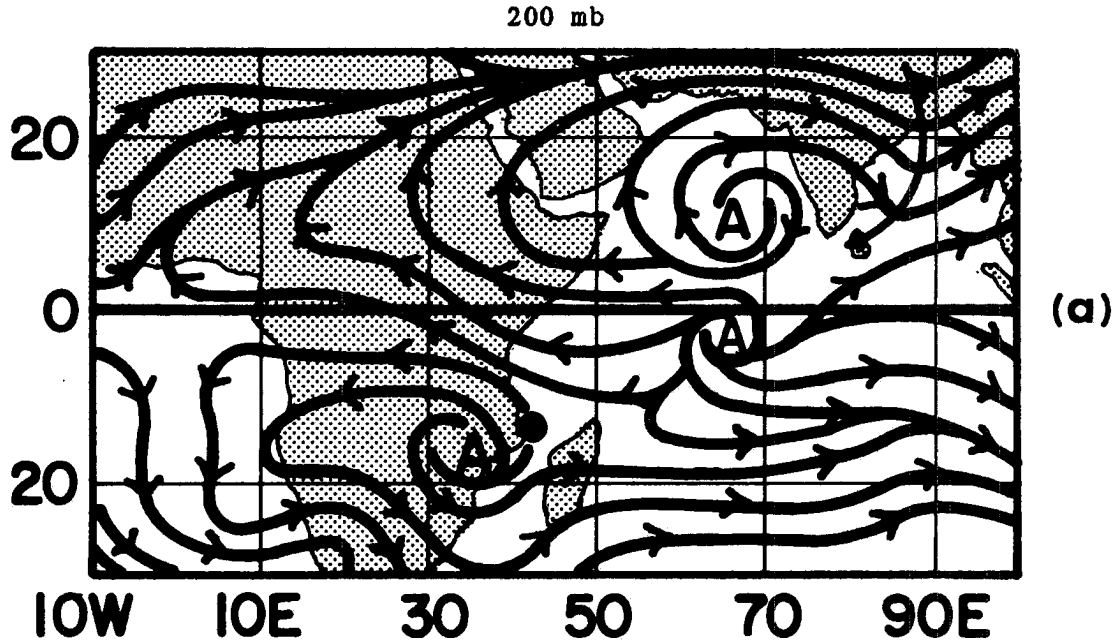


16 DECEMBER 00Z

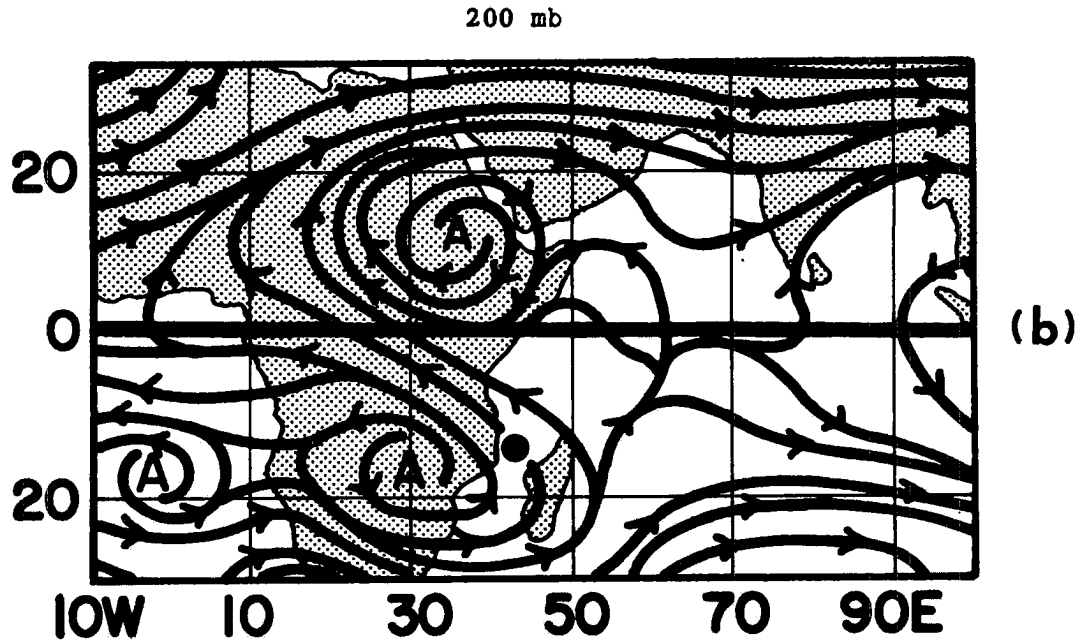


18 DECEMBER 00Z

Fig. 25a-b. Illustrating how tropical cyclone (Angele) in the Southern Hemisphere intensified to a hurricane when a 200 mb anticyclone over the Northern Hemisphere intensified and moved north of it. From 16 to 18 December Angele increased its intensity from a tropical depression to a hurricane (T5 90 kts).

anticyclone in the N.H. was over the North Indian Ocean (Fig. 25a). This anticyclone then built to a position over North Africa. It was then in a favorable longitudinal proximity with Tropical Cyclone Angele. This movement caused the development of strong 200 mb cross-equator flow and the establishment of Angele's equatorward outflow channel. Angele was then located over the Mozambique Channel (Fig. 25b). From 16 to 18 December Angele increased its intensity from a tropical depression to a cyclone of Dvorak T-no. 5 (90 kts).

b) Middle-Latitude or TUTT and Cyclone Interaction Influences

When a mid-latitude long-wave trough, moving eastward, approaches close enough to a tropical cyclone, conditions became favorable for the establishment or the strengthening of a poleward outflow channel.

On 19 December 1978, a tropical cyclone was present east of the Diego Garcia Island in the South Indian Ocean. A trough moving from west to east underwent strong deepening over the ocean east of Madagascar on 20 December (Fig. 26). This strengthened the poleward outflow channel of the tropical cyclone in front of the trough. From 20 to 21 December the tropical cyclone increased from a depression to a tropical storm.

These types of the middle latitude trough influences on tropical cyclone intensification are the feature most responsible for tropical cyclone intensification in the S.H.

Another model of a long-wave trough influence on intensification is the situation when a tropical cyclone becomes located at the tip of, or slightly to the rear of an upper level trough or TUTT. In contrast to the previous case this acts to enhance the tropical cyclone's equatorial outflow. This causes northern flow to prevail above the tropical

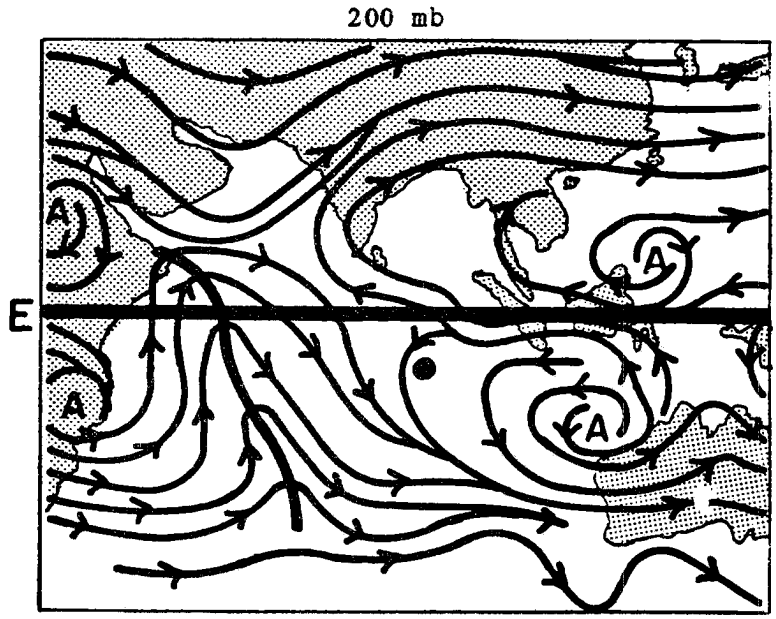


Fig. 26. Illustration of how a 200 mb poleward outflow channel is enhanced by a long wave trough west of the tropical cyclone. From 20 to 21 December the tropical cyclone increased from a tropical depression to tropical storm strength.

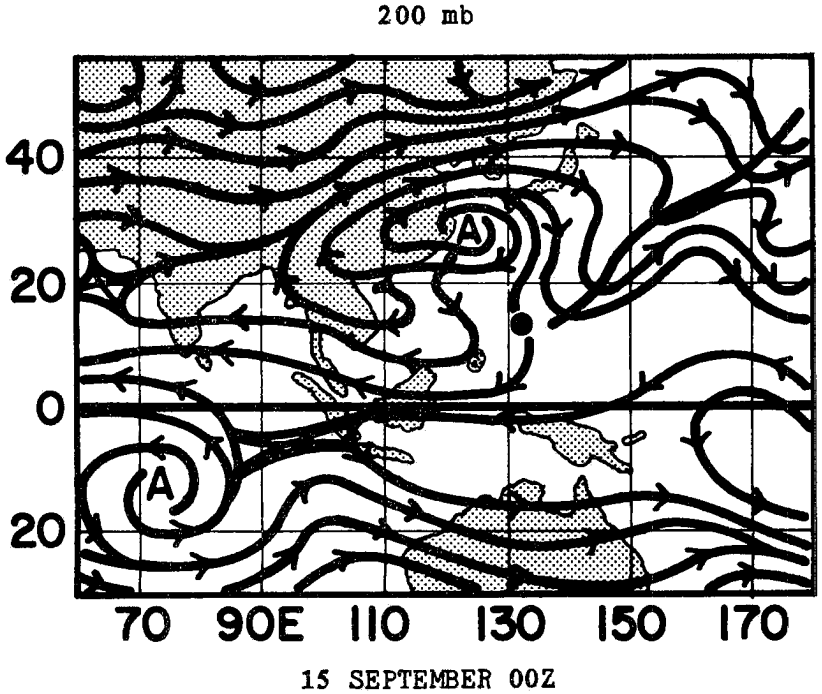


Fig. 27. Illustration of how a 200 mb equatorward outflow channel is enhanced by an upper level long wave trough or shear zone to the east of the tropical cyclone. From 15 to 16 September the maximum sustained wind of this cyclone (Mac) increased from 20 to 65 kts.

cyclone with an upper level anticyclone to the west of the storm. The long-wave trough (or TUTT shear line) acts to enhance an equatorial rather than the normally expected poleward outflow. This flow arrangement can also contribute to the intensification of a tropical cyclone.

Figure 27 shows the intensifying process of Typhoon Mac. A strong large-scale trough or shear line developed over the mid-Pacific. Mac was located in the area slightly to the rear of the trough, with prevailing northly flow and an equatorward outflow channel. From 15-16 September, the maximum sustained wind speed of Mac increased from 20 kts to 65 kts. Many other cases like this occur in the northwest Pacific during the summer season.

This type of outflow conforms with the $S_{Ee}$ pattern. In mid-summer (July-August), the development of a tropical cyclone over the northwest Pacific is frequently associated with such $S_{Ee}$ upper level patterns. The $S_{Ee}$ equatorward outflow channel can thus be brought about by either the rear effects of such a 200 mb TUTT type of trough or by the effects of a S.H. equatorial anticyclone.

c) Combined Influence

A tropical cyclone's intensification also can be positively influenced by the combined interaction of both the N.H. and S.H. flow patterns. Such a interaction can frequently have a powerful influence on very rapid tropical cyclone development and intensification.

When a mid-latitude long-wave trough and an equatorial upper level anticyclone of the opposite hemisphere approach to the north or south of a tropical cyclone from different directions, strong double outflow channels (D pattern) can be developed.

Typhoon Owen over the northwest Pacific had no obvious outflow channel before 24 September (Fig. 28). Two days later when a middle latitude trough and an opposite hemisphere anticyclone approached Owen simultaneously their combined influence was felt (Fig. 28b). These combined influences helped establish simultaneous double outflow channels. Owen's intensity increased rapidly. From 24-26 September, Owen's maximum sustained wind speed increased rapidly from 45 kts to 110 kts.

A second model shows how cyclone intensification can also be influenced by the combined effect or an equatorial anticyclone of the opposite hemisphere and that of the tip (or rear) of a TUTT. These combined influences can similarly lead to powerful enhancement of the equatorial outflow of the tropical cyclone and its rapid intensification.

Typhoon Hope over the North Pacific was in a depression phase on 28 July. During 27-29 July, an equatorial anticyclone of the Southern Hemisphere moved westward and intensified at the same time that a long-wave trough east of Hope deepened (Fig. 29). The combined effect of these two processes brought about a large enhancement of Hope's equatorial outflow channel. From 29-30 July, Hope's maximum sustained wind speed increased from 40 kts to 90 kts.

On 30 July, Hope was at the tip of the western extended trough over the mid-Pacific. Two streams of outflow were formed--a southwestward stream and a southeastward one (Fig. 29b). Satellite imagery also showed southwestward and southeastward cloud outflows -- both were equatorward. From 30-31 July, the maximum wind speed near the center of Hope increased from 90 kts to 130 kts.

200 mb

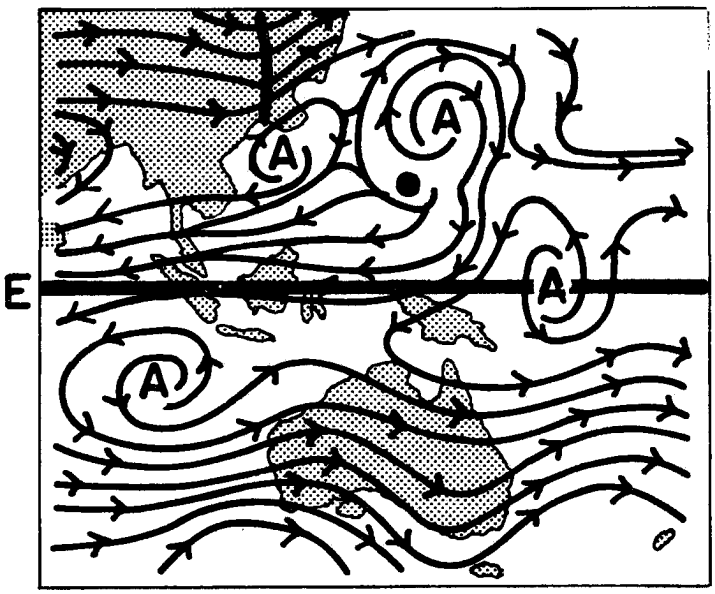


(a)

24 SEPTEMBER 00Z

200 mb

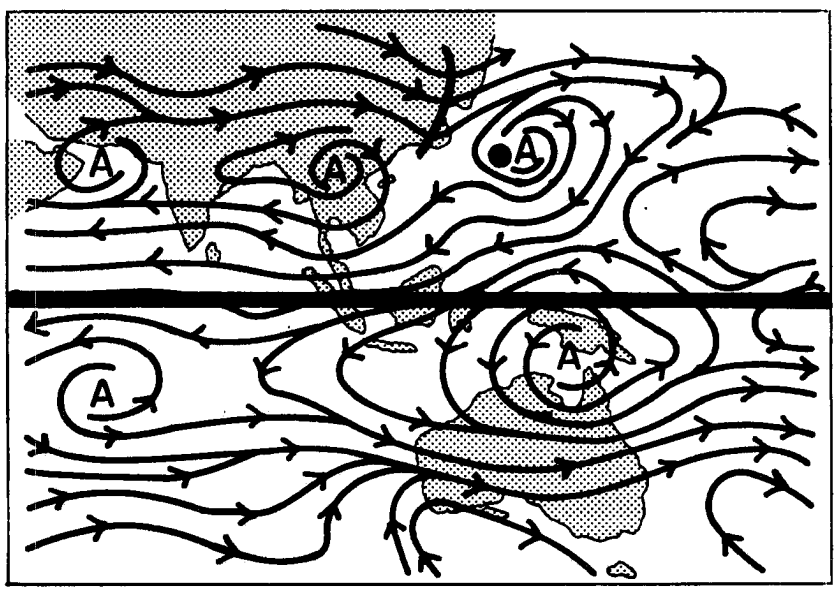


(b)

26 SEPTEMBER 00Z

Fig. 28a-b. Illustration of how 200 mb double outflow channel is enhanced by the combined influence of a trough west of the cyclone and an anticyclone over the opposite hemisphere. From 24 to 26 September the maximum sustained wind of this Typhoon Owen, increased from 45 to 110 kts.

200 mb

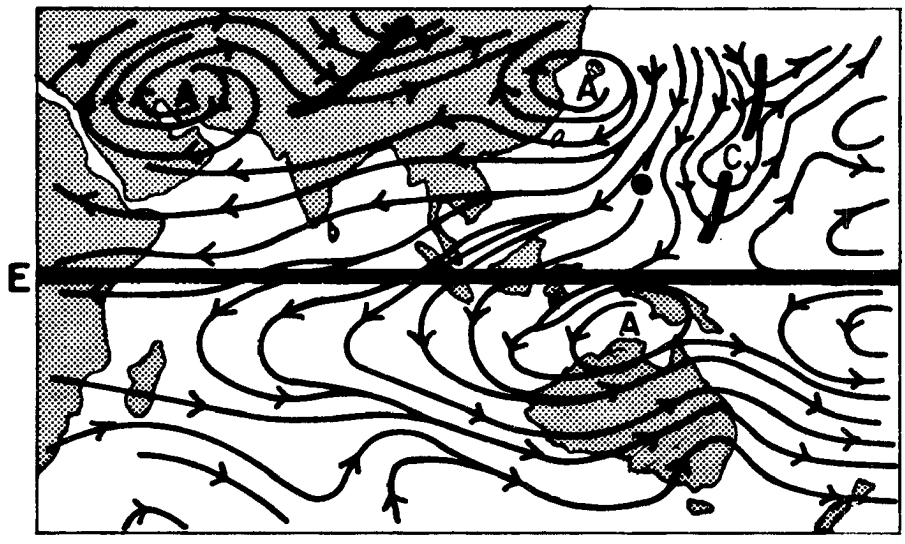


(a)

29 JULY 00Z

200 mb

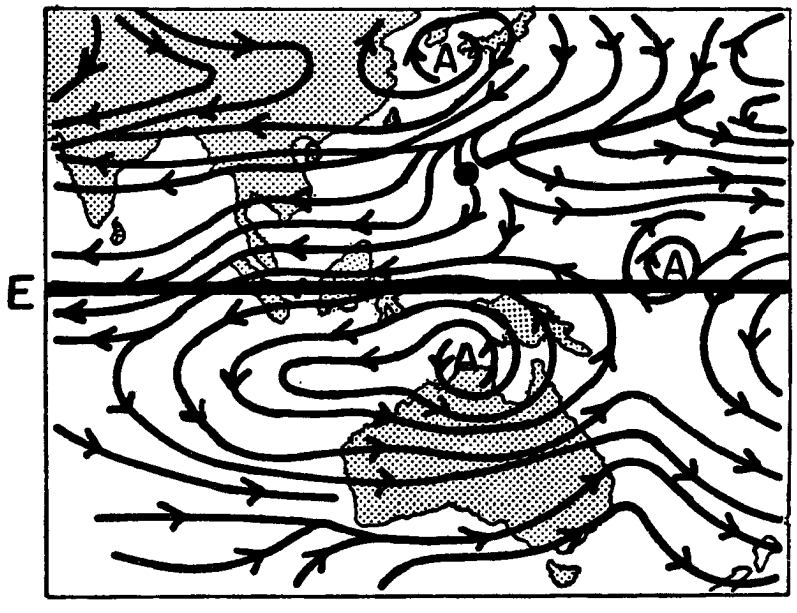


(b)

30 JULY 00Z

Fig. 29a-b. Illustration of how a 200 mb outflow towards the equator is enhanced by the combined influence of a trough east of the cyclone and an anticyclone over the other hemisphere. From 29 to 30 July 1979, the maximum sustained wind of this cyclone, Hope, increased from 40 to 90 kts. From 30 to 31 July, the maximum sustained wind of Typhoon Hope increaed from 90 to 130 kts.

Two mid-latitude troughs also can produce a combined outflow effect. For example, Hurricane Henri over the Atlantic was located west of an anticyclone between two mid-latitude troughs. The western trough helped enhanced poleward outflow, and the eastern trough helped to enhance equatorward outflow. This tropical cyclone established double-channel outflows and rapidly developed. From 15-17 September, the maximum wind speed near Henri's center increased from 25 kts to 75 kts (Fig. 30).

(2) Model Synthesis of Various Types of Interaction

We believe that these examples show how the positioning of a cyclone in conjunction with its upper tropospheric environment can have a very important influence on a tropical cyclone's intensification.

We have isolated six basic types of cyclone and environment 200 mb wind field interaction which occurred during the FGGE year and for which we have also observed to take place in other years. These are:

$I_1$ Equatorial anticyclone of the opposite hemisphere enhancing a single equatorward outflow channel ($S_e$).

$I_2$ Long-wave middle latitude trough moving eastward to the poleward and west side of the cyclone so as to enhance a single poleward outflow channel ($S_p$).

$I_3$ Tropical cyclone is located at the tip of or in the rear of a transverse long-wave trough (or TUTT). This arrangement acts to bring about the enhancement of a single equatorward outflow channel ($S_p$).

$I_4$ Mid-latitude long-wave trough (or TUTT) and equatorial anticyclone of the opposite hemisphere approach a tropical cyclone from

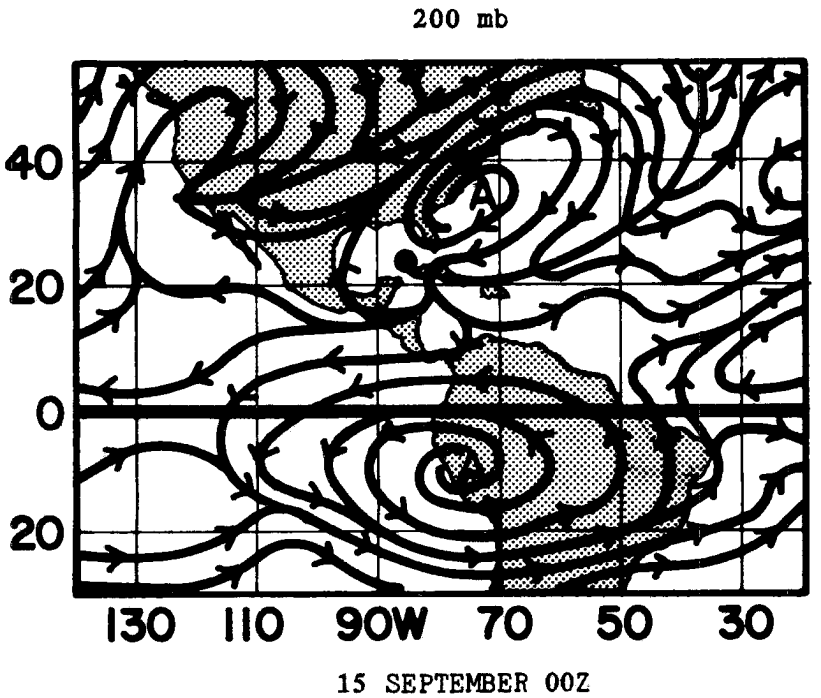


Fig. 30. Illustration of how 200 mb double outflow channels are enhanced by the combined influences of two large-scale troughs. From 15 to 17 September the maximum sustained wind of this hurricane, Henry, increased from 25 to 75 kts.

different directions and contribute to the establishment of double outflow channels (D) in both poleward and equatorial directions.

$I_5$ Combined effect of an equatorial anticyclone of the opposite hemisphere and the tip of a transverse upper shear line over the mid-ocean enhancing a single equatorial outflow channel ($S_e$).

$I_6$ Tropical cyclone flanked by western and eastern shear lines. This situation contributes to the establishment of double outflow channels (D).

Figure 31 shows a plan view of these six typical interaction types.

Some of these interaction models are more prevalent than other. Table 1 gives a statistical breakdown of the frequency of these various interaction models by class for the FGGE year. It is seen that 89% of the systems with poleward outflow channels ($S_p$ pattern) are associated with the approach of a mid-latitude long-wave trough or a TUTT. Only

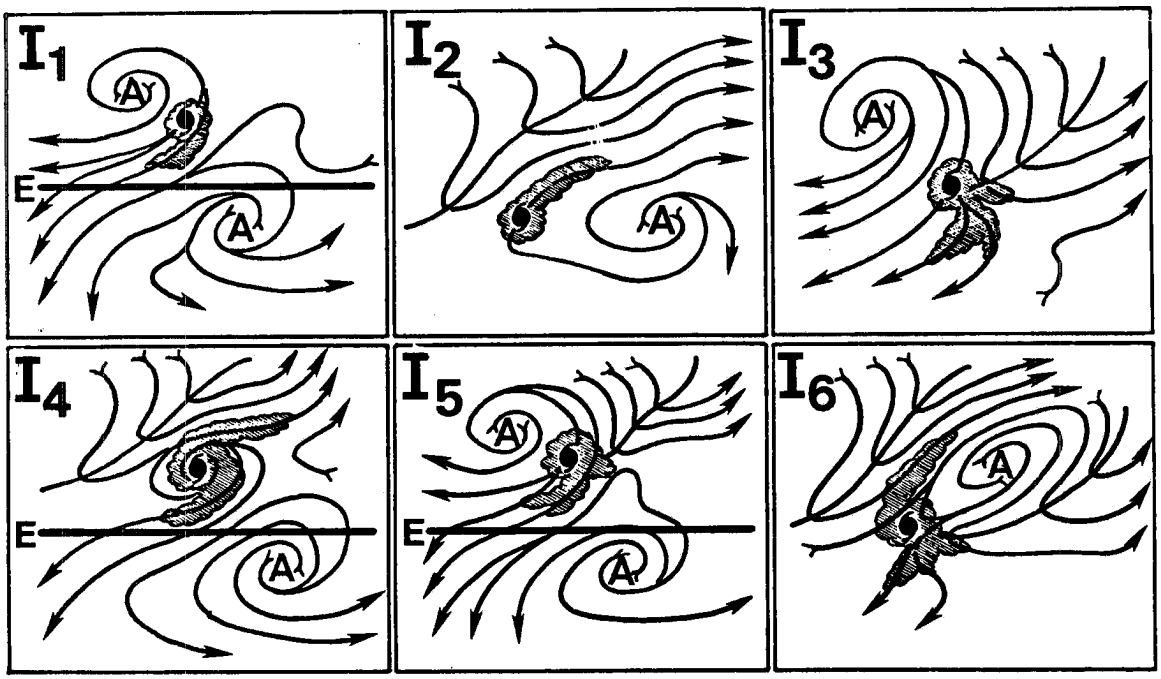


Fig. 31. Six types of interactions between a tropical cyclone and its surrounding.

TABLE 1

Frequency of interaction types in different outflow patterns during the FGGE year. X means that no interacting outflow cloud channels were detected with this flow configuration.

| Patterns | $S_P$ | | $S_E$ | | | | D | | N | | |
|---|---|---|---|---|---|---|---|---|---|---|---|
| Interaction Type | $I_2$ | X | $I_1$ | $I_5$ | $I_3$ | X | $I_4$ | $I_6$ | X | $I_1$ | |
| Number | 25 | 3 | 18 | 9 | 2 | 3 | 5 | 1 | 9 | 5 | |
| Total | 28 | | 32 | | | | 6 | | 14 | | Total 80 |

three cases have poleward outflow channels associated with other flow arrangements. Eighty-four percent of equatorward outflow channels are associated with favorable positioning of low latitude anticyclones of the opposite hemisphere. Thirty-four percent of equatorial outflows are associated with the tip or rear effects of a 200 mb trough or TUTT shear line. (Some equatorward channels are associated with both shear lines and anticyclones.)

Double channels occur with the lowest frequency. All but one double channel outflow were associated with the combined effects of an equatorial anticyclone of the opposite hemisphere and a mid-latitude long-wave trough of some configuration. This table also shows that of the 80 tropical cyclones occurring during the FGGE year which underwent intensification or development, 59 or 74% were observed to possess some type of distinct 200 mb outflow channel or channels. Upper tropospheric tropical cyclone and surrounding environmental interaction is thus a very common feature of tropical cyclone intensification.

These models of upper-level cyclone-environment interaction also possess seasonal and regional relationships. FGGE year data shows that in mid-summer in the northern hemisphere, intensification of tropical cyclones in the Pacific is frequently associated with the effect of an upper level anticyclone of the opposite hemisphere. On the other hand, the influence of a mid-latitude long-wave trough to the northwest of the cyclone (excluding tip and rear effects of upper shear line or TUTT trough over the mid-ocean), is primarily a feature of the autumn and winter.

All tip or rear of trough effects of a transverse shear line over the mid-ocean (models $I_3$, $I_5$, and $I_6$) occurred in the summer -- especially over the northwestern Pacific.

These outflow models also vary in the different ocean basins. The ocean basin most influenced by equatorial anticyclones of the opposite hemisphere is the northeastern Pacific (92%) and the northwestern Pacific (52%) basins. This is opposite to the situation in the S.H. Only 9% of S.H. FGGE year tropical cyclones were influenced by an equatorial anticyclone of the Northern Hemisphere. Most of the tropical cyclones which intensified in the S.H. (82% in the South Indian Ocean, and 63% in the Southern Pacific) are associated with a mid-latitude long-wave trough to their west ($I_2$ pattern that is inverted).

Poleward outflow patterns are also prevalent for tropical cyclones over the North Indian Ocean. These cyclones occur only in late spring and autumn. This is the time when middle latitude westerly waves are just able to pass to the south of the Tibetan plateu and draw in poleward directed outflow from the tropical cyclone.

Over the central Atlantic in summer, a quasi-stationary transverse shear line or TUTT typically exists. Tropical cyclones which intensified over the North Indian Ocean or the North Atlantic are thus mostly associated with the effects of middle latitude troughs and/or upper level shear lines (67%).

## 5. Regional and Seasonal Outflow Differences as a Response to Background 200 mb Climatology

These characteristic differences in outflow channel patterns are regionally and seasonaly well related to the background 200 mb climatology. These outflow patterns are better understood when this background climatology is studied region by region.

### a. The Northwest Pacific and the North Indian Ocean

Although tropical cyclones may occur in all seasons over the northwest Pacific, July through September is the main part of the season. Table 2 shows that the $S_E$ outflow pattern prevails during the summer. The poleward outflow channel ($S_P$) occurs mainly during non-summer months. Outflow channel patterns are closely linked with the seasonal variation of the upper level circulation.

The position of the jet stream axis of the upper westerlies over the northwest Pacific possesses a distinct seasonal shift. As indicated in Fig. 32, the jet stream axis reaches its northern limit ($45^{\circ}N$) in July and August, and its southern limit ($32^{\circ}N$) in January. In winter, the westerly stream may reach to a latitude as low as $10^{\circ}N$. Winter cyclones are almost always located to the west of the 200 mb climatological equatorial ridge (Fig. 33). Since winter tropical cyclones are always near the westerlies, the cyclone's outflow is almost always poleward, with very little possibility of its becoming equatorward. This is also true of cyclone in the late fall and early spring.

Following the northward shift of the jet stream, a strong anticyclone is formed in South Asia during July and August. A semi-

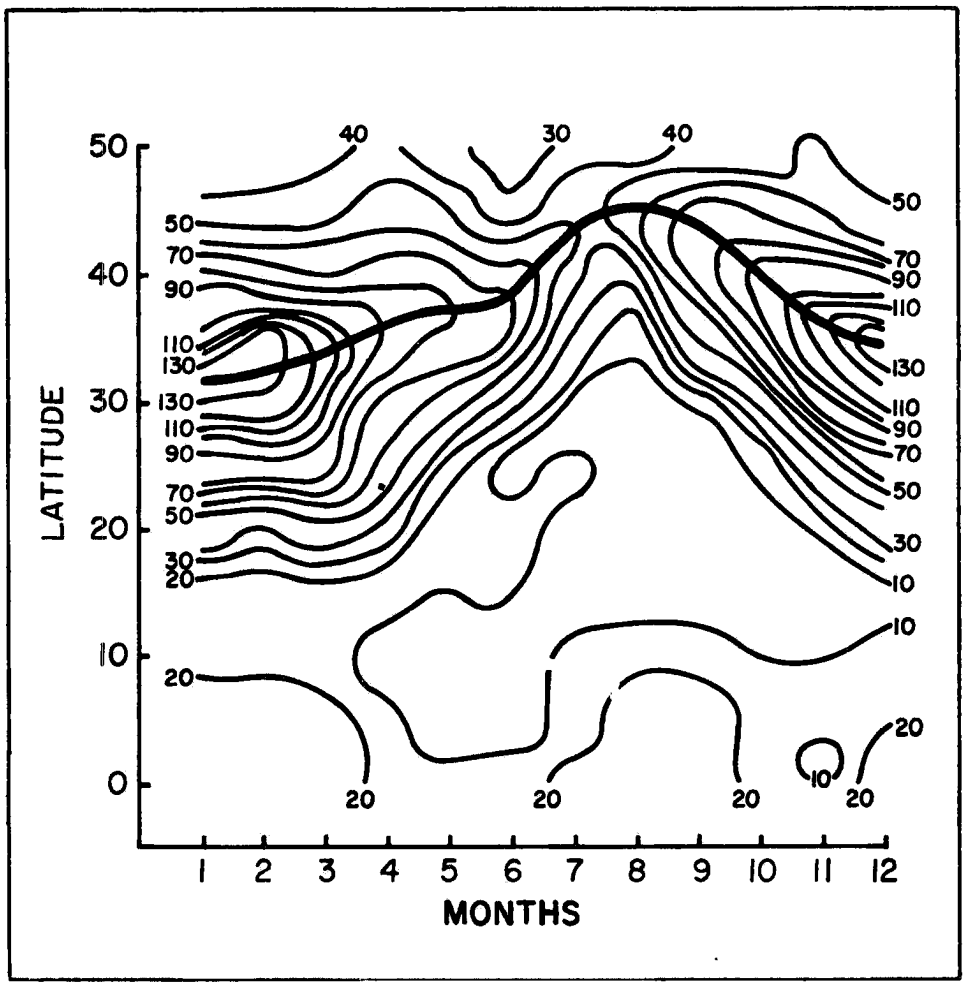


Fig. 32. The monthly variation of the 200 mb jet stream in the northwest Pacific basin (140°E) - (adopted from Sadler 1975).

stationary trough lies over the central Pacific. The tropical cyclone is usually at the western end of the shear line and under the influence of the northeastern flow of the eastern part of the South Asian anticyclone. There is thus a great difference in the 200 mb west Pacific flow patterns in July as compared with January. The mean climatological flow near the center of the summer cyclones has changed

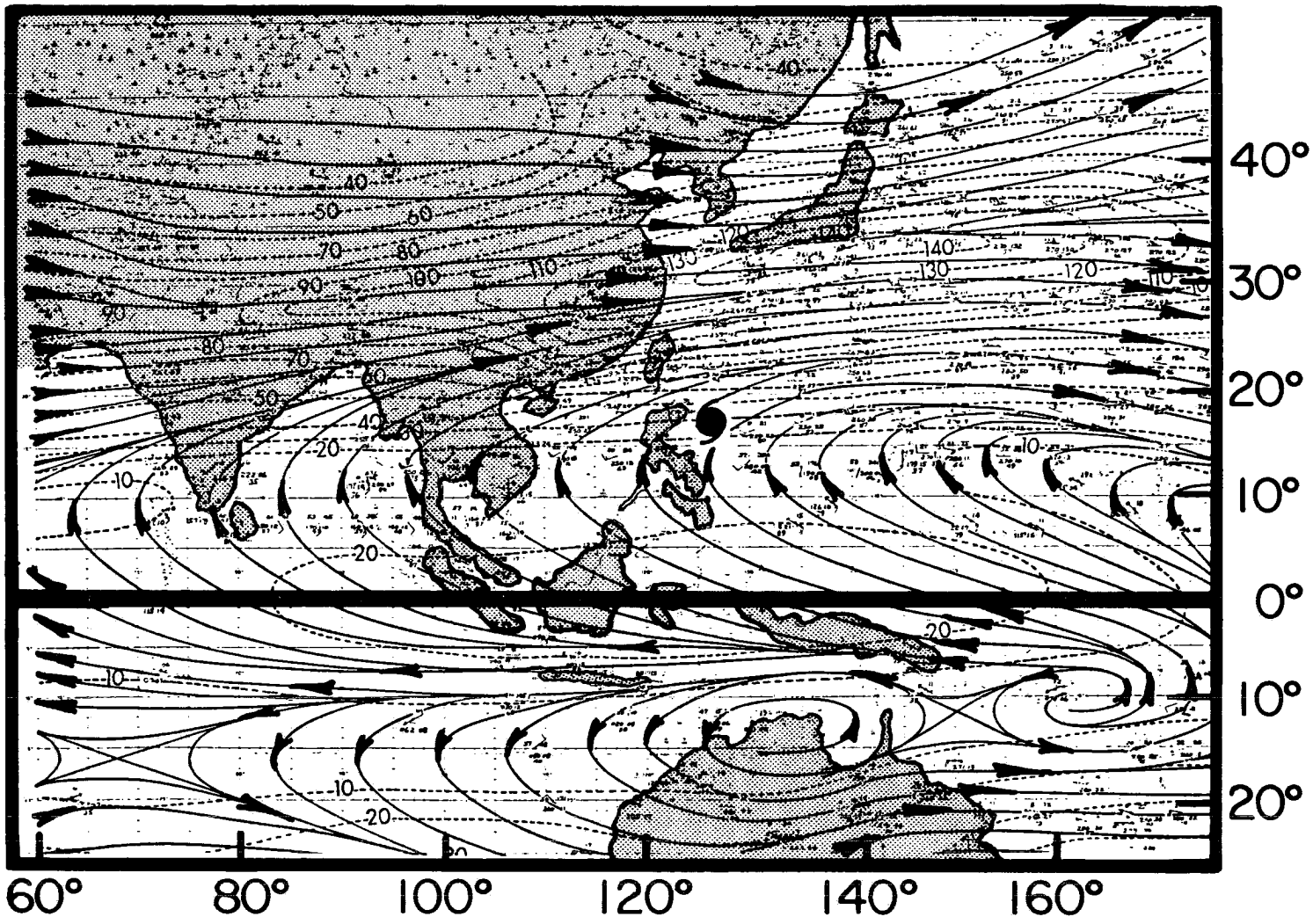


Fig. 33. 200 mb average wind for the northwest Pacific in January. (Adopted from Sadler (1976). The centraid of tropical cyclone location points is indicated by the large hurricane symbol.

from southwest to northeast (compare Fig. 34 with Fig. 33). These climatological flow patterns establish the background potential for the type of outflow channels and interaction that the cyclone is going to have with its environment. In mid-summer, the equatorial ridge of the S.H. winter is closer to the equator. Its intensification and movement can thus exert more influence on N.H. cyclones. Note also that the location of summer tropical cyclones are a considerable distance from the position of the climatological westerlies. This makes it difficult for summer cyclones to establish poleward outflow channels.

The two cases with double outflow channels occurred in the autumn season. This is typical. In the fall (Fig. 36), the jet stream axis of the westerlies advances markedly southward, and the south Asian anticyclone shrinks into a narrow west-east cell. The easterlies and westerlies on either side of the 200 mb anticyclone become considerably closer (Figs. 35 and 36) together. This provides a very favorable circulation background for the establishment of double outflow channels.

Tropical cyclones without outflow channels occur mostly at very low latitudes in mid-fall and winter (Table 2) when the South Asian anticyclone has retreated over the tropical Pacific and the southern part of the anticyclone is under flat easterlies. It is then more difficult to generate a poleward outflow at very low latitudes. Also, the equatorial ridge of the S.H. has moved further southward and away from the equator. It thus has less influence on tropical cyclones of the N.H. Therefore, conditions become more favorable in the late season and in winter for the occurrence of non-channel tropical cyclones.

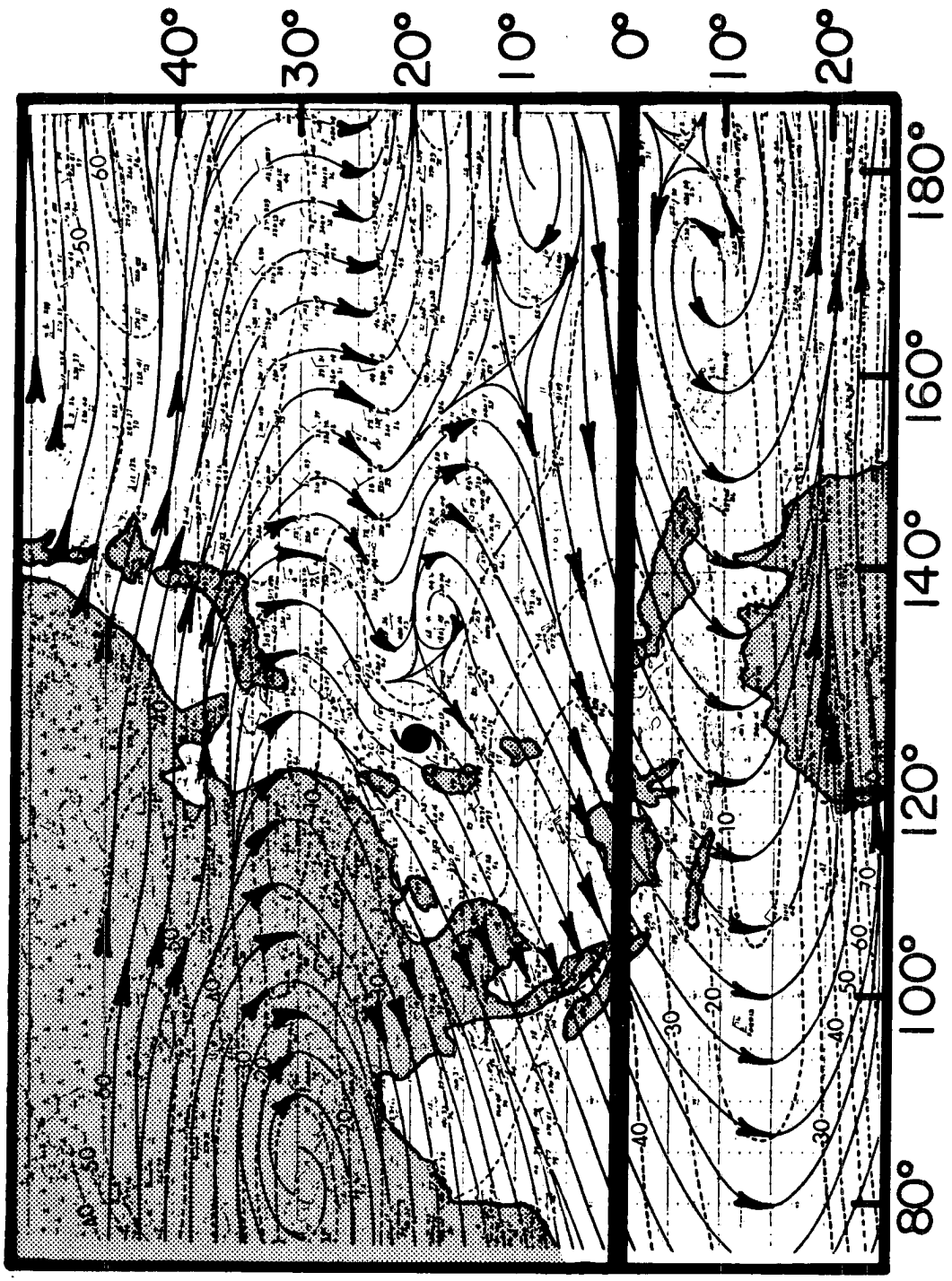


Fig. 34. Same as Fig. 33, but in July.

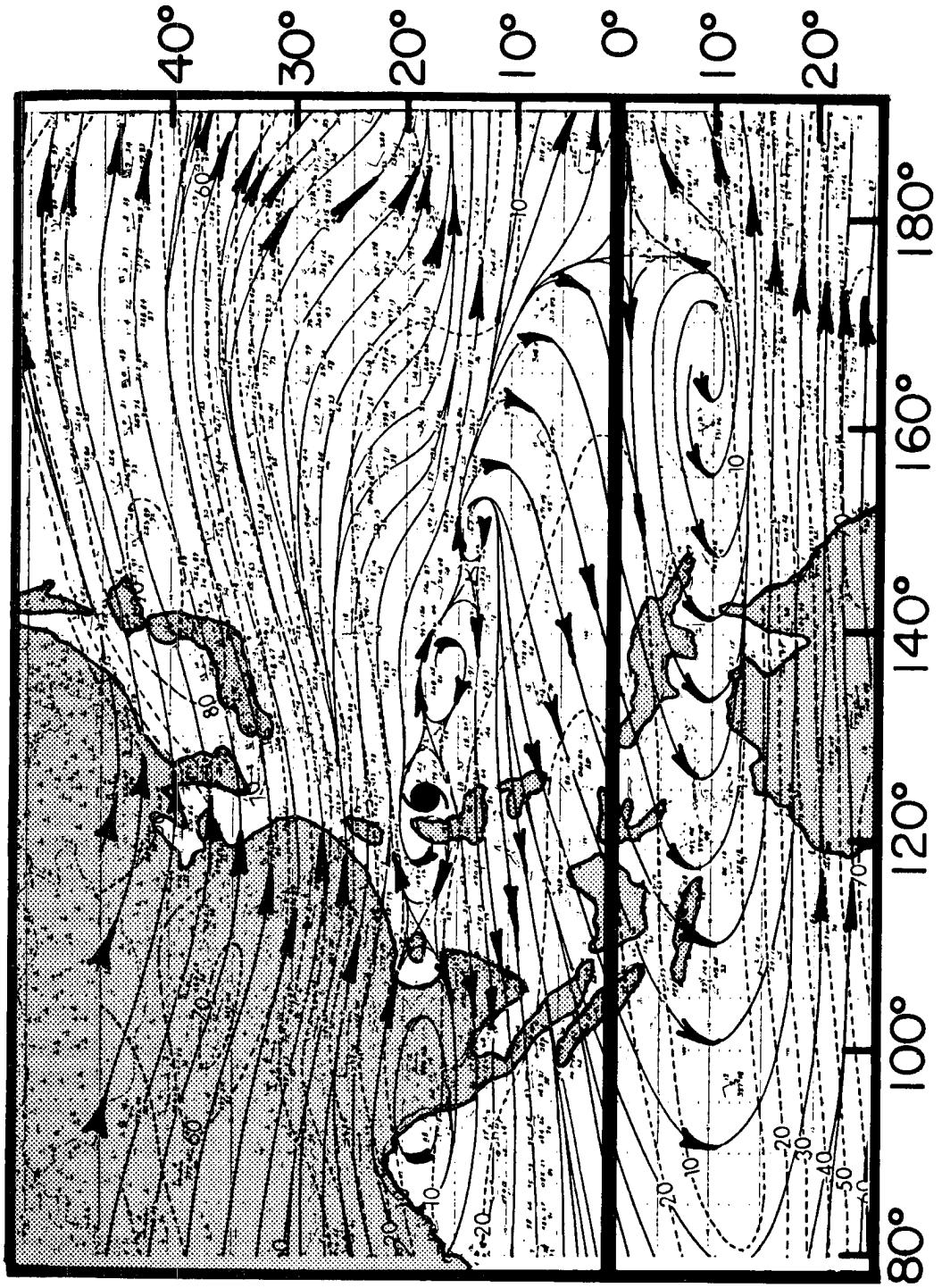


Fig. 35. Same as Fig. 33, but in October.

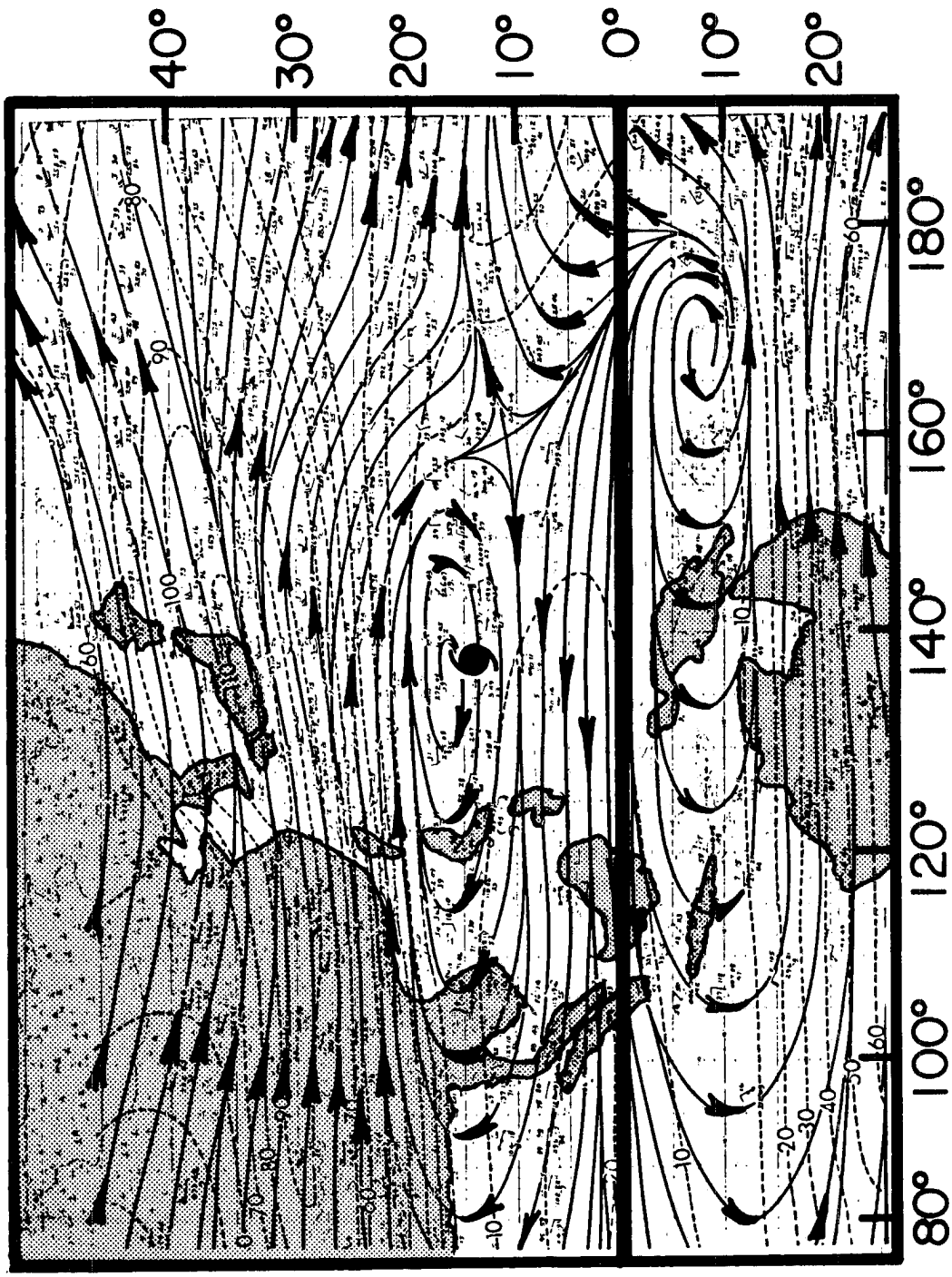


Fig. 36. Same as Fig. 33, but in November.

TABLE 2

Monthly frequency of the upper level outflow pattern of northwest Pacific FGGE year tropical cyclones.

| | | Dec | Jan | Feb | Mar | Apr | May | Jun | Jul | Aug | Sept | Oct | Nov | Total |
|---|---|---|---|---|---|---|---|---|---|---|---|---|---|---|
| S | SPw | | 1 | | 2 | | | | | | | | | 3 |
| | SPc | | | | | | | | | | 1 | 1 | | 2 |
| | SEc | | | | | | | | | | 1 | | | 1 |
| | SEe | | | | | | 1 | | 5 | 4 | 3 | 2 | | 15 |
| D | Dc | | | | | | | | | | 1 | | | 1 |
| | De | | | | | | | | | | | 1 | | 1 |
| N | Nw | | | | | | | | | | 1 | | | 1 |
| | Ns | | 1 | | | | | | | | | 1 | 2 | 4 |
| | Nc | | | | | | | | | | 1 | | 1 | 2 |
| | Ne | | | | | 1 | | | | | | | | 1 |

As indicated in Table 3 most of the tropical cyclones in the FGGE year over the North Indian Ocean have poleward outflow channels. This is because tropical cyclones over this basin occur primarily in late spring and fall. During these two seasons, the general circulation undergoes major changes. During April and May and after September, 200 mb southwesterlies prevail over the basin of the North Indian Ocean poleward of 10-15°N, (Fig. 37). This type of circulation is favorable for generating poleward outflow channels. After May, dramatic changes of circulations occur as the very intense South Asian anticyclone becomes formed over the northern part of the Indo-China peninsula. The circulation conditions that would normally generate equatorward outflow channels become well established over the North Indian Ocean (Fig. 38).

TABLE 3

Monthly frequency of the upper level outflow patterns during the FGGE year over the North Indian Ocean.

| | | Dec-Apr | May | Jun | Jul-Aug | Sept | Oct | Nov | Total |
|---|---|---|---|---|---|---|---|---|---|
| S | SPw | | 1 | | | 1 | | 1 | 3 |
| | SPc | | | | | | 1 | | 1 |
| | SEc | | 1 | | | | | | 1 |
| | SEe | | | 1 | | | | | 1 |

However, tropical cyclones typically do not form over this basin in mid-summer. Therefore, the frequency of poleward outflow channels with North Indian Ocean cyclones is higher than one might expect from a general consideration of the summer climatology.

b. The northwest Atlantic and the northeast Pacific

Tropical cyclones over the Northwest Atlantic occur at a relatively high latitude and mainly in August to October. Their frequency is only 30 percent of the northwest Pacific. They can readily generate double outflow channels, however. Table 4 shows that during the FGGE year the D type double outflow patterns in the Atlantic occurred 4 out of 9 times or in 44% of the cases. By contrast, over the northwest Pacific, only 6% of the cyclones experienced double outflow patterns.

The winter to summer shift of the 200 mb jet stream axis over the northwest Atlantic is not as distinct as that of the northwest Pacific. A permanent quasi-stationary 200 mb TUTT, much stronger than that over the Pacific, extends from the middle to the south western part of the Atlantic (Fig. 39). This results in southwest flows reaching low latitudes. In addition, the equatorial anticyclonic east-west ridge is

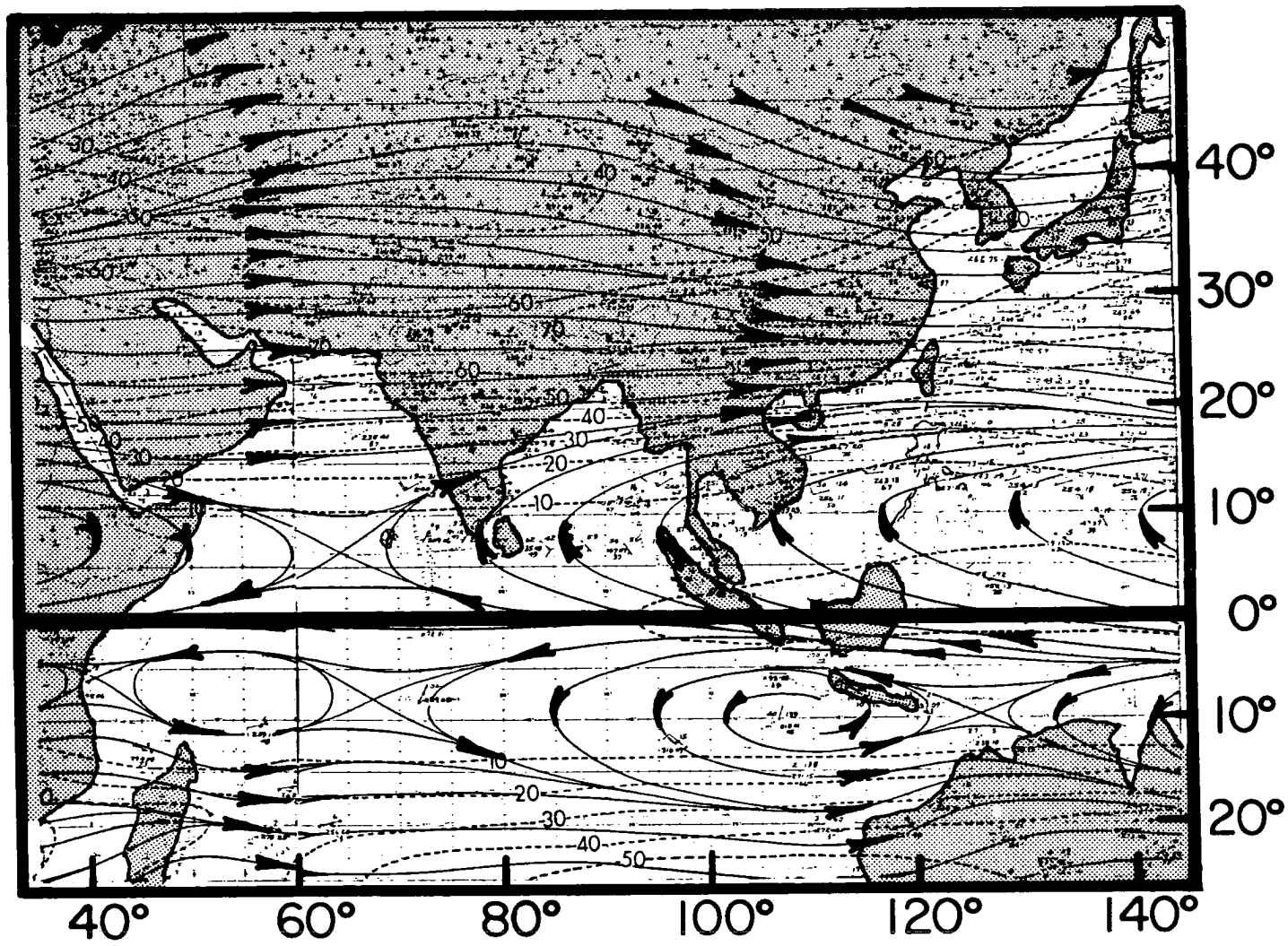


Fig. 37. 200 mb average wind over the North Indian Ocean in April (adopted from Sadler, 1978).

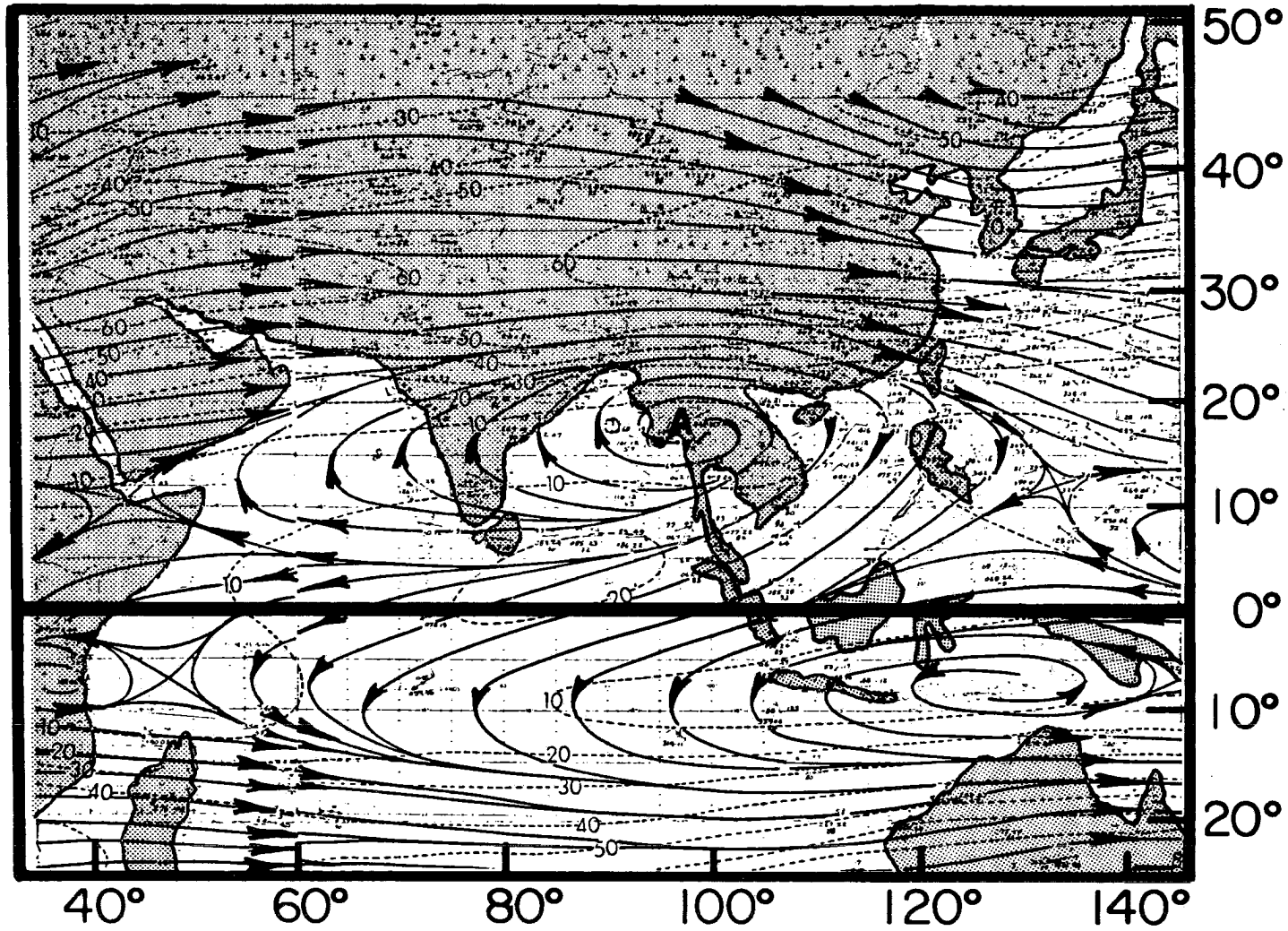


Fig. 38. Same as Fig. 37, but in May.

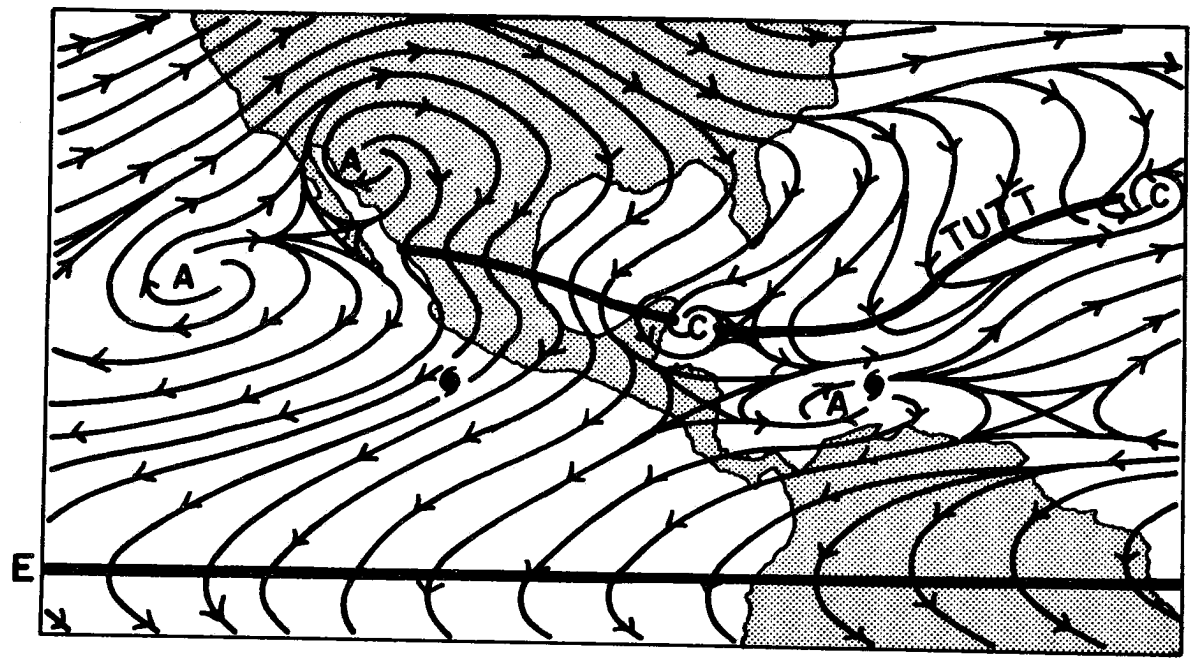


Fig. 39. Climatological 200 mb average wind for the northwest Atlantic and northeast Pacific in August (adopted from Sadler, 1976).

TABLE 4

Monthly frequency of the upper level outflow patterns over the Northwest Atlantic during the FGGE year.

| | | Dec-May | Jun | Jul | Aug | Sept | Oct-Nov | Total |
|---|---|---|---|---|---|---|---|---|
| S | $S_{Pw}$ | | 1 | | | 1 | | 2 |
| | $S_{Ec}$ | | | 1 | | | | 1 |
| D | $D_w$ | | | | 1 | 1 | | 2 |
| | $D_c$ | | | 1 | | 1 | | 2 |
| N | $N_s$ | | | | 1 | | | 1 |
| | $N_e$ | | | | 1 | | | 1 |

narrow with prevailing easterly winds on its southern side. These circulation conditions are favorable for generating double outflow channels. Tropical cyclones over the northeast Pacific occur mainly in June-October (Table 5.) The FGGE year was no exception. The upper level flow patterns of northeast Pacific tropical cyclones are subject to the influences of this strong climatologically positioned anticyclone. Most tropical cyclones form under the 200 mb northeast flow to the east of this upper level anticyclone (Fig. 39). It is not surprising then that equatorial outflow channels prevail over this ocean basin.

The frequency of equatorward outflow channels is very high for northeast Pacific tropical cyclones (see Table 5). Two-thirds (8 of 12) of these storms had equatorward outflow channels, only one had a poleward outflow channel and this occurred in November when 200 mb westerlies have just appeared. Two cyclones did not display outflow channels.

TABLE 5

Monthly frequency of the upper level outflow patterns over the Northeast Pacific during the FGGE year.

| | | Dec-May | Jun | Jul | Aug | Sept | Oct | Nov | Total |
|---|---|---|---|---|---|---|---|---|---|
| S | $S_{Pw}$ | | | | | | | 1 | 1 |
| | $S_{Ec}$ | | | 1 | | 1 | 1 | | 3 |
| | $S_{Ee}$ | | 2 | 1 | 1 | 1 | | | 5 |
| N | N | | | | 1 | | 1 | | 2 |
| | $N_c$ | | | | | | 1 | | 1 |

Before April, the whole northeast Pacific cyclone basin is controlled by 200 mb westerly winds. An anticyclone begins to develop in May. It remains stationary around 110°W (except in October when it retreats to about 95°W). After generation in May, the 200 mb anticyclone advances northward, and reaches its highest latitude in July and August (Fig. 40). In November, it retreats to lower latitude and disappears.

c. The Southwest Pacific and the South Indian Ocean

Tropical cyclones in the Southern Hemisphere (S.H.) occur mainly during December–April. Because the S.H. has a much larger area of oceans, winter to summer north-south shifts of the jet stream belt and the equatorial anticyclone are considerably less in the Northern Hemisphere. Even in mid-summer (Jan.-Feb.), westerlies may still reach 15°S. Thus, poleward outflow channels are much more prevalent in the S.H. During the FGGE year poleward outflow channels occur with 64% of the cyclones in the South Pacific and with 82% of the cyclones in the South Indian Ocean (Tables 6–7).

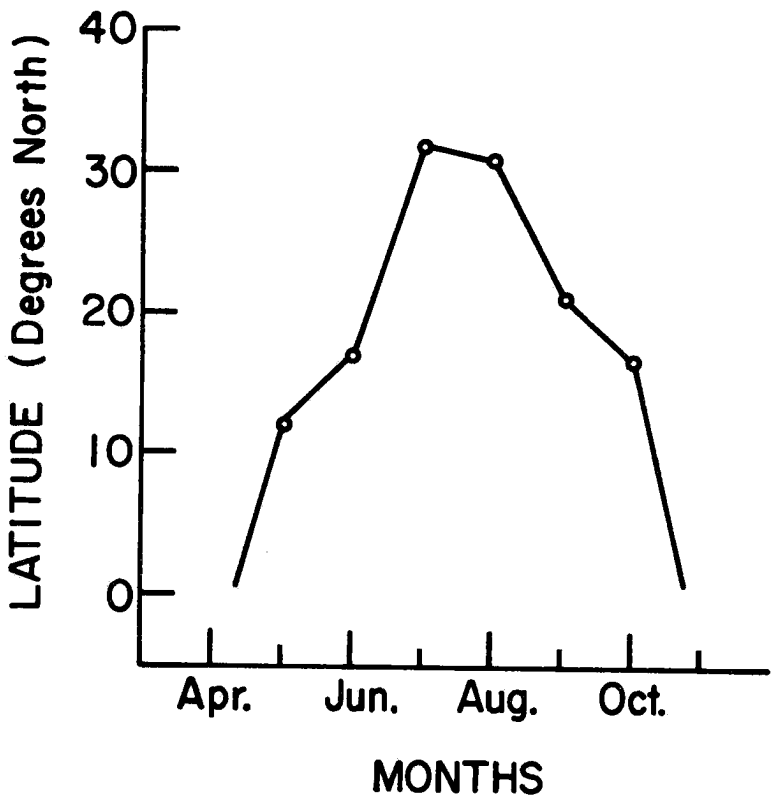


Fig. 40. Seasonal variation of the position of the center of an anticyclone at 200 mb over the east Pacific (between 100° - 140°W).

During January and February, the peak storm months in the S.H., the climatological position of the east-west ridge axis is between 10-15° latitude (Fig. 41). Easterly flow prevails between the equator and 8°S. This allows for the occurrence of equatorward oriented outflow channels. During the FGGE year 36% of the cyclones in the South Pacific and 9% in the South Indian Ocean cyclones developed equatorial outflow channels. When S.H. tropical cyclones occur at low latitudes and are located to the east of the climatological position of the 200 mb equatorial anticyclone (Fig. 41), then conditions are favorable for the formation of equatorward outflow channels.

TABLE 6

Monthly frequency of the upper level outflow patterns over the Southwest Pacific during the FGGE year.

| | | Dec | Jan | Feb | Mar | Apr | May-Nov | Total |
|---|---|---|---|---|---|---|---|---|
| S | $S_{Pw}$ | 2 | | 3 | | 1 | | 6 |
| | $S_{Pc}$ | | 1 | | | | | 1 |
| | $S_{Ec}$ | | 1 | | | | | 1 |
| | $S_{Ee}$ | | 1 | 1 | 1 | | | 3 |

TABLE 7

Monthly frequency of the upper level outflow patterns over the South Indian Ocean during the FGGE year.

| | | Dec | Jan | Feb | Mar | Apr | May-Nov | Total |
|---|---|---|---|---|---|---|---|---|
| S | $S_{Pw}$ | 1 | | 5 | 2 | | | 8 |
| | $S_{Pc}$ | | 1 | | | | | 1 |
| | $S_{Ee}$ | 1 | | | | | | 1 |
| N | $N_s$ | | | | | 1 | | 1 |

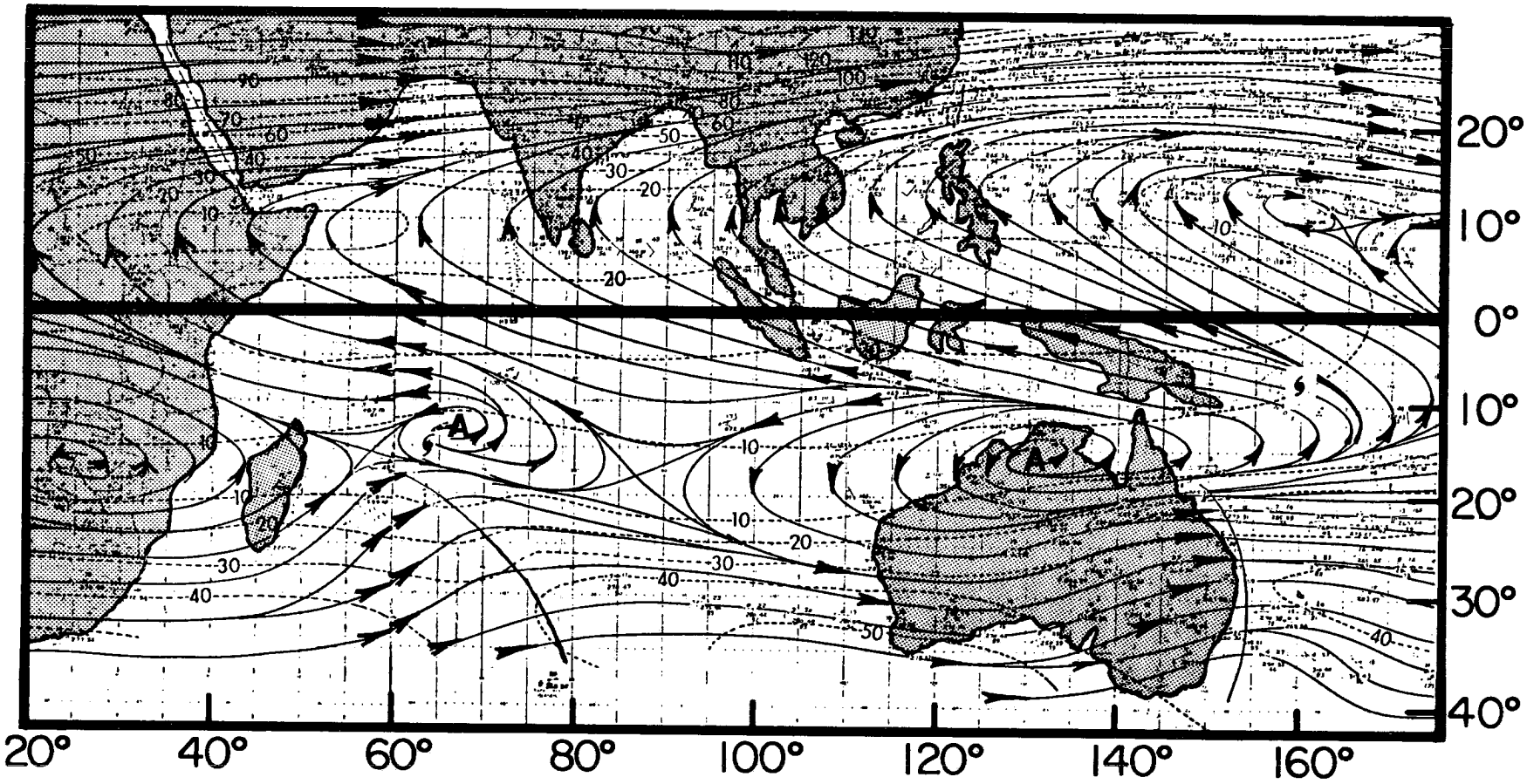


Fig. 40. 200 mb average wind in the Southern Hemisphere in February (adopted from Sadler, 1976).

A few S.H. tropical cyclones occur in a weak easterly sector to the equatorward side of the 200 mb anticyclone where wind conditions are not strong enough to favor the development of outflow channels.

d. Channel Discussion

Tables 8 and 9 show how frequently the various outflow channel patterns occur in the Northern and Southern Hemispheres, respectively. These results show that in the Northern Hemisphere, equatorward outflow channels occurred much more frequently than poleward outflow channels. Equatorial outflow patterns are twice as prevalent as equatorial outflow patterns. This situation is reversed in the S.H. where poleward outflow channels are much more frequent than equatorward outflow channels by a ratio of three to one. Global statistics show that poleward outflow channels and equatorward outflow channels occur with about the same frequency. During the FGGE year global tropical cyclone activity showed that single-channel outflows were three times as frequent as double or no-channel outflow.

TABLE 8

Outflow patterns of the different tropical cyclone basins of the Northern Hemisphere during the FGGE year with the percentages of each outflow pattern in parentheses.

| Outflow Patterns | $S_P$ | $S_E$ | D | N | Total |
|---|---|---|---|---|---|
| NW Pacific | 5(16) | 16(52) | 2(7) | 8(26) | 31(100) |
| N. Indian Ocean | 4(67) | 2(33) | | | 6(100) |
| NW Atlantic | 2(22) | 1(11) | 4(45) | 2(22) | 9(100) |
| NE Pacific | 1(8) | 8(67) | | 3(25) | 12(100) |
| Northern Hemisphere Total | 12(21) | 27(47) | 6(10) | 13(22) | 58(100) |

TABLE 9

Same as Table 8 but for the Southern Hemisphere.

| Outflow Patterns | $S_P$ | $S_E$ | D | N | Total |
|---|---|---|---|---|---|
| SW Pacific | 7(64) | 4(36) | | | 11(100) |
| S. Indian Ocean | 9(82) | 1(9) | | 1(9) | 11(100) |
| Southern Hemisphere Total | 16(73) | 5(23) | | 1(5) | 22(100) |

## 6. Outflow Channel Changes Associated with Tropical Cyclone Weakening

It is well known that when a tropical storm or hurricane passes over land, over a cold sea surface, or encounters strong vertical wind shear regions, its central intensity will decrease. Such inner-core cyclone intensity decrease can also occur over warm seas and away from baroclinic zones when the upper level outflow channels of the cyclone become cut-off. Cyclone intensity decrease is associated with a decrease in cyclone inner-core deep convection. As will be discussed later, cyclone outflow channel strength appears to be related to the strength of the inner-core deep convection.

Our case study analysis of FGGE year cyclones shows that prior to and during the weakening of a tropical cyclone over tropical waters that the upper level outflow and cloud outflow channel features often undergo marked changes. These changes are outlined in the following three models.

### a. Cut-off of the Upper Level Cloud Outflow Channel

Super Typhoon Judy over the northwest Pacific had a strong equatorward outflow channel for 6 days up until 23 August (Fig. 42a). This outflow channel was associated with the approach to and the enhancement of an equatorial anticyclone in the Southern Hemisphere (see previous Fig. 20). This outflow channel was then suddenly cut off (Fig. 42b) and Judy rapidly filled. A line from J to L of this figure shows the cut-off part of the cloud outflow ($21^{o}$N). The maximum sustained wind speed of Judy was 80 kts just before this cut-off occurred. After this cut-off, Judy weakened to only 30 kts maximum sustained speed on 25 August. This cyclone then disappeared on 26th of August.

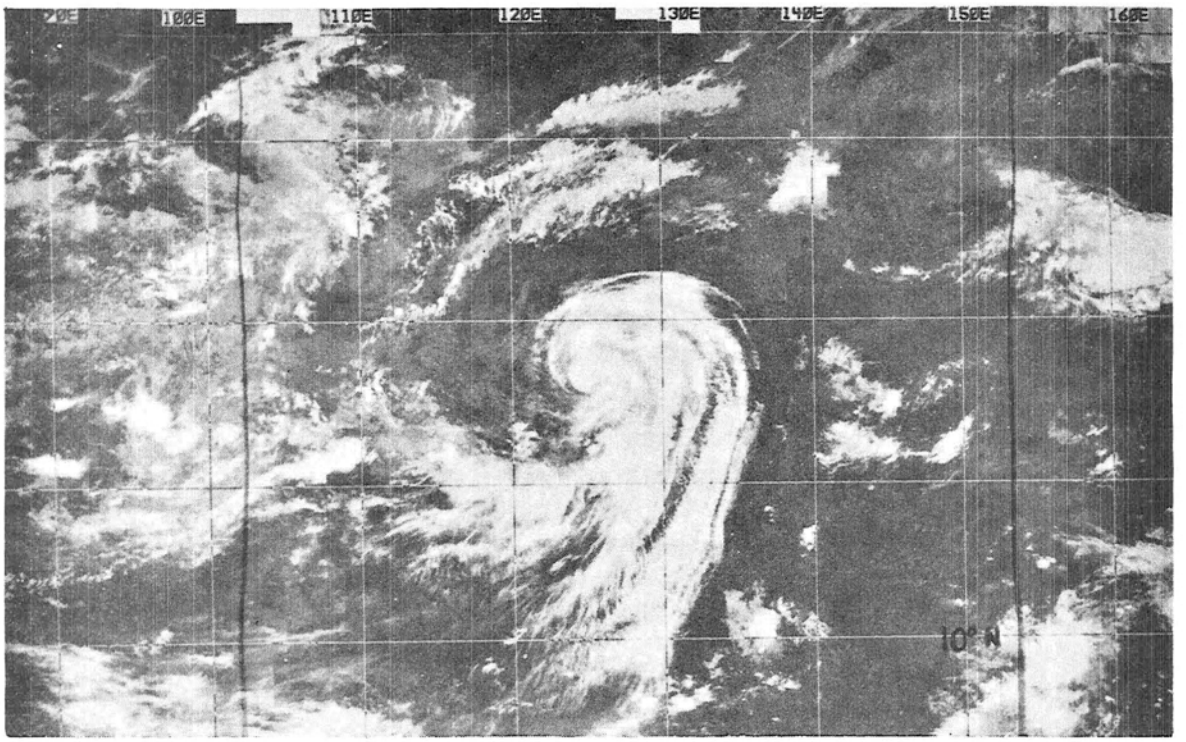


(a)

23 AUGUST 0615Z

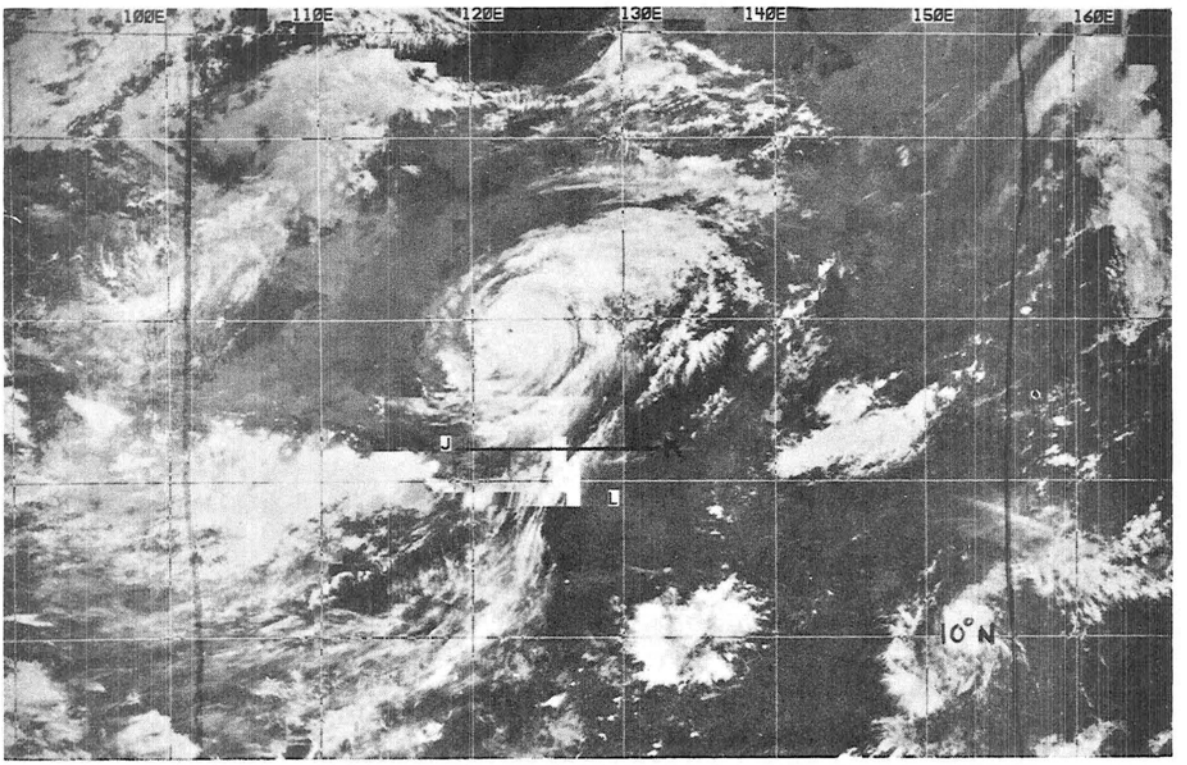


(b)

24 AUGUST 0612Z

Fig. 42. Illustrating the equatorial outflow channel cut-off which occurred with Pacific Typhoon Judy between 23 and 24 August.

By comparing Fig. 43a and 43b one can see that this outflow channel cut-off appears related to the eastward movement and weakening of the S.H. equatorial anticyclone (caused by the intense development of a long-wave trough off the east Australian coast). In addition, the typhoon moved northward and entered into a trough region between two highs.

Outflow channel cut-off can also occur when a tropical cyclone moves out of a large-scale environment which is conductive to outflow channel maintenance.

The depression out of which Typhoon Lola grew in the northwest Pacific was formed on 1 September; no outflow channel was present before 4 September. On the 5th an equatorward outflow channel was formed (Fig. 44a). From the 5th to the 6th, the maximum sustained wind speed increased from 75 kts to 90 kts. As Lola moved further westward the next day this outflow channel became cut off and disappeared on the 6th (Fig. 44b). Lola then rapidly weakened. From the 6th to the 7th, the maximum sustained wind speed dropped from 90 kts to 45 kts.

b. Merging of a tropical cyclone's poleward cloud outflow with a cloud band in the westerlies

It has been shown that when a longwave middle latitude baroclinic trough with a cloud band approaches a tropical cyclone, there is typically an intensification of the tropical cyclone. But, if the trough is strong and more closely approaches to the cyclone, the cyclone will quickly fill and occasionally disappear altogether due to the increase of the vertical wind shear over the system. When this happens it is frequently said that the cyclone has been "sheared". What is this critical distance for cyclone weakening? It depends upon such

200 mb

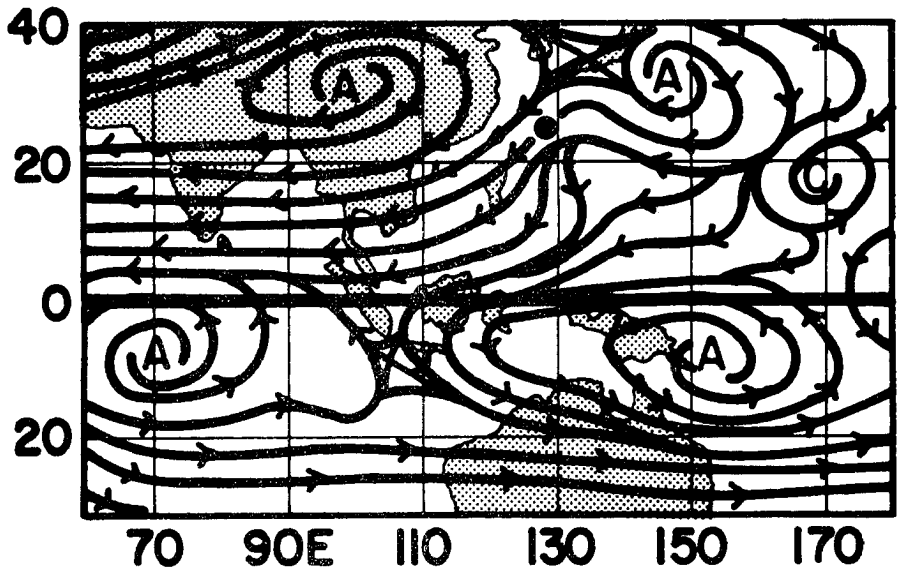


22 AUGUST 00Z

200 mb

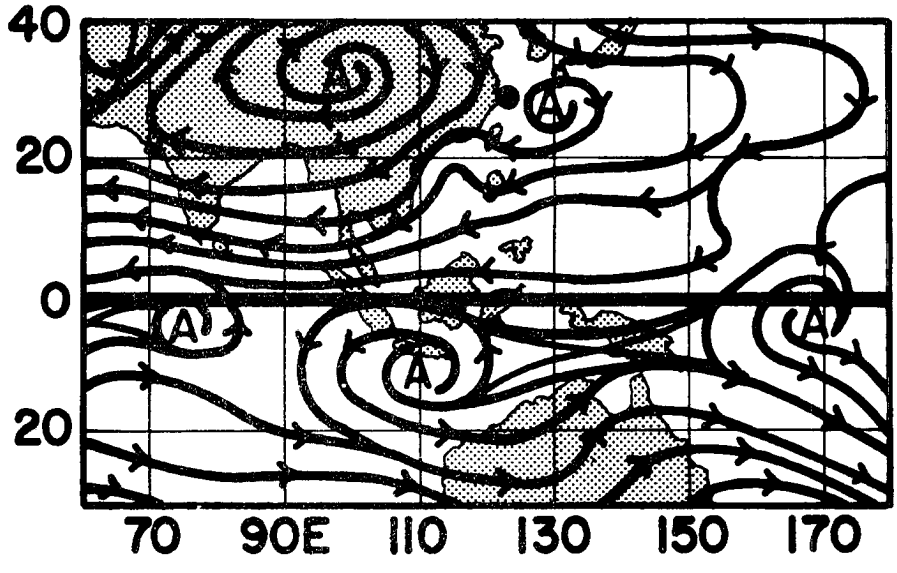


24 AUGUST 00Z

Fig. 43. Typhoon Judy's outflow channel was cut when the anticyclone over the Southern Hemisphere moved away from the storm. From 24-25 August Judy's maximum sustained wind decreased from 80 to 30 kts.

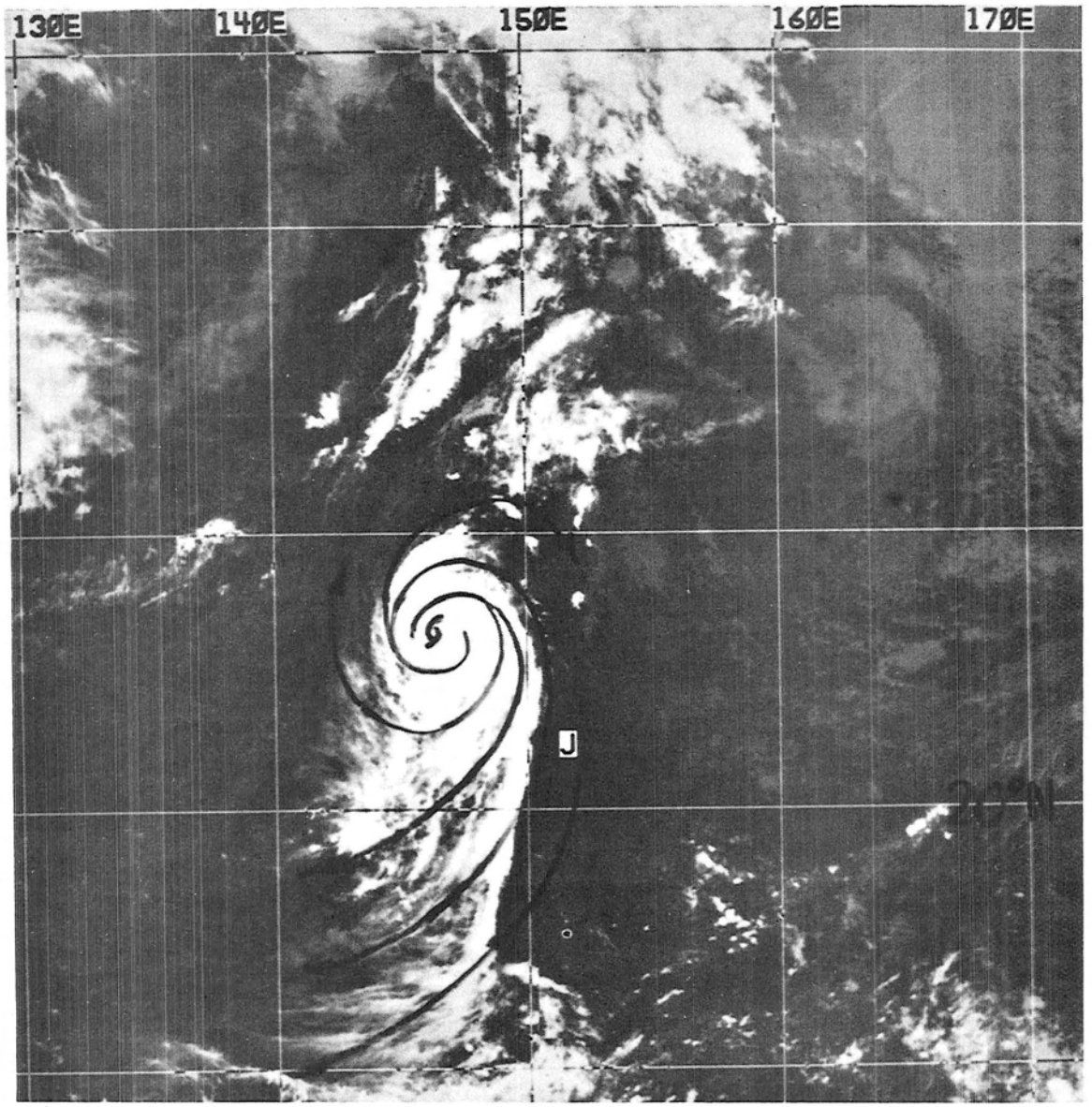


(a)

Fig. 44a-b. Illustration of Typhoon Lola's cloud outflow being cut off and this cyclone being to fill between the 5th (Diagram a) and the 6th (Diagram b next page) of September.

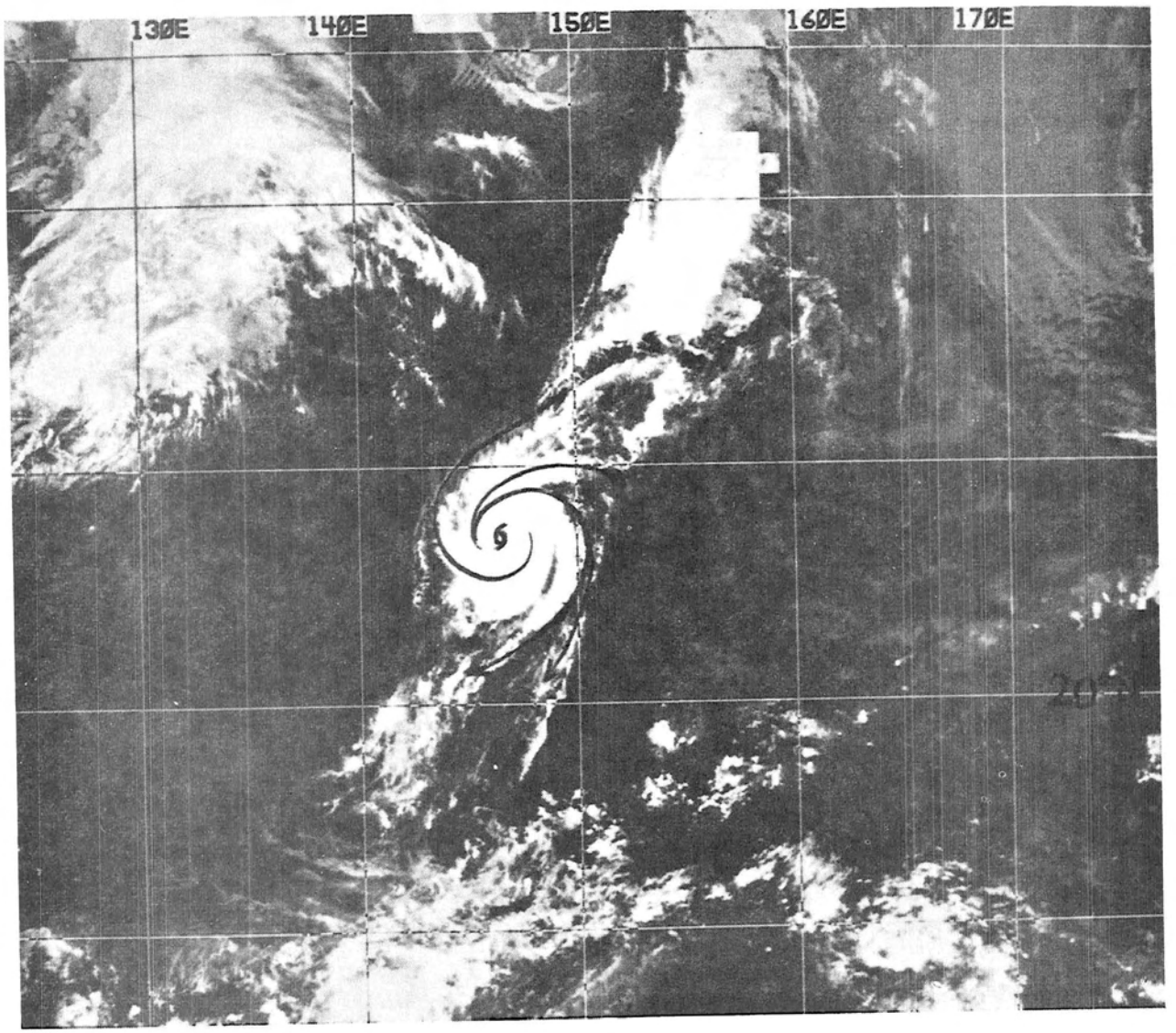


(b)

Fig. 44b. Continued.

factors as the typhoon's intensity, its size, and the intensity of cloud band and the baroclinic westerly winds. It is complicated. The satellite imagery, however, may provide some reference measure for how close the baroclinic region must come before cyclone weakening occurs. When the cloud band of westerlies links up with the poleward cloud outflow channel or with the central convection of the cyclone, the cyclone will typically undergo a rapid weakening.

Figure 45a shows future Typhoon Bess with a long poleward outflow channel. During the process of the typhoon's approach to the baroclinic westerlies, the maximum sustained wind speeds increased from 50 kts on 22 March to 90 kts on 23 March. The distance between Bess and cloud band 'B' of the westerlies was about 15 degrees at the time of this increase.

The next day as cloud band 'B' approached more closely to Bess, its cloud region linked up with the cyclone's long poleward cloud outflow channel (Fig. 46b). The two cloud bands merged on 24 March. From 24 to 25 March, the maximum sustained wind speed of Bess dropped from 90 kts to 25 kts, and the entire system dissipated.

Another Typhoon, Cecil, had similar features. Its depression was generated on 9 April. It developed rapidly during the 13th to 14th. It then made landfall in the Philippines on the 15th and recurved out to sea on the 17th. It then developed a poleward outflow channel (designated 'A' in Fig. 46). On the 18th this poleward outflow channel was about 15 degrees latitude from a cloud band 'B' of the westerlies designated 'B'. The two cloud bands linked together on the 19th, and merged on the 20th. From the 19th to the 20th, the maximum sustained

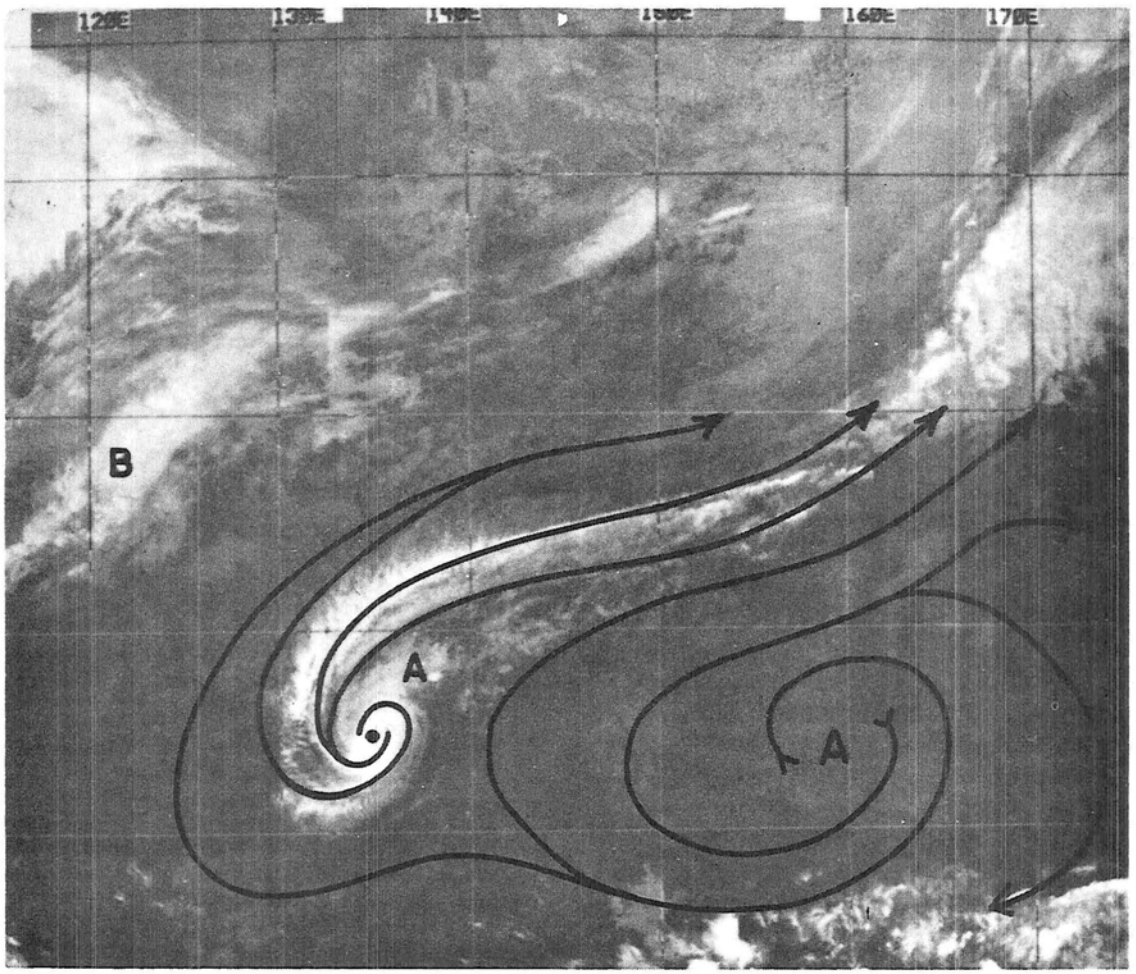


Fig. 45a. DMSP visual picture of Pacific Typhoon Bess on 22 March 1979 at 1600Z.

wind speed of Cecil decreased from 50 kts to 20 kts, and it disappeared over the sea (Fig. 47).

c. Entrance of a Tropical Cyclone Into an Upper Level Trough

A tropical cyclone also will be weakened when it encounters a baroclinic trough without a cloud band.

Figure 48a shows the situation one day before Hurricane Gloria weakened when an intensifying upper level trough and the anticyclone above Hurricane Gloria approach each other. The anticyclone in front of

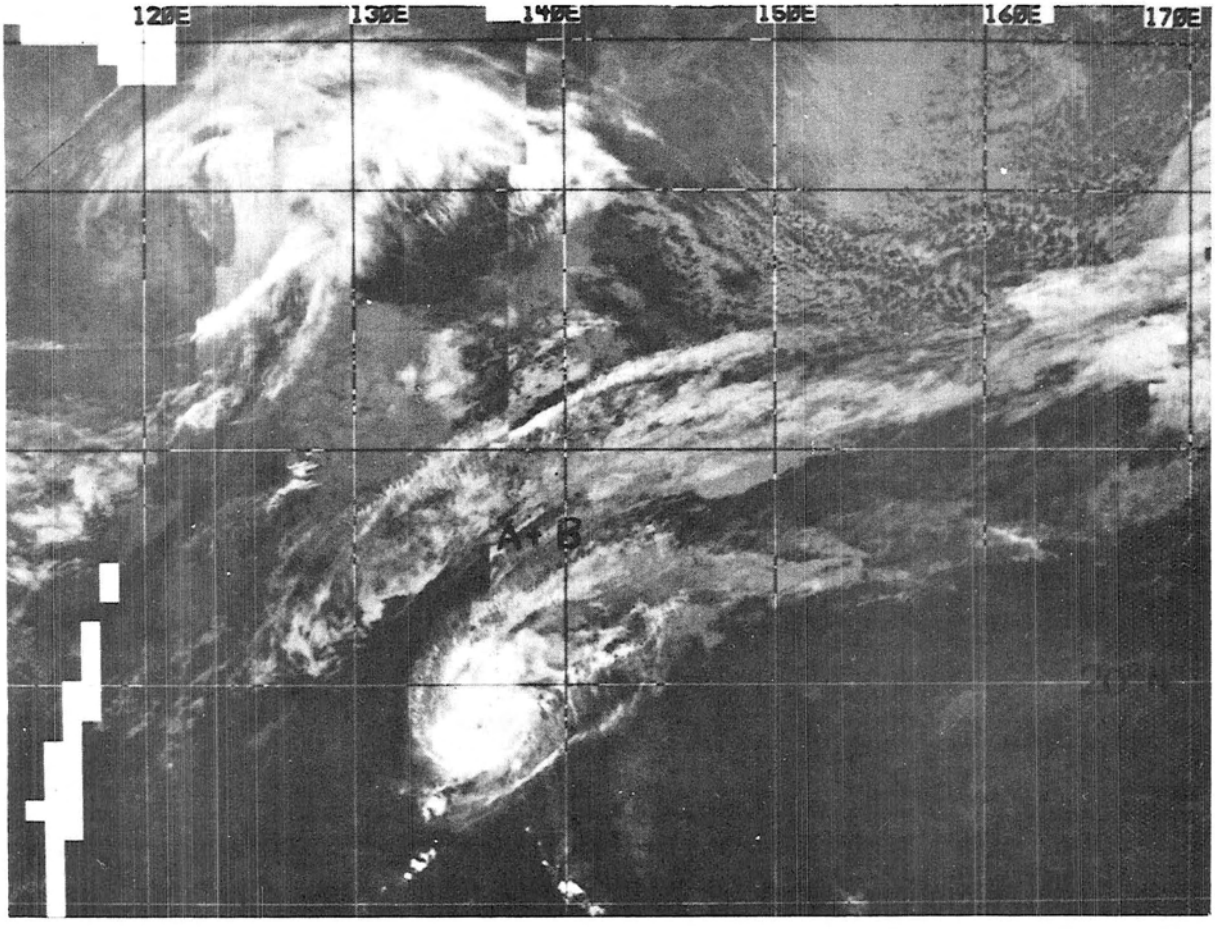


Fig. 45b. Linking up a poleward cloud outflow A and cloud band B of the westerlies. DMSP display of Typhoon Bess on 23 March 1979 - 1600 Z.

the trough was weakened by the strong trough which Gloria moved under (Fig. 49b). Gloria rapidly weakened. From 14 to 15 September, the maximum sustained wind speed of Gloria dropped 80 kts to less than 30 kts and the storm soon dissipated.

There are thus three primary types of synoptic processes that cause tropical storm weakening: cloud outflow towards the equator which is cut off (W1); the cyclone's polar outflow channel clouds merge with a westerly wind cloud band (W2); and the case when the tropical cyclone encounters an upper level trough (W3). Twenty-three weakening cases were analyzed during this FGGE year period (Table 10). Statistics show

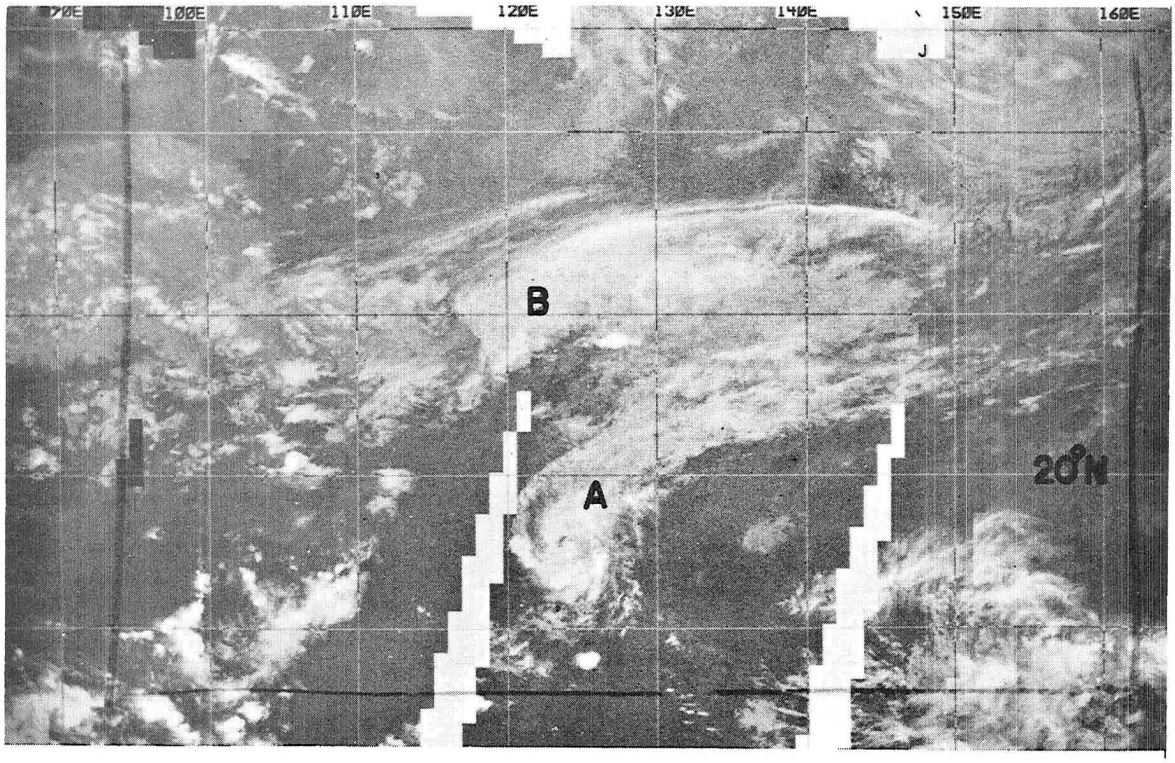


Fig. 46. DMSP display 1600Z 18 April 1979.

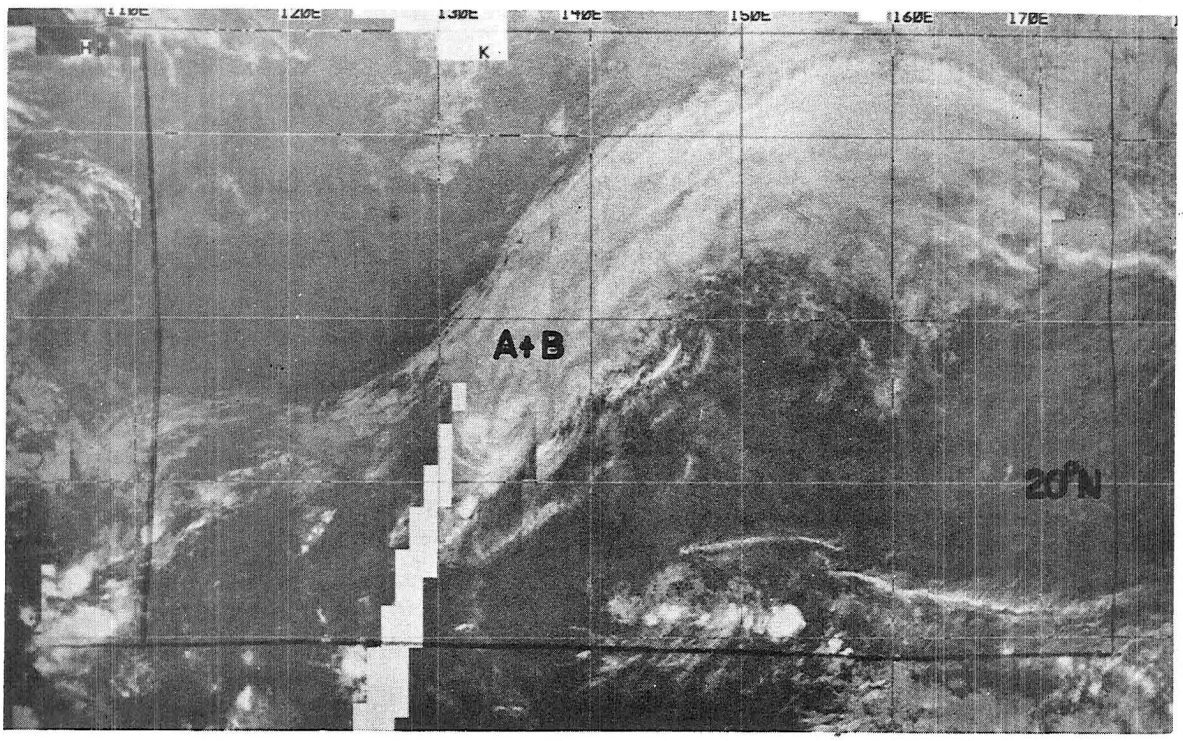


Fig. 47. DMSP display 1600Z 20 April 1979.

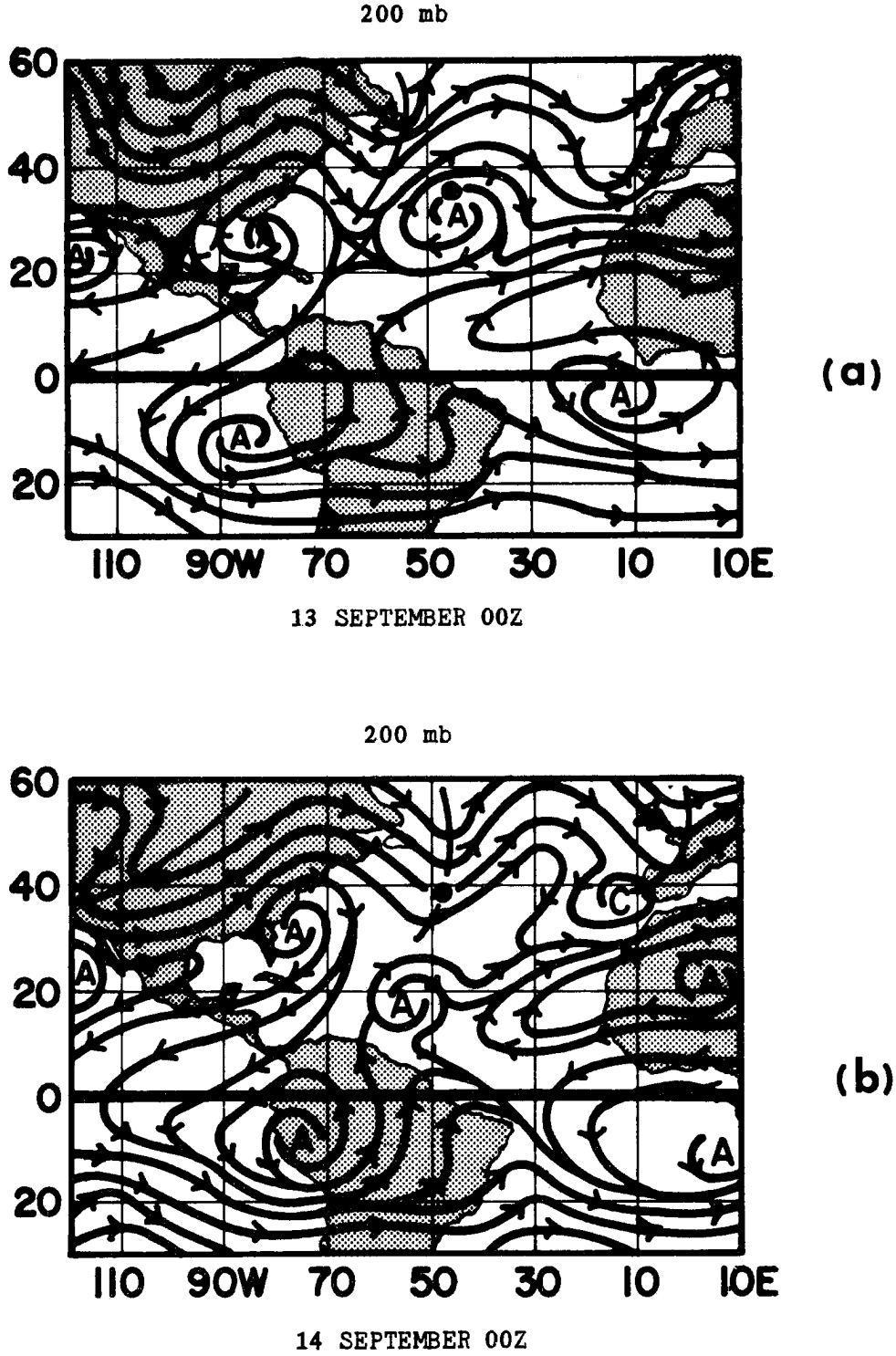


Fig. 48a-b. Tropical cyclone was covered by an upper level trough. a) 13 September 1979; and b) 14 September 1979.

TABLE 10

Frequency of weakening cases for different types of synoptic processes.

| Weakening Type | M1 | | M2 | | M3 | | Others | |
|---|---|---|---|---|---|---|---|---|
| | Number | % | Number | % | Number | % | Number | % |
| Frequency | 6 | 26 | 10 | 44 | 4 | 17 | 3 | 13 |
| Season | June-Sept | | Oct-Apr | | | | | |

that 20 or 87% of these cases belonged to these three types of weakening (26% of M1, 44% to M2, and 17% to M3).

The remaining 13% weaken from other processes. The M1 type of weakening tends to occur more in the summer half of the year and M2 more in the winter half of the year.

There is no doubt in our mind but that the upper tropospheric environment around the tropical cyclone can exert a very powerful influence on the intensity and the intensity change of the inner-core of the tropical cyclone.

## 7. How Upper Level Outflow Channels May Be Related to Cyclone Intensification

What physical processes are responsible for this apparent association of outflow channel concentration and inner storm intensification? We cannot yet answer this question with much certainty. We do, however, have preliminary suggestions based on recent research at CSU by Merrill (1985), Edson (1985), Holland and Merrill (1984), Holland (1983), and Schubert and Hack (1982).

Cyclone intensification is primarily related to the processes which bring about changes in the concentration of the tropical cyclone's inner core mean in-up-and-out mass circulation. Only positive increases in the cyclone's inner core transverse circulation can enhance the inner region convection, mechanically spin-up the storm's core momentum field, and cause a strong dynamically forced eye or center region subsidence.

There is now general agreement that tropical cyclone intensity and intensity change is not well related to the overall amount of deep cumulus convection and mean vertical motion occurring throughout the tropical cyclone as a whole (Arnold, 1977). Many tropical cyclones intensify with only a moderate amount of deep convection while other cyclones with massive amounts of deep convection over large areas fail to intensify or fill. It is not the magnitude of the overall mean vertical circulation within the total cyclone system which is the most important factor in its intensification, but rather the concentration of the deep convection near the cyclone's center.

The observations of this paper indicate that when a tropical cyclone's outer radius (~5-15$^{o}$) 200 mb outflow is concentrated in narrow

and strong channels (as opposed to broader and more uniform and weaker outflow channels) that favorable conditions for inner cyclone concentration of deep-convection are somehow met. When the tropical cyclone's upper level outflow is not concentrated in strong and narrow outflow channels, however, then the conditions necessary to concentrate inner-core deep convection are, in general, less favorable. Thus, the 200 mb mass outflow configuration as shown in the left diagram of Fig. 49 is more conducive to cyclone intensification than the outflow configuration of the right diagram.

a. How a Cyclone's Upper Tropospheric Environment may be Linked to the Inner Core Deep Convection

Although still speculative, the following ideas concerning inertial stability appear to offer some explanation as to why the tropical cyclone's upper tropospheric environmental processes can best explain the physical linkage to the cyclone's inner core circulation than do the low levels and why an association between concentrated outflow channels and cyclone inner-core convection exists. These ideas have been developed at CSU primarily by Holland and Merrill (1984), Holland (1983), Merrill (1984, 1985), and Schubert and Hack (1982).

The argument rests with the concepts of inertial stability ($I^2 = \chi \times \xi$) where $I^2$ stands for inertial stability, $\chi_a$ absolute vorticity and $\xi = f + \frac{2V_\theta}{r}$ where f is the Coriolis parameter, $V_\theta$ is the tangential wind, and r is radius. The mechanism for inertial stability can be viewed as the restoring ability between the pressure gradient, Coriolis, and centrifugal forces when a particle is offset in the radial distance from a balanced flow. Air particles can more easily move longer radial distances if their inertial stability is small (more anticyclonic). The

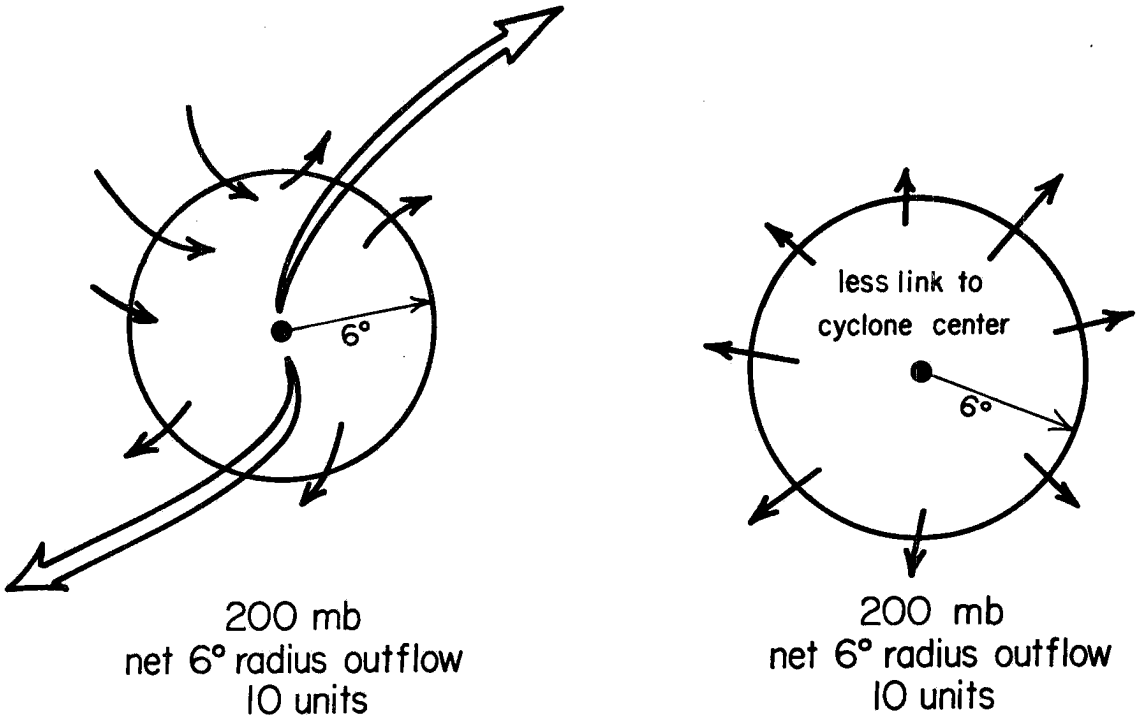


Fig. 49. Contrast of 200 mb cyclone outflow patterns with concentrated channels (left diagram) vs. a cyclone with uniform outflow and no concentrated outflow channels.

smaller $I^2$ is the less resistent are air particles to radial displacement. The $I^2$ in the anticyclonic shear of these upper level outflow channels is considerably lower than that which would exist in a more uniform symmetric cyclonic flow pattern at lower tropospheric levels. There can thus be a greater radial link between the inner core and its environment through these channels. It is the high inertial stability at low levels which insulates the cyclone's core circulation from its environment. This may explain why low level circulation features cannot be as well related to inner cyclone intensity change.

Physical Processes Occurring at Inner Core During Cyclone Intensification. Observational evidence within the inner core of the tropical cyclone from aircraft reconnaissance and eye dropsondes indicates that tropical cyclone intensity and intensity change is, in

general, proportional to the magnitude of the dynamically forced subsidence warming within the cyclone eye (or central region if no eye should be present). The strength of this central core subsidence appears, to a large extent, to be directly related to the intensity of eye-wall deep convection and inversely to the radius of the eye. For equal intensity eye-wall convection, the smaller the radius of maximum convection, the smaller the eye and in general the more intense is the subsidence warming and the lower the pressure drop. Thus, in order to observe an increase in tropical cyclone intensity one must also observe an increase in eye-wall (or central cyclone) deep convection and a consequent increased forced subsidence as idealized in Fig. 50. Arnold's (1977) Colorado State University composite satellite study gives evidence of systematic inner-core deep convection increases during the progressive developmental stages of a cloud cluster to super typhoon stage as does Dvorak's (1975, 1984) intensification technique. This inner core convective concentration goes on irrespective of the overall amount of deep convection within the entire tropical cyclone cloud region.

The mode of evolution of the cyclone's inner region deep convection is important in determining how the cyclone's inner deep convection can be maintained however. In general, deep Cb convection acts to warm and to stabilize the upper troposphere. All tropical cloud clusters with deep convection have warm upper tropospheric layers. Such upper level convective stabilization if continued in the central area of the tropical cyclone for very long would be expected to stabilize and

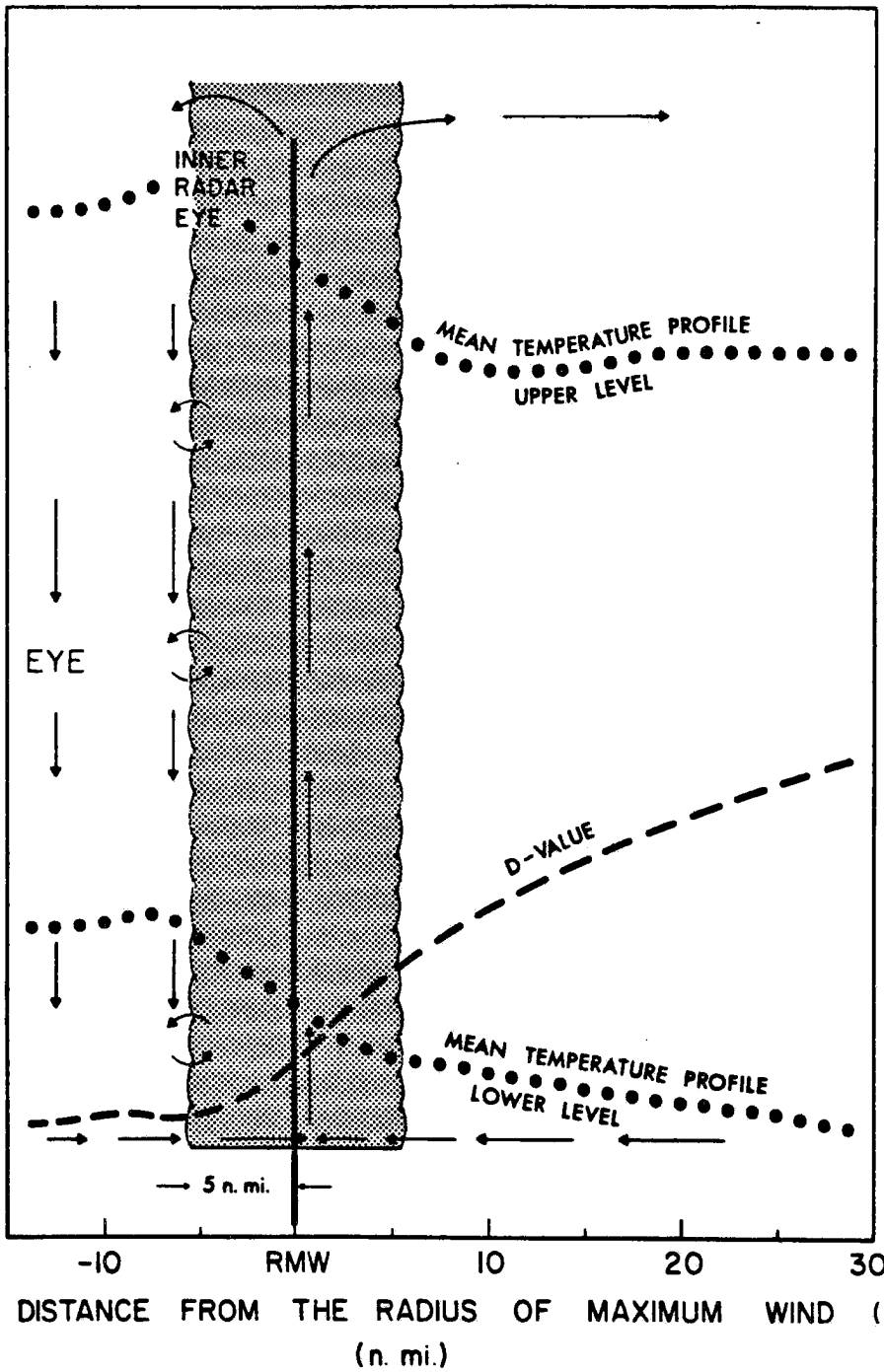


Fig. 50. Idealized portrayal of the mean flow conditions in the hurricane's inner core region. The horizontal and vertical arrows represent the radial and vertical velocities, respectively. Mean D-value (or pressure-height curve) and temperature profiles are as indicated.

reduce future deep convection. If such stabilization were to occur within the cyclone eyewall, convection would eventually weaken and eye subsidence for intensification would become less. A general cyclone filling would occur. Previous CSU research (Gray and Shea, 1973) indicates that the eye of the tropical cyclone is dynamic in fact it ventilates itself every 4-8 hours or so. Intensity is reduced in cyclones which cannot maintain continual eye subsidence and ventilation since intensity change requires an increase in eye subsidence.

To maximize a cyclone's central pressure drop and to minimize the buoyant stabilization aloft of the central area of deep convection it is important that the convectively induced core region warming outside the subsidence eye region occur as high as possible in the troposphere. In other words, the requirement for lowest surface pressure and highest cyclone intensity is that the cyclone's eye be as warm as possible but that the upper troposphere of the eye wall cloud (or the core convection region if there is no eye) be as cool and thus as unstable for deep convection as possible.

The lower the cyclone pressure the warmer (hydrostatic) the eye or central warming must become. The warmer the eye the stronger must be the dynamically forced subsidence and the eye-wall or core deep convection which is necessary to drive it. The higher this warming occurs the less buoyant stabilization of the upper and middle levels of 150-400 mb and the greater pressure thickness change which can occur for a given amount of warming.(1)

---

(1) For similar amounts of temperature ($\Delta T$) increase between equal pressure layers ($\Delta P$), larger thickness are obtained if such warming occurs at higher than at lower levels.

One of the distinctive features of the tropical cyclone's inner core region is the intense horizontal temperature gradient at the eye-wall. Approximately half the temperature increase from the storm's outer environment to the center of the eye occurs within the eye-wall cloud (see Fig. 50). Thus, the colder the upper levels of the eye-wall and outwards are in comparison with the eye's center, the more intense can be the eye-wall convection and the greater the dynamically forced subsidence inside the eye.

The larger a cyclone's inner core upper-tropospheric cyclonic tangential circulation becomes, the greater will be its eye-wall pressure drop (for a given amount of warming) and the less will be the stabilization at upper middle levels. Future deep convection will be less inhibited.

It should be realized that the well developed tropical cyclone has cyclonic flow at all levels in its inner core. Figure 51 illustrates a typical 200 mb pattern with anticyclonic flow at outer radii and the usual cyclonic flow at inner radii.

New wind compositing research at CSU (Edson, 1985; Merrill, 1985) is showing that intensifying tropical cyclones are best distinguished from non-intensifying (or less intensifying) cyclones by their increasing tangential wind velocity in the upper troposphere at inner radii of 1-3° and less - See Fig. 52. In this case, cylindrical thermal wind balance considerations would dictate that upper tropospheric warming would be also higher up and buoyant stability near the cyclone's core (but not in the eye) be reduced when the upper tangential winds are more like curve (a) than curve (b) in Fig. 53. Thermal wind requirements would also dictate that there be much more warming outside

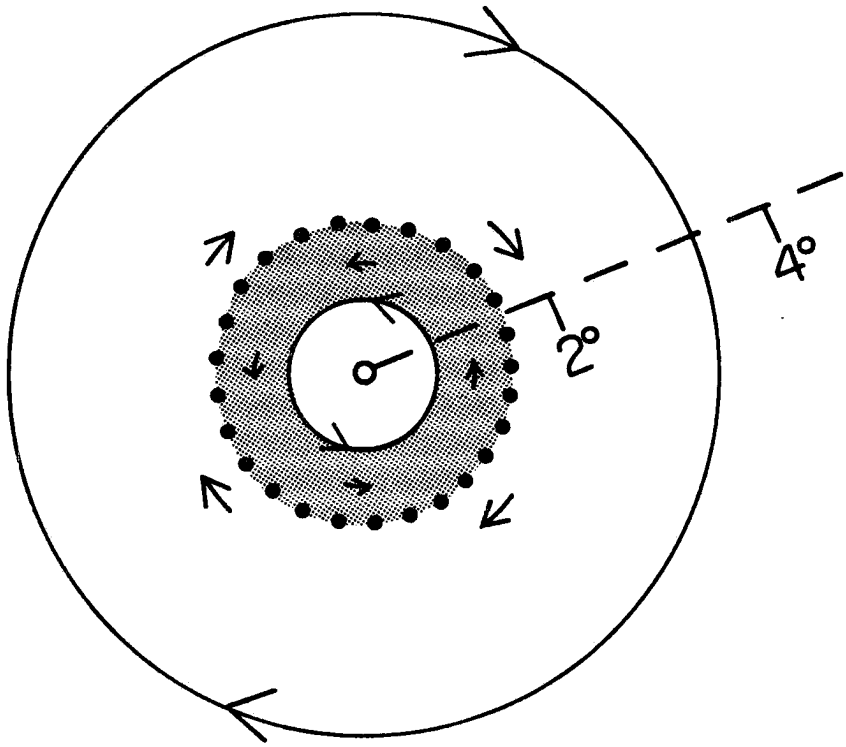


Fig. 51. Typical 200 mb circulation around the center of a hurricane. The shaded region shows the area of cyclonic circulation.

the eye between the levels of 400-150 mb to balance the vertical wind profile of curve (b) than that of curve (a).

Any process (either external or internal) which leads to inner cyclone upper tropospheric tangential wind increase will (other influences remaining constant) allow for surface pressure decrease in the eye and less upper level stabilization for a specified amount of tropospheric warming near the convective eye wall. An outward sloping eye with height would also be beneficial to maintaining convection buoyancy. For instance, our project's composite rawinsonde observations of intensifying versus non-intensifying tropical cyclones (Merrill, 1985; Edson, 1985) show distinct differences in the initial upper tropospheric temperature. Intensifying cyclones of similar central pressure in comparison with non-intensifying cyclones are distinctly cooler at levels from 125-400 mb by amounts of about 1-4$^{o}$C. This allows

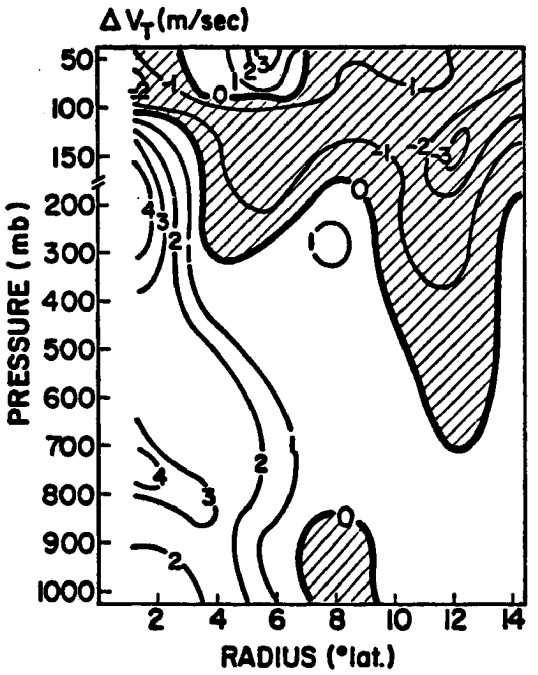


Fig. 52. Changes in tangential wind velocity in 24 hours for western North Pacific tropical cyclones undergoing moderate rates of intensity change of > 18 mb/24 hrs (from Edson, 1985).

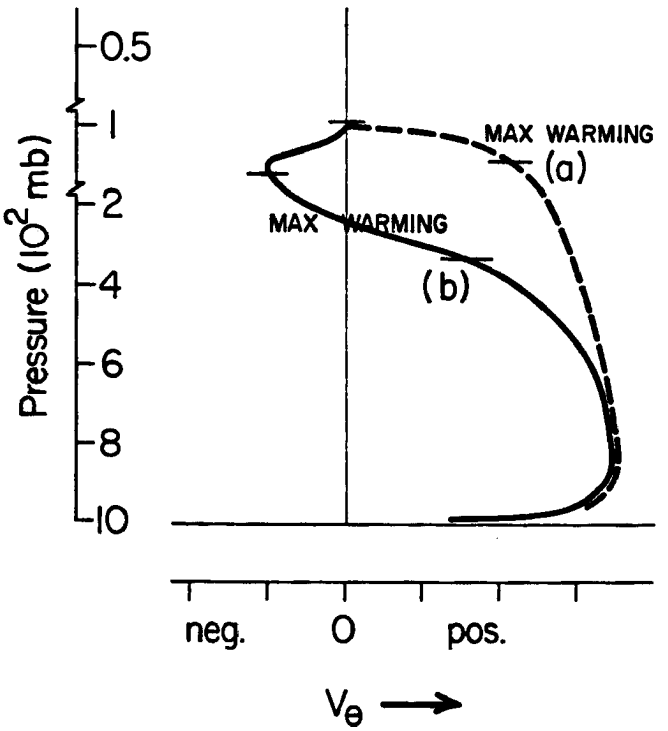


Fig. 53. Favorable vertical tangential wind profile near the convective cloud center of a tropical cyclone to allow maximum surface pressure drop and minimum lapse rate stability (curve a) versus a tangential wind profile which would cause less surface pressure and greater lapse rate stability in the upper troposphere (curve b).

the convective heating for the intensifying case to have a less stabilizing effect.

The larger part of the upper tropospheric tangential wind increase at the eye-wall as a cyclone develops is due to convective momentum import from lower levels. It is likely, however, that an important extra source of tangential momentum to these upper layers also come from horizontal tangential momentum imports into the eye-wall region from the outer cyclone environment due to inward horizontal eddy fluxes (Merrill, 1985). If this contention is correct and 200 mb outflow channels were to act to enhance 200 mb inner core cyclonic wind increase, then a direct physical association between these outflow channels and cyclone central core intensification could be made.

Environmental Linkages to the Inner Core. The observations and hypothesis of Merrill (1985) and the observational results of this paper imply that tropical cyclones with strong outflow channels likely have a greater upper level eddy import of tangential momentum to the region of central convection than do tropical cyclones without such concentrated outflow channels. The physical link between tropical cyclone eye-wall convection enhancement and outflow channels is thus believed to take place through the association of such outflow channels with enhanced inward tangential eddy momentum flux to the cyclone's central region of maximum convection.

When outflow is concentrated in strong anticyclonically curved outflow channels as shown by the left diagram in Fig. 49, mass requirements dictate that there also be a degree of compensating inflow. This upper level inflow may move towards the center with a tangential momentum larger than the outflowing air at the same radius. This may

result in an inward eddy momentum flux which would not be possible were the outflow more nearly symmetric as shown by the right diagram of Fig. 49.

This is an overly simplified view. The actual dynamics of this inward eddy momentum flux appear to be very complicated. Merrill (1985) has presented evidence and has hypothesized that this needed upper level inward momentum flux may occur due to standing wave (Wave No. 1 or 2) momentum fluxes. These waves are developed through upper level barotropic instability process at radii between about 2-5° or so. When such an intermediate radius barotropic wave becomes azimuthally superimposed upon an environmental wave or special flow pattern on the tropical cyclone's flank at radius of 10-15°, an important outer to inner core upper level momentum transport may result. The reader should refer to Merrill's study for a more detailed discussion of this hypothesis. Although Merrill's intensification ideas have been developed for hurricanes undergoing intensification change in the Atlantic basin it is believed that the general physical processes as he has advanced them likely apply in a similar fashion in the other tropical cyclone basins. The hypothesized physical linkages might be summarized in the following flow diagram of Fig. 54.

These upper tropospheric linkages between the tropical cyclone and its environment need much more research. Although not well understood at this time, the observations of this paper and the majority of the experienced tropical cyclone forecasters indicate that such upper level linkages are typically present with cyclone intensification cases.

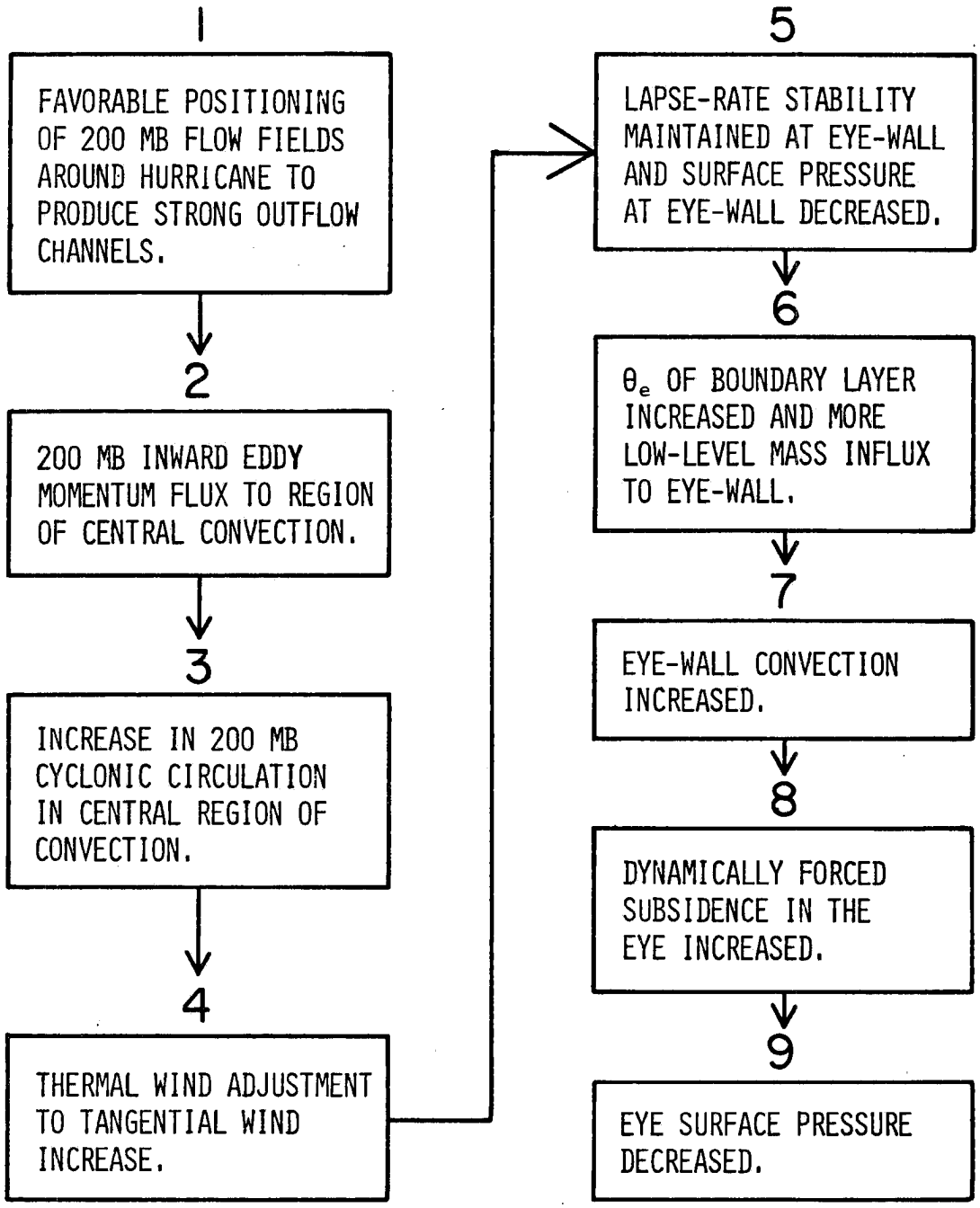


Fig. 54. Idealized view of how favorable environmental conditions at 200 mb might lead to an increase in tropical cyclone inner-core intensity change.

## 8. Concluding Discussion

Tropical cyclone upper level outflow patterns vary in the different ocean basins. Certain outflow patterns occur only in specific ocean basins and in certain seasons of the year. The type of outflow patterns which occur in each ocean basin and season are largely dependent upon the background general circulation climatology of that particular region.

The prediction of tropical cyclone intensity change remains a complicated subject. While many associations of 200 mb outflow with tropical cyclone intensity change have been demonstrated here, other factors such as sea-surface temperature (SST), moisture content, lower tropospheric circulation conditions, etc. can also influence a tropical cyclone's potential for intensity change. Sometimes tropical cyclone intensity change will not occur despite the presence of highly favorable outflow conditions. Other times when outflow conditions are only marginally satisfactory, a tropical cyclone may intensify anyway because these other factors are very favorable. Nevertheless, the outflow channel and intensity change relationships shown here appear to be associated with a substantial fraction of the intensity change which typically occurs. Outflow characteristics should be utilized as much as possible when making intensity changes predictions. The reader should consult the new CSU study by Merrill (1985) for an extensive discussion of the interplay of a cyclone's outflow, SST, and other factors on its intensity and intensity change. Even though Merrill has treated only Atlantic hurricanes and tropical cyclones, we believe his findings should, in a general sense, be applicable to the other global storm basins.

It is hoped that this study of cyclone outflow channels will provide the tropical cyclone forecaster and researcher with a little better background for assessing cyclone intensity change.

The global satellite observations in this paper, by necessity, have largely been taken from the polar orbiting US military DMSP system. Geostationary Meteorological Satellite (GMS) derived cyclone outflow channel wind information would have likely given a much superior measurement and better space and time resolution to our outflow channel assessments. Unfortunately GMS cyclone outflow winds were not available for most of these FGGE year cyclone cases. It is hoped that more research studies of these outflow and core intensity relationships will be made in the tropical cyclone basins where GMS outflow wind information are now available and, in time, in the other ocean basins when geostational satellite data becomes available. Merrill (op.cit) study of west Atlantic tropical cyclones has shown how a much superior assessment of cyclone intensity change potential can be made through a painstakingly combination of GMS satellite, aircraft and rawinsonde winds.

How are the results of this paper related to the very excellent research of V. Dvorak (1975, 1984) on determining tropical cyclone intensity directly from an inspection of satellite images? We believe this research is auxillary to Dvorak's intensity determination method and that these results might be used at times as a supplementary aid to the Dvorak scheme. The outflow information of this paper will hopefully give the forecaster a little better understanding of the importance of assessing tropical cyclone 200 mb outflow patterns on a larger space and time scale than the Dvorak scheme is able to do from satellite images

alone. While this study uses both satellite pictures and the available upper level synoptic data, Dvorak uses only satellite imagery. Dvorak concentrates primarily on the cyclone's inner 5-6° radius cloud characteristics and banding features and how these are related to current cyclone intensity. By contrast this study deals primarily with the environmental wind and outflow channels of the cyclone at radii > 5°. We also have not attempted a current cyclone intensity estimate as Dvorak does but only to identify the environmental patterns which are most conducive to cyclone intensity change.

It is hoped that some of the tropical cyclone outflow information of this paper might be used as a modest supplement to the Dvorak scheme.

Acknowledgements

The authors are grateful for the many discussions they have had on this subject with their CSU colleagues, particularly Roger Edson, Robert T. Merrill, and Edward Rodgers while he was on extended leave to CSU from NASA. We are very appreciative of the careful review of this paper given by Roger Edson. We would like to thank the NOAA satellite archive facility in Boulder, Colorado, for the loan of many of the DMSP pictures used in this study.

This research has been financially supported by the National Aeronautics and Space Adminstration Grant Number NAG 5-299. The authors are appreciative of the encouragement rendered them for this type of observational research by Dr. Joanne Simpson of the NASA Goddard Laboratory.

This research was accomplished while the first author was on a two-year research visit to CSU from the Beijing Central Meteorological Bureau of the People's Republic of China.

References

Alaka, M. A., 1962: The occurrence of dynamic instability in incipient and developing hurricanes. Mon. Wea. Rev., 90, 49-68.

Arnold, C. P., 1977: Tropical cyclone cloud and intensity relationships Dept. of Atmos. Sci. Paper No. 277, Colo. State Univ., Ft. Collins, CO, 154 pp.

Bjorheim, K., et al., 1981, 1982: FGGE III-b daily global analysis parts I, II, III, and IV. ECMWF publication (available for ECMWF, Reading, U.K.).

Chen, L. S., 1974: On the relationships between typhoon formation and four aspects of the surrounding large scale flow. Tech. Report of Chinese National Typhoon Conference.

Dvorak, V. F., 1975: Tropical cyclone intensity analysis and forecasting from satellite imagery. Mon. Wea. Rev., 103, 420-430.

Dvorak, V. F., 1984: Tropical cyclone intensity analysis using satellite data. NOAA Tech. Report NESDIS 11, 47 pp. (available from the National Environmental Satellite Data and Information Service, Washington, D.C.

Edson, Roger, 1985: Synoptic scale view of the differences in tropical cyclone intensity vs. strength change. Paper presented at 16th Technical Conference on Hurricanes and Tropical Meteorology, AMS, Houston, TX.

Gray, W. M., 1982: Tropical cyclone genesis and intensification. Topics in Atmospheric and Oceanographic Sciences, Intense Atmospheric Vortices, (Ed. by L. Bengston/J. Lighthill), Springer-Verlag Berlin Heidelberg (ISPN 3-540-11657-5), 3-20.

Holland, G. J., 1983: Tropical cyclones in the Australian/southwest Pacific region. Dept. of Atmos. Sci. Paper No. 363, Colo. State Univ., Ft. Collins, CO 264 pp.

Holland, G. J. and R. T. Merrill, 1984: On the dynamics of tropical cyclone structural changes. Quart. J. Roy. Meteor. Soc., 110, 723-745.

Merrill, R. T., 1984: A comparison of large and small tropical cyclones. Mon. Wea. Rev., 112, 7, 1408-1418.

Merrill, R. T., 1984: Structure of the tropical cyclone outflow layer. Proceedings of the 15th Technical Conference on Hurricanes and Tropical Meteorology, AMS, January 9-13, Miami, FL.

Merrill, R. T., 1985: Environmental influences on hurricane intensification. Dept. of Atmos. Sci. Ph.D. thesis, Colo. State Univ., Ft. Collins, CO.

Rodgers, Edward, 1984: The justification for using VAS data to improve tropical cyclone forecasting. Proceedings of the 15th Technical Conference on Hurricanes and Tropical Meteorology, AMS, January 9-13, Miami, FL.

Sadler, J. C., 1975: The upper tropospheric circulation over the global tropics. UH MET 75-05. Univ. of Hawaii Research Report, 36 pp.

Sadler, J. C., 1976: A role of the tropical upper tropospheric trough in early season typhoon development. Mon. Wea. Rev., 104, 1266-1278.

Sadler, J. C., 1978: Mid-season typhoon development and intensity changes and the tropical tropospheric trough. Mon. Wea. Rev., 106, 1137-1152.

Sawyer, J. S., 1947: Notes on the theory of tropical cyclones. Quart. J. Roy. Meteor. Soc. 73, 101-126.

Sawyer, J. S., 1949: The significance of dynamic instability in atmospheric motion. Quart. J. Roy. Meteor. Soc., 75, 364-373.

Schubert, W. H. and J. J. Hack, 1982: Inertial stability and trpical cyclone development. J. Atmos. Sci., 39, 1687-1697.

Simpson, R. H., 1970: A reassessment of the hurricane prediction problem. ESSA Tech. Memo WBTM SR-50, 16 pp.

Weatherford, C. and W. M. Gray, 1984: Relating typhoon intensity to outer 1-4$^{o}$ radius circulation as measured by reconnaissance aircraft. Proceedings of the 15th Technical Conference on Hurricanes and Tropical Meteorology, AMS, January 9-13, Miami, FL.

Weatherford, C., 1985: Tropical structural variability. Dept. of Atmos. Sci. Paper No. 391, Colo. State Univ., Ft. Collins, CO, 77 pp.

W. M. GRAY'S FEDERALLY SUPPORTED RESEARCH PROJECT REPORTS SINCE 1967

| CSU Dept. of Atmos. Sci. Report No. | Report Title, Author, Date, Agency Support |
|---|---|
| 104 | The Mutual Variation of Wind, Shear and Baroclinicity in the Cumulus Convective Atmosphere of the Hurricane (69 pp.). W. M. Gray. February 1967. NSF Support. |
| 114 | Global View of the Origin of Tropical Disturbances and Storms (105 pp.). W. M. Gray. October 1967. NSF Support. |
| 116 | A Statistical Study of the Frictional Wind Veering in the Planetary Boundary Layer (57 pp.). B. Mendenhall. December 1967. NSF and ESSA Support. |
| 124 | Investigation of the Importance of Cumulus Convection and Ventilation in Early Tropical Storm Development (88 pp.). R. Lopez. June 1968. ESSA Satellite Lab. Support. |
| Unnumbered | Role of Angular Momentum Transports in Tropical Storm Dissipation over Tropical Oceans (46 pp.). R. F. Wachtmann. December 1968. NSF and ESSA Support. |
| Unnumbered | Monthly Climatological Wind Fields Associated with Tropical Storm Genesis in the West Indies (34 pp.). J. W. Sartor. December 1968. NSF Support. |
| 140 | Characteristics of the Tornado Environment as Deduced from Proximity Soundings (55 pp.). T. G. Wills. June 1969. NOAA and NSF Support. |
| 161 | Statistical Analysis of Trade Wind Cloud Clusters in the Western North Pacific (80 pp.). K. Williams. June 1970. ESSA Satellite Lab. Support. |
| --- | A Climatology of Tropical Cyclones and Disturbances of the Western Pacific with a Suggested Theory for Their Genesis/ Maintenance (225 pp.). W. M. Gray. NAVWEARSCHFAC Tech. Paper No. 19-70. November 1970. (Available from US Navy, Monterey, CA). US Navy Support. |
| 179 | A diagnostic Study of the Planetary Boundary Layer over the Oceans (95 pp.). W. M. Gray. February 1972. Navy and NSF Support. |
| 182 | The Structure and Dynamics of the Hurricane's Inner Core Area (105 pp.). D. J. Shea. April 1972. NOAA and NSF Support. |

| CSU Dept. of Atmos. Sci. Report No. | Report Title, Author, Date, Agency Support |
|---|---|
| 188 | Cumulus Convection and Larger-scale Circulations, Part I: A Parametric Model of Cumulus Convection (100 pp.). R. E. Lopez. June 1972. NSF Support. |
| 189 | Cumulus Convection and Larger-scale Circulations, Part II: Cumulus and Meso-scale Interactions (63 pp.). R. E. Lopez. June 1972. NSF Support. |
| 190 | Cumulus Convection and Larger-scale Circulations, Part III: Broadscale and Meso-scale Considerations (80 pp.). W. M. Gray. July 1972. NOAA-NESS Support. |
| 195 | Characteristics of Carbon Black Dust as a Tropospheric Heat Source for Weather Modification (55 pp.). W. M. Frank. January 1973. NSF Support. |
| 196 | Feasibility of Beneficial Hurricane Modification by Carbon Black Seeding (130 pp.). W. M. Gray. April 1973. NOAA Support. |
| 199 | Variability of Planetary Boundary Layer Winds (157 pp.). L. R. Hoxit. May 1973. NSF Support. |
| 200 | Hurricane Spawned Tornadoes (57 pp.). D. J. Novlan. May 1973. NOAA and NSF Support. |
| 212 | A Study of Tornado Proximity Data and an Observationally Derived Model of Tornado Genesis (101 pp.). R. Maddox. November 1973. NOAA Support. |
| 219 | Analysis of Satellite Observed Tropical Cloud Clusters (91 pp.). E. Ruprecht and W. M. Gray. May 1974. NOAA/ NESS Support. |
| 224 | Precipitation Characteristics in the Northeast Brazil Dry Region (56 pp.). R. P. L. Ramos. May 1974. NSF Support. |
| 225 | Weather Modification through Carbon Dust Absorption of Solar Energy (190 pp.). W. M. Gray, W. M. Frank, M. L. Corrin, and C. A. Stokes. July 1974. |
| 234 | Tropical Cyclone Genesis (121 pp.). W. M. Gray. March 1975. NSF Support. |

| CSU Dept. of Atmos. Sci. Report No. | Report Title, Author, Date, Agency Support |
|---|---|
| --- | Tropical Cyclone Genesis in the Western North Pacific (66 pp.). W. M. Gray. March 1975. US Navy Environmental Prediction Research Facility Report. Tech. Paper No. 16-75. (Available from the US Navy, Monterey, CA). Navy Support. |
| 241 | Tropical Cyclone Motion and Surrounding Parameter Relationships (105 pp.). J. E. George. December 1975. NOAA Support. |
| 243 | Diurnal Variation of Oceanic Deep Cumulus Convection. Paper I: Observational Evidence, Paper II: Physical Hypothesis (106 pp.). R. W. Jacobson, Jr. and W. M. Gray. February 1976. NOAA-NESS Support. |
| 257 | Data Summary of NOAA's Hurricanes Inner-Core Radial Leg Flight Penetrations 1957-1967, and 1969 (245 pp.). W. M. Gray and D. J. Shea. October 1976. NSF and NOAA Support. |
| 258 | The Structure and Energetics of the Tropical Cyclone (180 pp.). W. M. Frank. October 1976. NOAA-NHEML, NOAA-NESS and NSF Support. |
| 259 | Typhoon Genesis and Pre-typhoon Cloud Clusters (79 pp.). R. M. Zehr. November 1976. NSF Support. |
| Unnumbered | Severe Thunderstorm Wind Gusts (81 pp.). G. W. Walters. December 1976. NSF Support. |
| 262 | Diurnal Variation of the Tropospheric Energy Budget (141 pp.). G. S. Foltz. November 1976. NSF Support. |
| 274 | Comparison of Developing and Non-developing Tropical Disturbances (81 pp.). S. L. Erickson. July 1977. US Army Support. |
| --- | Tropical Cyclone Research by Data Compositing (79 pp.). W. M. Gray and W. M. Frank. July 1977. US Navy Environmental Prediction Research Facility Report. Tech. Paper No. 77-01. (Available from the US Navy, Monterey, CA). Navy Support. |
| 277 | Tropical Cyclone Cloud and Intensity Relationships (154 pp.). C. P. Arnold. November 1977. US Army and NHEML Support. |
| 297 | Diagnostic Analyses of the GATE A/B-scale Area at Individual Time Periods (102 pp.). W. M. Frank. November 1978. NSF Support. |

| CSU Dept. of Atmos. Sci. Report No. | Report Title, Author, Date, Agency Support |
|---|---|
| 298 | Diurnal Variability in the GATE Region (80 pp.). J. M. Dewart. November 1978. NSF Support. |
| 299 | Mass Divergence in Tropical Weather Systems, Paper I: Diurnal Variation; Paper II: Large-scale Controls on Convection (109 pp.). J. L. McBride and W. M. Gray. November 1978. NOAA-NHEML Support. |
| --- | New Results of Tropical Cyclone Research from Observational Analysis (108 pp.). W. M. Gray and W. M. Frank. June 1978. US Navy Environmental Prediction Research Facility Report. Tech. Paper No. 78-01. (Available from the US Navy, Monterey, CA). Navy Support. |
| 305 | Convection Induced Temperature Change in GATE (128 pp.). P. G. Grube. February 1979. NSF Support. |
| 308 | Observational Analysis of Tropical Cyclone Formation (230 pp.). J. L. McBride. April 1979. NOAA-NHEML, NSF and NEPRF Support. |
| --- | Tropical Cyclone Origin, Movement and Intensity Characteristics Based on Data Compositing Techniques (124 pp.). W. M. Gray. August 1979. US Navy Environmental Prediction Research Facility Report. Tech. Paper No. CR-79-06. (Available from the US Navy, Monterey, CA). Navy Support. |
| --- | Further Analysis of Tropical Cyclone Characteristics from Rawinsonde Compositing Techniques (129 pp.). W. M. Gray. March 1981. US Navy Environmental Prediction Research Facility Report. Tech. Paper No. CR-81-02. (Available from the US Navy, Monterey, CA). Navy Support. |
| 333 | Tropical Cyclone Intensity Change - A Quantitative Forecasting Scheme. K. M. Dropco. May 1981. NOAA Support. |
| --- | Recent Advances in Tropical Cyclone Research from Rawinsonde Composite Analysis (407 pp.). WMO Publication. W. M. Gray. 1981. |
| 340 | The Role of the General Circulation in Tropical Cyclone Genesis (230 pp.). G. Love. April 1982. NSF Support. |
| 341 | Cumulus Momentum Transports in Tropical Cyclones (78 pp.). C. S. Lee. May 1982. ONR Support. |

| CSU Dept. of Atmos. Sci. Report No. | Report Title, Author, Date, Agency Support |
|---|---|
| 343 | Tropical Cyclone Movement and Surrounding Flow Relationships (68 pp.). J. C. L. Chan and W. M. Gray. May 1982. ONR Support. |
| 346 | Environmental Circulations Associated with Tropical Cyclones Experiencing Fast, Slow and Looping Motions (273 pp.). J. Xu and W. M. Gray. May 1982. NOAA and NSF Support. |
| 348 | Tropical Cyclone Motion: Environmental Interaction Plus a Beta Effect (47 pp.). G. J. Holland. May 1982. ONR Support. |
| --- | Tropical Cyclone and Related Meteorological Data Sets Available at CSU and Their Utilization (186 pp.). W. M. Gray, E. Buzzell, G. Burton and Other Project Personnel. February 1982. NSF, ONR, NOAA, and NEPRF Support. |
| 352 | A Comparison of Large and Small Tropical Cyclones (75 pp.). R. T. Merrill. July 1982. NOAA and NSF Support. |
| 358 | On the Physical Processes Responsible for Tropical Cyclone Motion (200 pp.). Johnny C. L. Chan. November 1982. NSF, NOAA/NHRL and NEPRF Support. |
| 363 | Tropical Cyclones in the Australian/Southwest Pacific Region (264 pp.). Greg J. Holland. March 1983. NSF, NOAA/NHRL and Australian Government Support. |
| 370 | Atlantic Seasonal Hurricane Frequency, Part I: El Nino and 30 mb QBO Influences; Part II: Forecasting Its Variability (105 pp.). W. M. Gray. July 1983. NSF Support. |
| 379 | A Statistical Method for One- to Three-Day Tropical Cyclone Track Prediction (201 pp). Clifford R. Matsumoto. December, 1984. NSF/NOAA and NEPRF support. |
| --- | Varying Structure and Intensity Change Characteristics of Four Western North Pacific Tropical Cyclones. (100 pp.). Cecilia A. Askue and W. M. Gray. October 1984. US Navy Environmental Prediction Research Facility Report No. CR 84-08. (Available from the US Navy, Monterey, CA). Navy Support. |

| CSU Dept. of Atmos. Sci. Report No. | Report Title, Author, Date, Agency Support |
|---|---|
| --- | Characteristics of North Indian Ocean Tropical Cyclone Activity. (108 pp.). Cheng-Shang Lee and W. M. Gray. December 1984. US Navy Environmental Prediction Research Facility Report No. CR 84-11. (Available from the US Navy, Monterey, CA). Navy Support. |
| 391 | Typhoon Structural Variability. (77 pp.). Candis L. Weatherford. October, 1985. NSF/NOAA Support. |
| 392 | Global View of the Upper Level Outflow Patterns Associated with Tropical Cyclone Intensity Change During FGGE. L. Chen and W. Gray, 126 pp. NASA support. |
| | Tropical cyclone structure and intensity change (290 pp.). Edwin Nunez. NSF Support. |

| BIBLIOGRAPHIC DATA SHEET | 1. Report No. ATS-392 | 2. | 3. Recipient's Accession No. |
|---|---|---|---|

4. Title and Subtitle

Global View of the Upper Level Outflow Patterns Associated with Tropical Cyclone Intensity Changes During FGGE

5. Report Date: October, 1985

6.

7. Author(s)

Lianshou Chen and William M. Gray

8. Performing Organization Rept. No. ATS-392

9. Performing Organization Name and Address

Atmospheric Science Department
Colorado State University
Fort Collins, CO 80523

10. Project/Task/Work Unit No.

11. Contract/Grant No.

NASA NAG 5-299

12. Sponsoring Organization Name and Address

NASA/Goddard #NASA NAG 5-299
Office of Space Science and Applications
Greenbelt, Maryland 20771

13. Type of Report & Period Covered

Project Report

14.

15. Supplementary Notes

16. Abstracts

This paper discusses the characteristics of the upper tropospheric outflow patterns which occur with tropical cyclone intensification and weakening over all of the global tropical cyclone basins during the year long period of the First GARP Global Experiment (FGGE). By intensification we mean the change in the tropical cyclone's maximum wind or central pressure, not the change of the cyclone's outer 1-3° radius mean wind which we classify as cyclone strength. All the 80 tropical cyclones which existed during the FGGE year are studied. 200 mb wind fields were derived from the analysis of the European Centre for Medium Range Weather Forecasting (ECMWF) which made extensive use of upper tropospheric satellite and aircraft winds. Corresponding satellite cloud pictures from the polar orbiting U.S. Defense Meteorological Satellite Program (DMSP) and other supplementary polar and geostationary satellite data are also used.

17. Key Words and Document Analysis. 17a. Descriptors

Typhoons
Tropical Cyclones
Typhoon Intensity Change

17b. Identifiers/Open-Ended Terms

17c. COSATI Field/Group

| 18. Availability Statement | 19. Security Class (This Report) UNCLASSIFIED | 21. No. of Pages 126 pp. |
|---|---|---|
| | 20. Security Class (This Page) UNCLASSIFIED | 22. Price |

FORM NTIS-35 (REV. 3-72)
THIS FORM MAY BE REPRODUCED
USCOMM-DC 14952-P72